3-2004

Geocation of an Audio Source in a Multipath Environment Using Time-of-Arrival

Jeffrey A. Boggs

GEOLOCATION OF AN AUDIO SOURCE IN A MULTIPATH ENVIRONMENT USING TIME-OF-ARRIVAL

THESIS

Jeffrey A. Boggs, 1st Lieutenant, USAF

AFIT/GCS/ENG/04-03

DEPARTMENT OF THE AIR FORCE
AIR UNIVERSITY

AIR FORCE INSTITUTE OF TECHNOLOGY

Wright-Patterson Air Force Base, Ohio

AFIT/GCS/ENG/04-03

GEOLOCATION OF AN AUDIO SOURCE IN A MULTIPATH ENVIRONMENT USING TIME-OF-ARRIVAL

THESIS

Presented to the Faculty

Department of Electrical and Computer Engineering

Graduate School of Engineering and Management

Air Force Institute of Technology

Air University

Air Education and Training Command

In Partial Fulfillment of the Requirements for the

Degree of Master of Science

Jeffrey A. Boggs, BS

1st Lieutenant, USAF

March 2004

AFIT/GCS/ENG/04-03

GEOLOCATION OF AN AUDIO SOURCE IN A MULTIPATH ENVIRONMENT USING TIME-OF-ARRIVAL

Jeffrey A. Boggs, BS

1st Lieutenant, USAF

Approved:

//SIGNED//	9 Mar 04
Maj. Rusty O. Baldwin, PhD, USAF (Chairman)	Date
//SIGNED//	9 Mar 04
Dr. John F. Raquet, (Member)	Date
//SIGNED//	9 Mar 04
Dr. Richard A. Raines, (Member)	Date

Acknowledgments

I would like to express my sincere appreciation to my faculty advisor, Major Rusty Baldwin, for his guidance and support throughout the course of this thesis effort. The insight and experience was certainly appreciated. I would also like to thank my family for their continuous support throughout this endeavor and my Air Force career.

A special thanks go to Dr. Henry Potoczny for making my AFIT experience most memorable and enjoyable. The extended discussions in Data Security and Algorithms as well as the challenging midterms and finals in those classes were the high point of my graduate studies.

I would finally like to personally thank “Squatch”, “Cable Guy”, “Sally”, “Sparky”, “Tar”, “Rage”, Serial”, “Snap”, “Switch”, and “FNG” for stress management through the hard parts.

Jeffrey A. Boggs

Table of Contents

Page

Acknowledgments vi

List of Figures x

List of Tables xii

Abstract 1

I. Introduction 2

Background 2

Problem Statement 3

Research Objectives/Questions/Hypotheses 4

Preview 4

II. Literature Review 5

Chapter Overview 5

Understanding the Fundamentals of GPS Geolocation 5

Sound Wave Propagation 10

Waveform Analysis 11

Current research 12

Summary 18

III. Methodology 19

Chapter Overview 19

Problem Definition 19

Goals and Hypothesis 19

Approach 20

System Boundaries 20

System Services ... 21

Performance Metrics ... 22

System Parameters ... 22

Workload Parameters ... 23

Factors ... 24

Evaluation Technique ... 30

Workload ... 30

Experimental Design ... 30

Analyze and Interpret results ... 31

Summary ... 31

IV. Analysis and Results ... 32

Chapter Overview ... 32

Sample of experiment output ... 32

Individual topology output ... 36

Topology #1: 1000m x 1000m x 50m, 25 receivers ... 37

Topology #2: 5000m x 5000m x 50m, 25 receivers ... 39

Topology #3: 150m x 150m x 50m, 9 receivers ... 42

Topology #4: 150m x 150m x 60m, 27 receivers ... 44

Topology #5: 150m x 150m x 60m, 27 receivers ... 47

Consolidated output ... 49

Output Distributions ... 53

ANOVA ... 57

Summary.....58

V. Conclusions and Recommendations.....59

Chapter Overview.....59

Conclusions of Research.....59

Significance of Research.....59

Recommendations for Future Research.....60

Summary.....61

Appendix A, Raw Data.....62

Bibliography.....92

Vita.....94

List of Figures

Page

Figure 2.1 Trilateration [MiE01] 6

Figure 2.2 Pictorial representation of GPS geolocation [MiE01]...................................... 7

Figure 2.3 Illustration of good versus poor satellite geometry [AcL94] 10

Figure 2.4 Sniper bullet trajectory and supersonic shockwave [DGB96] 13

Figure 2.5 Proof-of-Principle System Processing Block Diagram [DGB96] 14

Figure 3.1 A graphical representation of the SUT and CUT 21

Figure 3.2 X/Y Plane representation of Topology #1: 1000m x 1000m x 50m 25

Figure 3.3 X/Y Plane representation of Topology #2: 5000m x 5000m x 50m 26

Figure 3.4 X/Y Plane representation of Topology #3: 150m x 150m x 20m 27

Figure 3.5 X/Y Plane representation of Topology #4: 150m x 150m x 50m 28

Figure 3.6 X/Y Plane representation of Topology #5: 150m x 150m x 50m 29

Figure 4.1 Sample input: 25 receivers and 1 source shown in X/Y plane 33

Figure 4.2 Sample output: all valid locations generated by 4-tuples 34

Figure 4.3 Sample output: Valid locations within 100m of population average 35

Figure 4.4 Sample output: Mode of valid locations population...................................... 36

Figure 4.4 Population Average Errors for Topology 1 37

Figure 4.5 100m Cluster Average Errors for Topology 1 38

Figure 4.6 Population Mode Errors for Topology 1 39

Figure 4.7 Population Mode X/Y Errors for Topology 1 39

Figure 4.8 Population Average Errors for Topology 2 40

Figure 4.9 Population Average Errors for Topology 2 40

Figure 4.10 Population Mode Errors for Topology 2 41

Figure 4.11 Population Mode X/Y Errors for Topology 2 41

Figure 4.12 Population Average Errors for Topology 3 42

Figure 4.13 Population Average Errors for Topology 3 43

Figure 4.14 Population Mode Errors for Topology 3 44

Figure 4.15 Population Mode X/Y Errors for Topology 3 44

Figure 4.16 Population Average Errors for Topology 4 45

Figure 4.17 Population Average Errors for Topology 4 46

Figure 4.18 Population Mode Errors for Topology 4 46

Figure 4.19 Population Mode X/Y Errors for Topology 4 47

Figure 4.20 Population Average Errors for Topology 5 47

Figure 4.21 Population Average Errors for Topology 5 48

Figure 4.22 Population Mode Errors for Topology 5 48

Figure 4.23 Population Mode X/Y Errors for Topology 5 49

Figure 4.24 Population Average Errors for All Topologies 51

Figure 4.25 Population Average Errors for All Topologies 51

Figure 4.26 Population Mode Errors for All Topologies... 52

Figure 4.27 Population Mode X/Y Errors for All Topologies.. 52

Figure 4.28 Population Location Error Histrogram Distribution................................... 53

Figure 4.29 100M Cluster Location Error Histrogram Distribution.............................. 54

Figure 4.30 Population Mode Location Error Histogram Distribution........................... 55

Figure 4.31 Population Mode X/Y Location Error Histrogram Distribution 56

List of Tables

Page

Table 2.1 Effectiveness results of the ACSS tests [DGB96] 15

Table 2.2 SECURES Accuracy in Austin TX Demonstration 16

Table 3.1 System Parameters 23

Table 3.2 Factors 24

Table 4.1 Least Squares Fit 57

Table A1 Topology #1, 0% echo 62

Table A2 Topology #1, 20% echo 63

Table A3 Topology #1, 40% echo 64

Table A4 Topology #1, 60% echo 65

Table A5 Topology #1, 80% echo 66

Table A6 Topology #1, 100% echo 67

Table A7 Topology #2, 0% echo 68

Table A8 Topology #2, 20% echo 69

Table A9 Topology #2, 40% echo 70

Table A10 Topology #2, 60% echo 71

Table A11 Topology #2, 80% echo 72

Table A12 Topology #2, 100% echo 73

Table A13 Topology #3, 0% echo 74

Table A14 Topology #3, 20% echo 75

Table A15 Topology #3, 40% echo 76

Table A16 Topology #3, 60% echo 77

Table A17 Topology #3, 80% echo 78

Table A18 Topology #3, 100% echo 79

Table A19 Topology #4, 0% echo 80

Table A20 Topology #4, 20% echo 81

Table A21 Topology #4, 40% echo 82

Table A22 Topology #4, 60% echo 83

Table A23 Topology #4, 80% echo 84

Table A24 Topology #4, 100% echo 85

Table A25 Topology #5, 0% echo 86

Table A26 Topology #5, 20% echo 87

Table A27 Topology #5, 40% echo 88

Table A28 Topology #5, 60% echo 89

Table A29 Topology #5, 80% echo 90

Table A25 Topology #5, 100% echo 91

AFIT/GCS/ENG/04-03

Abstract

The Air Force and the Department of Defense (DoD) are continually searching for ways to protect U.S. forces, both stateside and abroad. One continuing threat, especially in the current world environment, is gunfire from an unseen sniper. Designated areas, such as a forward deployed base or motorcade route, need to be continuously monitored for sniper fire. Once detected, these gunmen need to be located in real time. One possible method for accomplishing this task is to geolocate the audio signals generated using time-of-arrival (TOA) algorithms. These algorithms rely on direct-path measurements for accuracy. Multipath environments therefore pose a problem when measuring signals from the audio spectrum.

The errors induced by a multipath environment can be reduced by introducing additional audio receivers to the detection system. By sampling all possible combinations of a minimum set of receivers (four), a more accurate location can be calculated. An accuracy of six meters can be achieved roughly 69 percent of the time, though most of the error occurs in the vertical component. An accuracy of six meters in the X/Y plane can be achieved approximately 97 percent of the time.

GEOLOCATION OF AN AUDIO SOURCE IN A MULTIPATH ENVIRONMENT USING TIME-OF-ARRIVAL

I. Introduction

In this chapter, a brief discussion is presented on the need for an audio geolocation system and the general problem is defined. Several objectives are identified and relevant questions relating to the research are posed. The major focus of the research is also defined here. Finally, an overview of the methodology is addressed and some basic assumptions about the research are laid out.

Background

With the ever-increasing threat of violence to our armed forces and citizens, the need for an accurate and timely sniper detection and location system is immense. US military personnel are at risk daily in deployed locations from unseen sniper gunfire and mortar fire. In addition, urban crime is a large concern. There is a definite need for a sniper detection system which can quickly and effectively locate an unseen sniper and relay this information to appropriate authorities. In a real time environment, an area of interest could be monitored by numerous audio receiver units, which could communicate with a central processing computer. A hostile sniper or mortar crew could be located in real time and be countered. The lives of American military personnel, as well as civilians, could be saved. In addition, confidence is the U.S. military could be bolstered by its ability to deal with this threat.

One way to locate snipers is to geolocate using the time-of-arrival (TOA) of the audio signals generated by the gun or mortar fire. This is very similar to the way GPS is used to geolocate a single receiver near the surface of the earth. GPS calculates the travel time of each radio signal sent from a satellite to the receiver. This is accomplished using a highly accurate clock and knowing when the signal was sent and when it was received. Using the calculated travel time and the speed the signal is traveling (for radio waves the speed of light), the line-of-sight distance from satellite to receiver can be calculated. With three or more satellites in line-of-sight view of a receiver, a system of equations is constructed with three unknowns: the X, Y, and Z components of the receiver's location. A fourth unknown, the bias or clock error in the system, is also calculated for more accuracy.

In a very similar fashion, sound waves can be used in a TOA algorithm to geolocate an audio source. In a sniper detection system, the event time is not known and therefore is a variable to be calculated in the system of equations generated. Another source of concern is the fact that sound waves have a higher degree of reflectivity than radio waves. Echo or multipath is the signal must be addressed to minimize the location error.

Problem Statement

An area of concern such as a deployed base and a downtown city block needs to be monitored for gunfire or mortar fire and authorities need to be notified in real time of when and where gunfire was detected. A sniper detection system must be able to geolocate an audio source (sniper) to within 6 meters of the actual source, in three dimensions.

Research Objectives/Questions/Hypotheses

The objectives of this research are to prove the feasibility of a sniper detection system which uses only the time-of-arrival of the audio signal generated from sniper gunfire or mortar fire. Such a system should be able to geolocate this audio source to within 6 meters of the actual location. In addition, this system should be able to handle echo or multipath signals and maintain the same accuracy.

Preview

Chapter 2 outlines the fundamentals of GPS geolocation. A review of current research conducted on sniper identification and location is presented. Chapter 3 defines the methodology used in conducting the experiments of this research. The system under test and component under test are defined. Chapter 4 provides analysis of the data produced by the research. The results are compared to the desired accuracy and conclusions are drawn which assert the effectiveness of the proposed geolocation algorithm. In Chapter 5 a summary of the research and recommendations for future study in this area are presented.

II. Literature Review

Chapter Overview

In this chapter, three fundamental topics are discussed: TOA geolocation, sound wave propagation and waveform analysis. The basic formulas used by GPS location are defined. Previous research on geolocation is discussed, as well as waveform analysis.

Understanding the Fundamentals of GPS Geolocation

The Global Positional System (GPS) is a widely used navigational aid. It provides an accurate (to within 1-3 meters optimally) location in three-dimensional space near the surface of the earth (up to 200km altitude). The GPS constellation consists of 27+ active satellites in medium earth orbit. The number of satellites and their orbital planes results in four or more satellites in view from almost any point on the surface of the earth. GPS receivers typically require input from four or more satellites to produce an accurate location in three-dimensional space.

The principle upon which GPS is based is called trilateration[MiE01]. This technique uses three distance measurements from three known locations and finds their intersection to determine a fourth location. A radionavigation system using trilateration is referred to as a *time-of-arrival* (TOA) system [MiE01]. GPS is such a TOA system. Figure 2.1 illustrates the principle of trilateration.

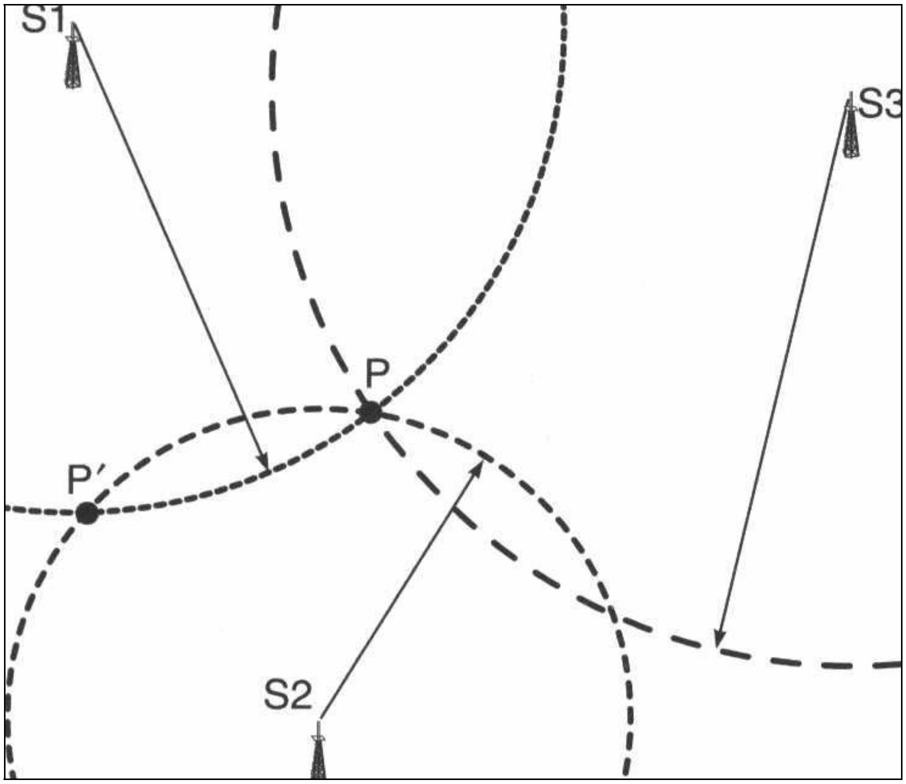

Figure 2.1 Trilateration [MiE01]

A TOA system operates by sending a radio signal from three different transmitters whose location is known. The receiver knows, to a high level of accuracy, exactly when each incoming signal was transmitted and when each was received. The speed of a radio wave is assumed constant over short distances and therefore the distance each radio signal traveled can be calculated. Using this information, the receiver can determine its position through trilateration; by determining the intersection of the three spheres whose radius is the distances traveled by the radio waves and are centered on the known location of each transmitter. For example, consider Figure 2.1. S1, S2, and S3 are the transmitting antennae. P' is a possible intersection point for signals from S1 and S2. P is the intersection point of all three signals.

The location of each GPS satellite relative to the center of the earth is predictable. Further, each satellite contains a highly accurate clock. A timing signal is encoded in each satellite's transmissions along with its location. Therefore, a GPS receiver has both pieces of information needed to perform a trilateration: transmitter location and time-of-flight for the incoming signal. A fourth satellite is used to compensate for any bias or error within the receiver.

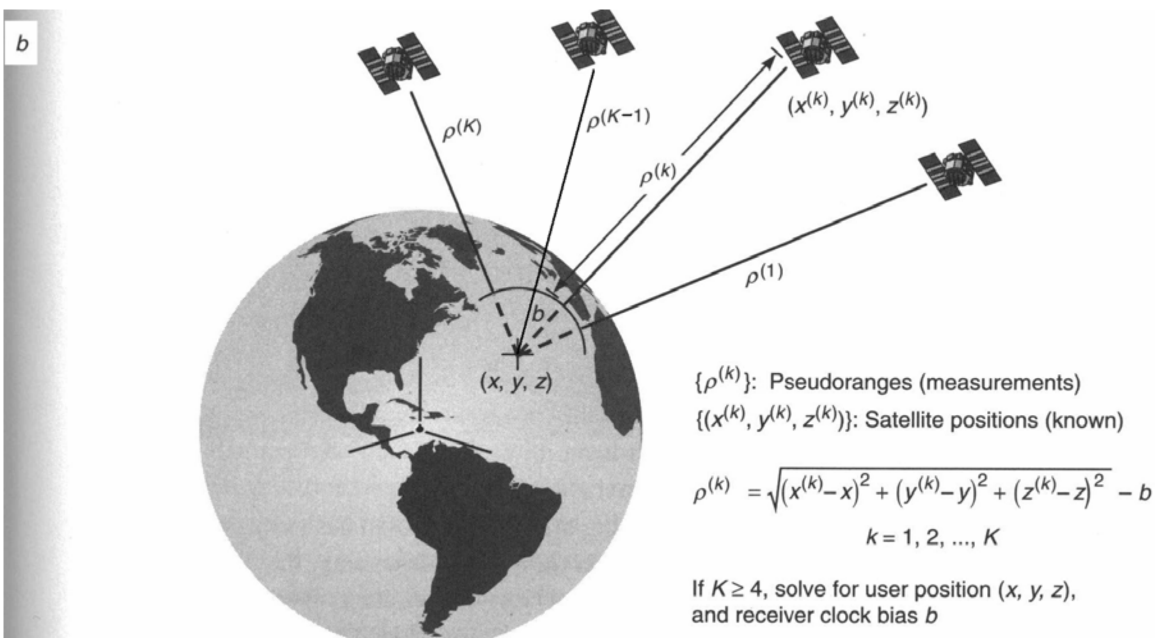

Figure 2.2 Pictorial representation of GPS geolocation [MiE01].

Consider the satellites in Figure 2.2. The geolocation equations for this four satellite system is

$$\rho^{(1)} = \sqrt{\left(x^{(1)} - x\right)^2 + \left(y^{(1)} - y\right)^2 + \left(z^{(1)} - z\right)^2} - b \tag{1}$$

$$\rho^{(2)} = \sqrt{\left(x^{(2)} - x\right)^2 + \left(y^{(2)} - y\right)^2 + \left(z^{(2)} - z\right)^2} - b \tag{2}$$

$$\rho^{(3)} = \sqrt{\left(x^{(3)} - x\right)^2 + \left(y^{(3)} - y\right)^2 + \left(z^{(3)} - z\right)^2} - b \qquad (3)$$

$$\rho^{(4)} = \sqrt{\left(x^{(4)} - x\right)^2 + \left(y^{(4)} - y\right)^2 + \left(z^{(4)} - z\right)^2} - b \qquad (4)$$

where, $\boldsymbol{\rho}^{\mathbf{k}}$ is the pseudoranges (distance from observer to satellite k), $\mathbf{(x^{(k)},y^{(k)},z^{(k)})}$ is satellite k's known position in three-dimensional space measured from the center of the earth, and **b** is the clock bias (error in timing within the system) times the speed of light. This system of four equations contain four unknowns: **x,y,z** coordinates of receiver's location and the clock bias **b** [MiE01].

A simple approach to solving K equations is to linearize them about an approximate user position, and solve iteratively. The idea is to start with rough estimates of the user position and clock bias, and refine them in stages so that the estimates fit the measurements better. This approach is generally referred to as *Newton-Raphson method* [Una93]. Let $\mathbf{x}_0=(x_0,y_0,z_0)$ and b_0 be the first estimates of the user position and receiver clock bias, respectively [MiE01]. An approximation of the pseudorange based on the initial guesses x_0 and b_0 is

$$\rho_0^{(k)} = \left\| x^{(k)} - x_0 \right\| + b_0 . \qquad (5)$$

The iterative least-squares solution equation is

$$\Delta x = (H^T C_\rho^{-1} H)^{-1} H^T C_\rho^{-1} \Delta\rho , \qquad (6)$$

where Δx is the iterative update to the position vector of the receiver (x,y,z,b), H is the partial derivative matrix constructed from equations (1)-(4) with respect to the calculated distance from satellite to receiver, C_ρ is the measurement covariance matrix, and $\Delta\rho$ is the difference between estimated pseudorange, $\rho_0^{(k)}$ and the actual pseudorange, $\rho^{(k)}$.

The iterative process for solving the system of equations is:

1. Estimate the receiver's position and clock bias.
2. Calculate $\rho_0^{(k)}$ with equation (5).
3. Calculate $\Delta\rho$ by subtracting $\rho_0^{(k)}$ from $\rho^{(k)}$.
4. Calculate the H matrix.
5. Calculate Δx with equation (6).
6. Calculate a new receiver position by adding Δx to the previous position vector.

Steps 2-6 are repeated until Δx becomes sufficiently small (approaches zero) or becomes prohibitively large (approaches infinity). If Δx approaches or becomes zero, a location solution has been calculated.

The topology of the satellites in the celestial hemisphere plays a large role in the error introduced into the system. Accurate geolocation requires a degree of separation between satellites with respect to the receiver. Figure 2.4 illustrates a good versus poor topology of satellites [AcL94]. The geolocation algorithm requires substantial planar separation between the satellites and the receiver to provide an accurate location in that plane. That is to say that if the satellites are (nearly) grouped into a single plane with the receiver, then that component of the location answer will contain substantive error.

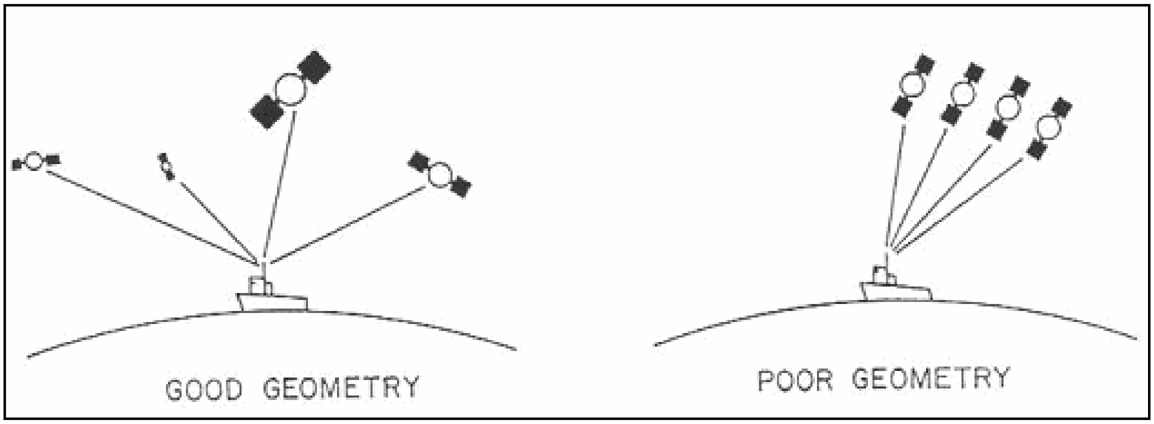

Figure 2.3 Illustration of good versus poor satellite geometry [AcL94] .

Sound Wave Propagation

The propagation of sound is affected by atmospheric conditions including humidity and temperature. $c = \left[\left(\frac{\gamma}{M} \right) \cdot R \cdot T_0 \right]^{\frac{1}{2}}$ is the speed of sound in an ideal gas at a constant pressure where γ, M, R, and T_0 are the specific heat ratio, molar mass, universal gas constant, and the absolute temperature (in Kelvins), respectively [WoE85]. At a constant temperature, the ratio of the speed of sound in humid air to the speed of sound in dry air is

$$\frac{c_h}{c_0} = \left[\frac{\left(\frac{\gamma_h}{M_h} \right)}{\left(\frac{\gamma_0}{M_0} \right)} \right]^{\frac{1}{2}} \qquad (5)$$

where c_h, γ_h, M_h and c_0, γ_0, M_0 are the speed of sound, specific heat ratio and the molar mass of the air at two different humidity values [WoE85]. It has been shown that c_h/c_0 increases with humidity and temperature [WoE85]. The ratio between 0˚ – 30˚ Celcius is

$$\frac{c_h}{c_0} = 1 + h\left(9.66x10^{-4} + 7.2x10^{-5} \cdot t + 1.8x10^{-6} \cdot t^2 + 7.2x10^{-8} \cdot t^3 + 6.5x10^{-11} \cdot t^4\right) \qquad (6)$$

where *h* is relative humidity (dimensionless) and *t* is temperature in degrees Celsius [WoE85].

Variations in the speed of sound could adversely affect geolocation algorithm based on sound wave propagation. If, in such a system, the temperature and humidity varies significantly between receivers, the calculated pseudoranges could contain significant errors. Atmospheric errors are expected to grow as the travel distance of the audio signal grows. Shorter travel distances will most likely incur smaller atmospheric errors.

Waveform Analysis

There are three basic properties associated with sound waves which are important for waveform analysis: frequency, amplitude and relative arrival time [Wei03]. These three elements characterize each received sound wave such that the individual audio source can be differentiated, associated and located.

Geolocation of an audio event using TOA calculations works best with direct path sound waves. Echoes alter the pseudorange calculated from the signal travel time and can induce error into the system [Una00].

The frequency of each sound wave can be used to differentiate most sources. Sound waves can be attenuated, which is the loss of intensity for whatever reason, and they can be absorbed, where the energy is transformed into another form, usually heat [Cal03]. In addition, the speed of sound changes when traveling through different mediums, such as water and earth. But the frequency of sound waves, once produced, remains constant through a single medium. Therefore, these signals can be differentiated and associated between receivers [Cal03].

The amplitude of each incoming signal describes the strength of the signal and can be used to roughly calculate the relative position of the sound source to each of the receivers [KFC82].

The relative arrival time of each sound source is a key element to measuring the distance from the sound source to the receiver. With a known, or determined, event time and the relative arrival time at each sensor, the distance between the event and each sensor can be determined using the speed of sound [MiE01].

Current research

There are several acoustic sniper-tracking systems either proposed or fielded, though none solely use TOA measurements to calculate location, most likely due to the line-of-sight restrictions. One such system was developed by BBN Systems and Technologies of Cambridge, MA [DGB96].

The Acoustic Counter-Sniper System (ACSS) is a low-cost, portable system that detects and localizes (vs. locates) a sniper in both urban and rural environments. The system uses observations of the shock wave from supersonic bullets to estimate the bullet trajectory, Mach number, and caliber. If muzzle blast observations are also available from unsilenced weapons, the exact sniper location along the trajectory is also estimated [DGB96].

ACSS concentrates on observing the shock wave of a supersonic bullet due to the available countermeasures to hide muzzle blast and flash. A silencer can be used to hide both the sound and muzzle flash of a discharged rifle. The acoustic shockwave emitted by these supersonic bullets is a unique, recognizable signature and can be used to determine the caliber of the bullet. The optimum configuration for ACSS is either two small four-element tetrahedral microphone arrays on opposing sides of the protected target, or six omnidirectional microphones spread over the protected area. Figure 2.5 illustrates how the acoustic shockwave is created from a supersonic bullet during flight. As the bullet slows, the (shockwave) wavefront becomes curved. The speed of a sound wave is constant for a given temperature and humidity level and therefore, due to temperature or humidity, the sound wave shouldn't suffer from curving [Woe85].

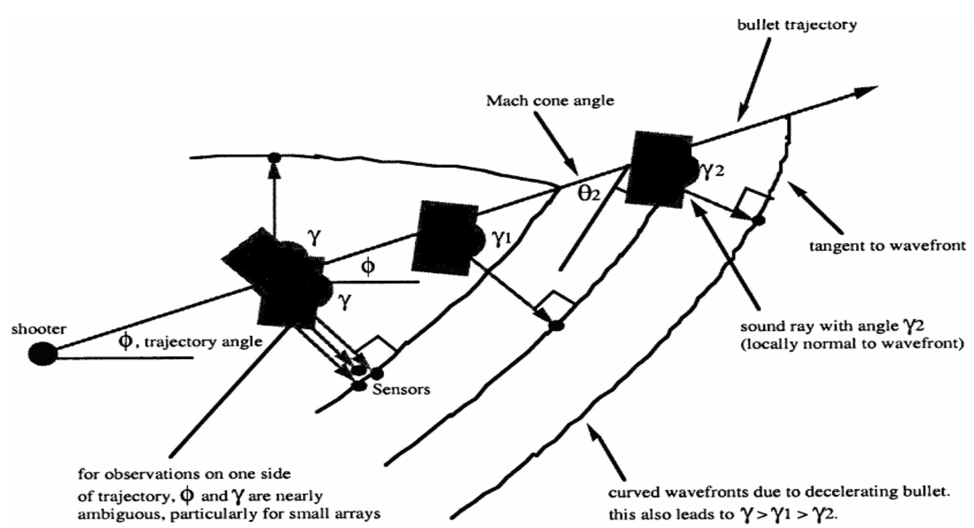

Figure 2.4 Sniper bullet trajectory and supersonic shockwave [DGB96]

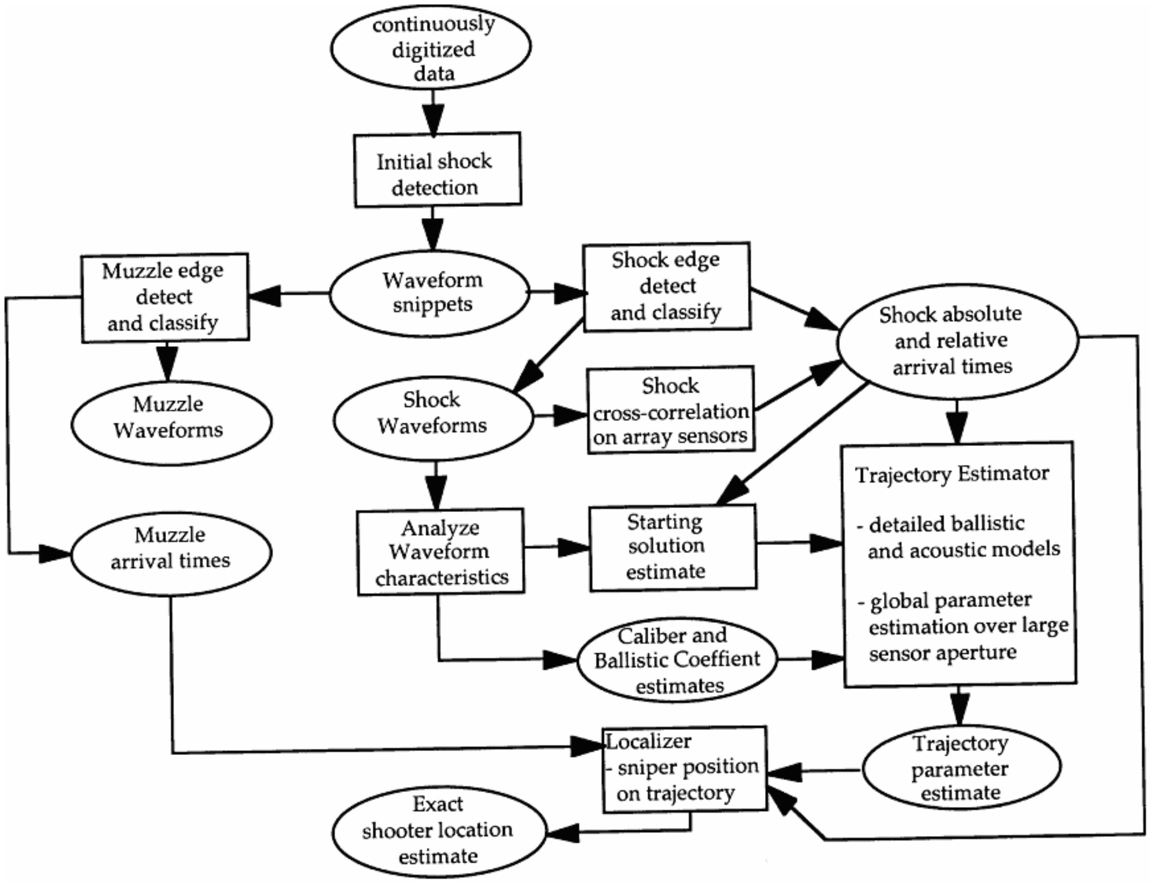

Figure 2.5 Proof-of-Principle System Processing Block Diagram [DGB96]

Figure 2.5 illustrates how the system processes information in a block diagram format. This figure also shows the interdependencies of inputs, shockwave and muzzle blast, to the outputs, location, trajectory, and caliber.

The ACSS was tested at Camp Pendleton's MOUT facility using two tetrahedral arrays and the five systems to be delivered to the government. The results, listed in Table 2.1, demonstrate the effectiveness of this type of system.

Table 2.1 Effectiveness results of the ACSS tests [DGB96]

- 90% of the total shots were detected by the system
- On these the following performance was obtained:

Caliber: 90% had were estimated correctly

Azimuth: 72% had errors less than 1 degree

93% had errors less than 5 degrees

96% had errors less than 10 degrees

Elevation: 38% had errors less than 1 degree

91% had errors less than 5 degrees

Range: 28% had errors less than 1%

60% had errors less than 5%

70% had errors less than 10%

Planning Systems Incorporated (PSI) has fielded two acoustic systems used to detect and locate gunfire: the System for the Effective Control of Urban Environment Security (SECURES) and the Tactical Asset for Gunfire Identification and Targeting – Counter Sniper (TAGIT-CS). Both systems operate by observing the muzzle blast. SECURES is designed to detect and analyze short range, sub-sonic weaponry while the TAGIT-CS is designed for long range, supersonic, high velocity weaponry.

The SECURES system consists of a wide array of microphone sensors positioned around the monitored area. Each sensor is a stand-alone processor that monitors background noise for suspect waveforms. Once an incoming signal is suspect, it's passed to a second processor which compares its shape width and frequency to known gunfire profiles. If the incoming signal passes the second processor, an RF transmitter notifies the base station with a "hit". The base station displays the triggering unit on a map of the monitored area. There's no geolocation involved with in the SECURES system, only detection of suspect sound signals, basic waveform analysis with known gunfire profiles and association of suspect waveforms to a receiver location. Table 2.2 shows the performance accuracy of SECURES as measured in the 2002 Austin TX demonstration.

Table 2.2 SECURES Accuracy in Austin TX Demonstration

Performance with two-dimensional localization using a minimum of four pole units provides:

- 78% probability of detection of 9mm and 380 pistol fire (single shot)
- 33% probability of detection of bottle rockets
- 3% probability of detection of firecrackers

Performance with three-dimensional localization:

- 75% probability of detection of 9mm and 380 pistol fire (single shot)
- 24% probability of detection of bottle rockets
- 3% probability of detection of firecrackers

The TAGIT-CS system consists of 5-15 Sensor Units (SU) distributed in the surveillance area, with each SU being a small, batter-powered unit which transmits gunshot event messages to the Sniper Locator Display Unit (SLDU). The event time-of-arrival differences from several sensors are used by the SLDU software to triangulate the sniper location. Using the PSI multi-path and shock-wave-resistant localization algorithm, the TAGIT-CS system is optimized for the detection of muzzle blasts of high-powered rifles. Local weather is also an input to the SLDU calculations [LCS02].

Similar to the sensor units in the SECURES system, the SUs of the TAGIT-CS system monitor the background noise for suspect waveforms. A second processor is used to compare the signal's shape and frequency to known sniper shot profiles. If a signal passes the second filter, an RF signal is sent to the SLDU for triangulation.

The SLDU, run from a laptop computer, receives "hits" from the SUs which are time-stamped. It then uses the proprietary PSI algorithm to triangulate the sniper's location in two-dimensions. The exact location of each SU, measured using GPS receivers during placement, is critical in the triangulation algorithm. The algorithm also employs special data redundancy techniques to reduce multi-path solutions caused by echoing. It also discriminates against the acoustic shock wave of supersonic bullets. At least five triggering sensors are required for an accurate location solution in 2-D.

A third sniper detection & location system has been fielded by Lockheed Martin IR Imaging Systems, called the Integrated Sniper Location System (I-SLS). This system combines an Acoustic Warning System (AWS) with an uncooled Infrared Warning System (IRWS).

The AWS detects both the muzzle blast, for unsilenced sniper fire, and the bullet's acoustic shockwave, if supersonic, and provides a course location of the shooter [FiS99].

Summary

Geolocation using time-of-arrival is a proven method. It provides an accurate location given an accurate arrival time and a constant speed of the signal. Several sniper detection systems are currently being developed or fielded, though none rely solely on TOA calculations to locate. In this chapter, the fundamentals of GPS location were presented. The principles of sound wave propagation were also discussed as well as defining the basic waveform analysis needed to process the incoming audio signals. And finally, several sniper detection and location systems currently in development or production were reviewed.

III. Methodology

Chapter Overview

In this chapter, overall experiment design is discussed in detail. Each factor affecting the experiment is explained as well as the assumptions made in formulating the experiment. The experimental boundaries are defined as well as expected outcomes.

Problem Definition

The techniques used to calculate an unknown location using GPS can be adapted to locate an audio source using sound waves instead of radio waves. One such application is locating a sniper using the audio signature of a rifle shot. This research will explore the feasibility of such a system and its expected accuracy in geolocation.

Goals and Hypothesis

Before a sniper detection system can be realized, an algorithm must be developed to compute the location of a sound source. This algorithm uses the location of each audio receiver station and the relative arrival time of the suspect audio signal. The hypothesis of this research is that the algorithm will produce similar accuracy as GPS, even though the distances are much shorter and the speed of sound is much slower than the speed of light. The goal is to calculate the location of the audio event and the confidence level of that location.

Approach

The approach to solving the problem uses TOA calculations and an audio signature. The algorithm used in the geolocation is derived from the GPS TOA calculation formulas. The speed of sound is substituted for the speed of light. Unlike the radio waves used in GPS, the speed of sound is affected by temperature and humidity and must be taken into account. Furthermore, the acoustic signature of a discharged firearm must be modeled so the processing software can identify an audio event from noise.

Temperature and humidity are assumed to be constant over the entire region of interest and therefore the speed of sound will be constant. In addition, this experiment focuses on the geolocation algorithm and assumes that the waveform analysis has been accomplished.

System Boundaries

Figure 3.1 graphically illustrates the breakout of the system under test (SUT) and component under test (CUT). The SUT is the sniper detection system. This includes the audio receivers, data transfer capability, and data processing computer. Each receiver contains a microphone, a sound card, a signal analyzer, and a clock which is synchronized with the algorithm processing system's clock. The microphone and sound card translate the audio signal into a digital waveform. The signal analyzer determines when a suspect waveform (gunfire or mortar fire) is received. The synchronized clock is needed to ensure the relative accuracy of each incoming audio signal. The data transfer capability is wired or wireless computer network between the receivers and the processing system.

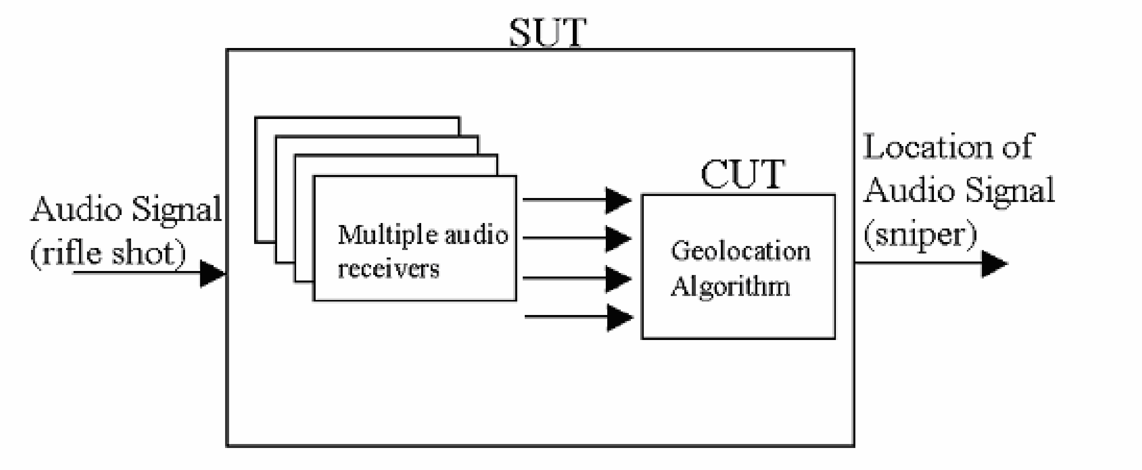

Figure 3.1 A graphical representation of the SUT and CUT

The CUT is the geolocation algorithm. The algorithm uses the location of each receiving station in three-dimensional space, and the relative arrival time of each suspect audio signal. It uses this to calculate the location of the audio source using TOA formulas derived from GPS.

System Services

The primary service provided by the system is the location of the suspect audio source, in this case a sniper. This location is calculated with respect to the receiver stations. A secondary service provided by the system is the confidence level associated with the location.

The possible outcomes of the service are:

- The data is not accepted by the system
- The data is accepted but the geolocation algorithm fails to produce a result

- The data is accepted but the algorithm produces a result outside desired error limits
- The data is accepted and the algorithm produces a result within desired error limits

This research doesn't consider the first outcome.

Performance Metrics

The performance of the system is measured by the magnitude of the error in the location produced by the geolocation algorithm. The error is calculated as the Euclidean distance from the estimated location and the actual location of the audio source.

System Parameters

The resolution of the audio input signals affects the amount of work required by the execution engine to decode and time-stamp each input signal. The sampling rate of the input signal has a direct impact on the accuracy and granularity of the time-stamp associated with the suspect audio signal. This will prove to be crucial to the confidence level of the geolocation answer.

Similarly, the accuracy and resolution of the clocks have a large impact on both the location and the confidence level. The relative arrival time of the audio signal at each receiver is used to calculate the travel time between audio source and receiver. This travel time is only one of four variables used in the geolocation algorithm.

The topology of the receivers in relation to the audio event source is also a decisive element in the geolocation algorithm. A wide dispersion of receivers in relation to the audio source helps to mitigate the errors associated with difference between a receiver computer's clock and the algorithm processing computer's clock. Widely dispersed receivers also produce higher angles of incidence in the intersection of the spheres produced by the trilateration. Tightly clustered receivers produce lower angles of incidence and yield a lower accuracy in location estimates.

The number of receivers is a final parameter in the workload submitted to the SUT. The geolocating algorithm has four unknowns: the X,Y,Z coordinates and the event time of the source. Four or more receivers are needed to accurately calculate the location of the event source. Fewer receivers or input signals require an estimation calculation and affect the confidence level significantly.

Reflection, or echo, adds error to the geolocation as well. The location can be improved greatly by adding more than four receivers to the system and sampling all possible 4-tuples.

Workload Parameters

The workload is the audio event generated by a rifle shot which is presumed to be fed directly into the system. The clock accuracy, clock resolution and sampling accuracy is combined into one figure, namely that the event arrival time at each receiver is within +/- 3ms of the arrival time as seen by the algorithm processing computer's clock.

Table 3.1 System Parameters

System Parameters	Workload Parameters
Resolution of the input signal	Audio event fed directly into system
Sampling rate of the input signal	
Accuracy and Resolution of system clocks	
Topology of the receivers in relation to source	
Number of receivers in the system	
Amount of echo/multipath in system	

Factors

The factors chosen are the receiver topology and percentage of receivers experiencing echo. There are five different topologies explored. Each topology is tested at six levels of echo. The amount of echo is randomly generated between 0% to 100%.

The five topologies of the receivers are:

1. 1000m x 1000m x 50m area with source inside, 25 receivers
2. 5000m x 5000m x 50m area with source inside, 25 receivers
3. 150m x 150m x 50m area with source outside, 9 receivers
4. 150m x 150m x 60m area with source outside, 27 receivers
5. 150m x 150m x 60m area with source inside, 27 receivers

In each of the first three topologies the X/Y components are divided equally into grids such that one receiver is randomly placed in each grid. Topologies one and two produce a five by five grid. Topology three is divided into a three by three grid. In the last two topologies, each area is divided into 50x50x20 cubes with one receiver placed within each. These topologies model a building of dimensions 150m x 150m x 60m. The topologies are graphed in Figures 3.2 – 3.6.

Table 3.2 Factors

Factors	Levels
Topology	1000m x 1000m x 50m, source inside, 25 sensors
	5000m x 5000m x 50m, source inside, 25 sensors
	150m x 150m x 50m, source outside, 9 sensors
	150m x 150m x 60m, source outside, 27 sensors
	150m x 150m x 60m, source inside, 27 sensors
% of receivers experiencing echo	0%, no receivers experiencing echo
	20% of receivers experiencing echo
	40% of receivers experiencing echo
	60% of receivers experiencing echo
	80% of receivers experiencing echo
	100% of receivers experiencing echo

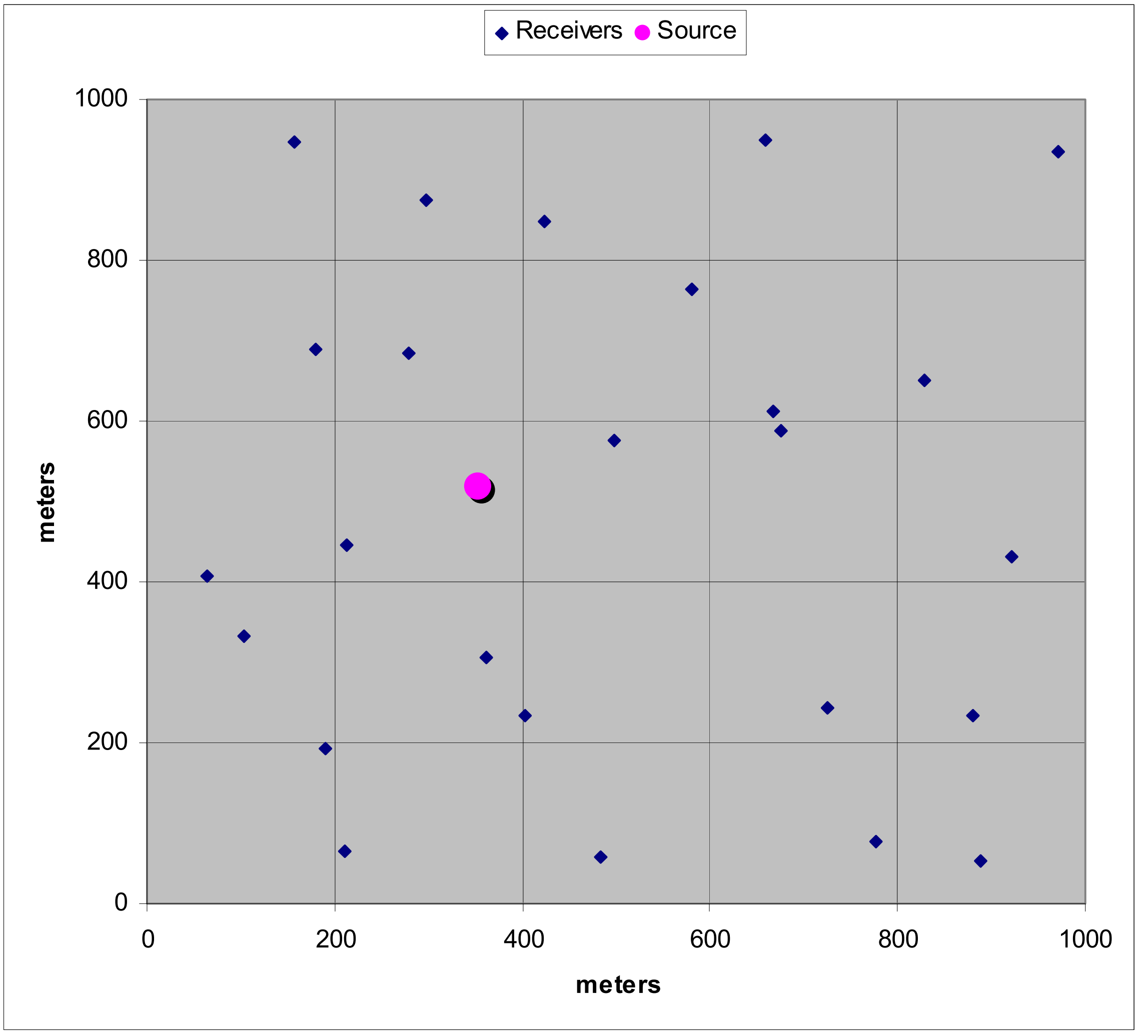

Figure 3.2 X/Y Plane representation of Topology #1: 1000m x 1000m x 50m

Topology #1 models an outdoor scenario of a 1000 meters by 1000 meters area which is relatively flat. The detection area is divided into 25 subregions as shown in figure 3.2. For each replication of the experiment, receivers are randomly placed within the subregions which are 200 meters by 200 meters by 50 meters. The audio source is randomly placed within the entire 1000m x 1000m x 50m region.

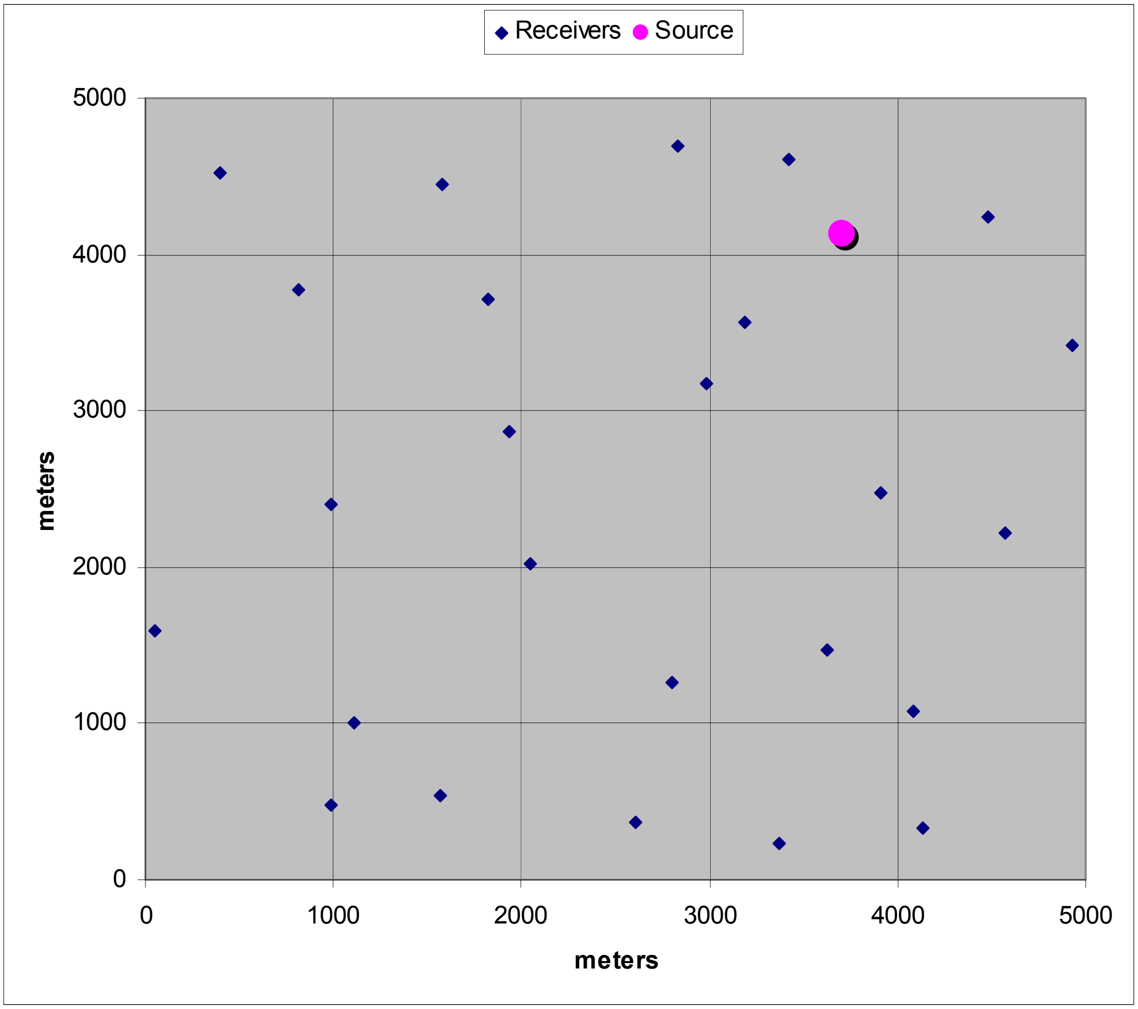

Figure 3.3 X/Y Plane representation of Topology #2: 5000m x 5000m x 50m

Topology #2 is also an outdoor scenario, though in a larger area. This scenario is 5000 meters square and 50 meters high. The detection area is again divided into 25 subregions (Figure 3.3). For each replication, receivers are allowed to be placed anywhere within a 1000m x 1000m x 50m subregion with an audio source located anywhere within the entire 5000m x 5000m x 50m region.

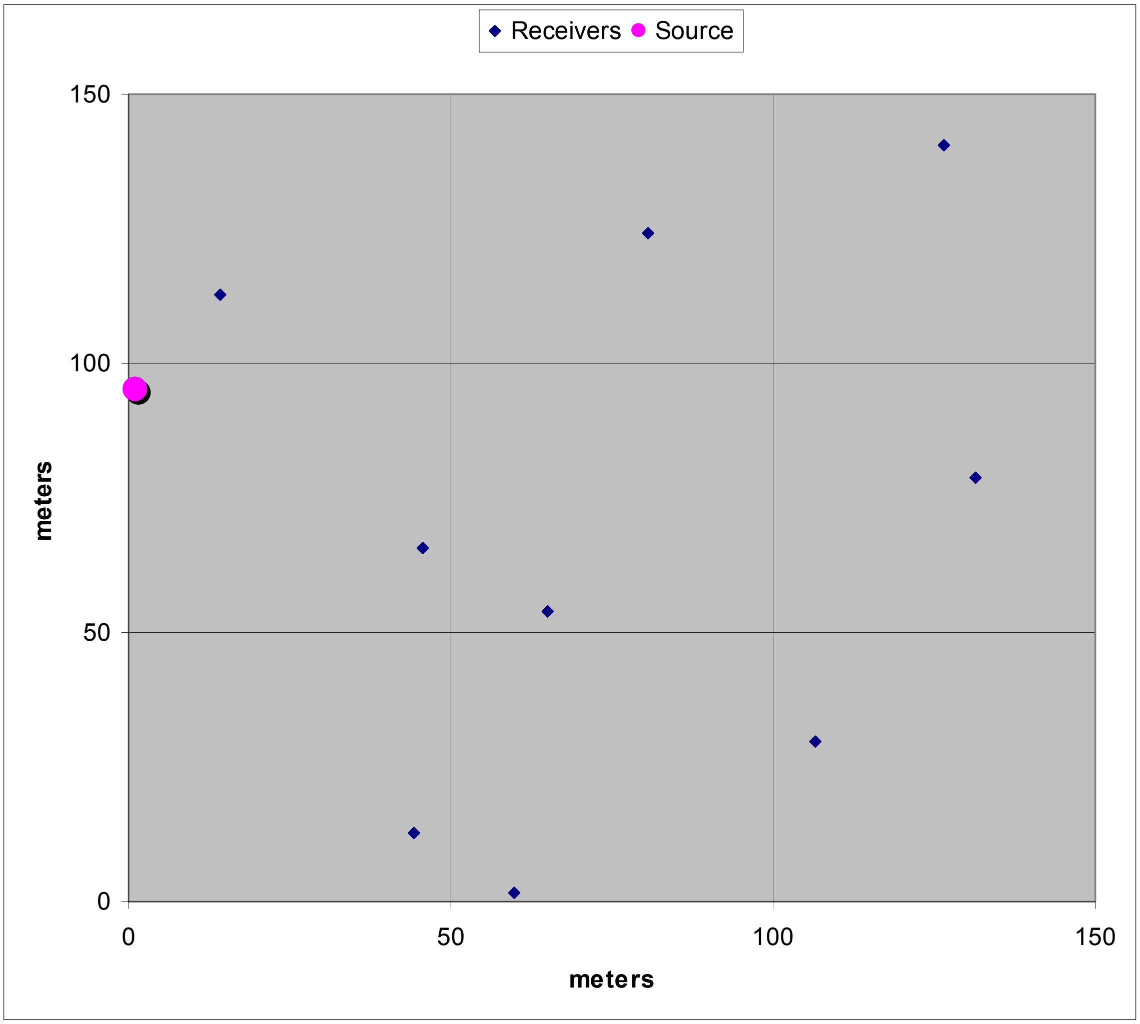

Figure 3.4 X/Y Plane representation of Topology #3: 150m x 150m x 20m

Topology #3 models an urban scenario, where a sniper is firing from a building window into an open area. This scenario's detection zone is 150 meters square in the horizontal and 20 meters high. The detection area is divided into 9 subregions (Figure 3.4). For each replication, the receivers are allowed to be placed anywhere within the

50m x 50m x 20m subregion. To simulate firing from a building window, the audio source is placed along the left side of the region, (1m x 60m x 50m).

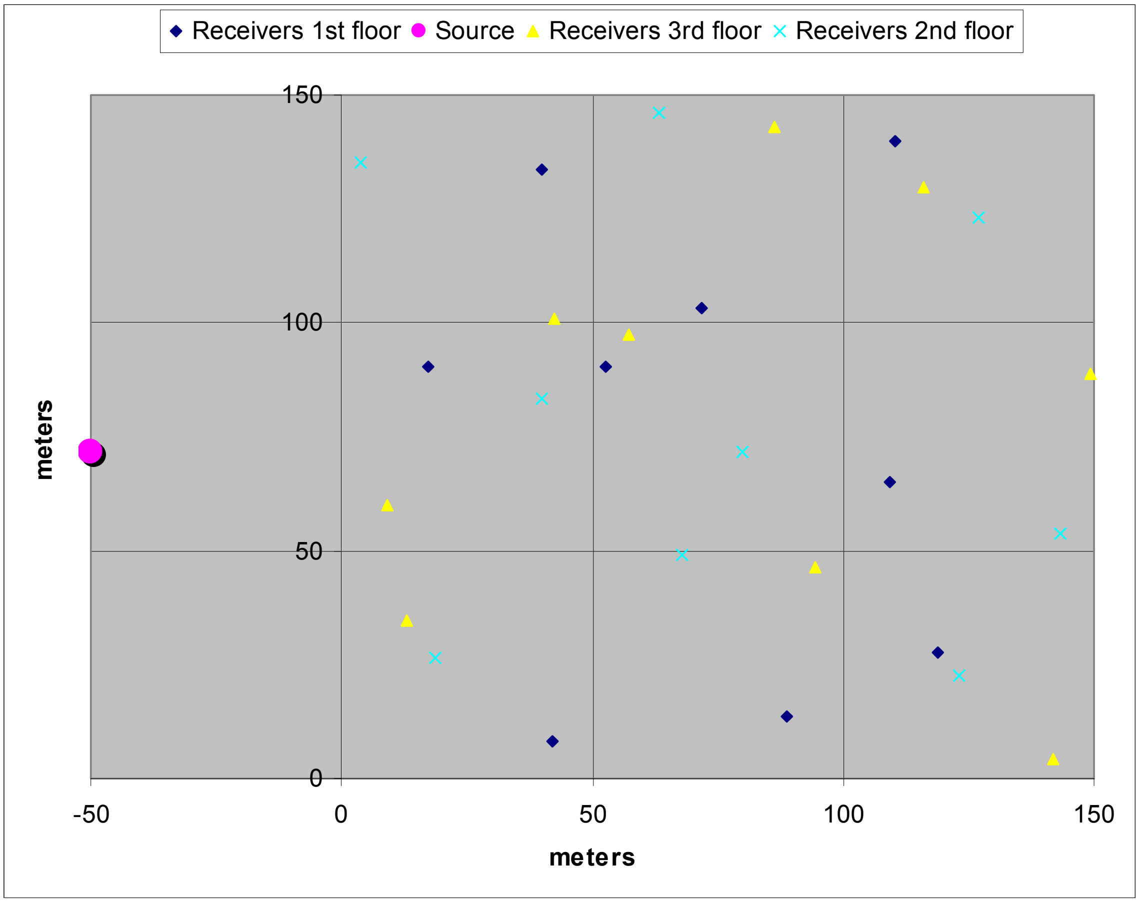

Figure 3.5 X/Y Plane representation of Topology #4: 150m x 150m x 50m

Topology #4 is another urban scenario. It assumes a sniper is firing from a building window into another building. It is unclear in which direction the threat is based so the entire building is monitored, which in this case is 150 meters square in the horizontal and 60 meters high. The detection area is divided into 27 subregions (Figure 3.5), 3 regions by 3 regions by 3 regions. For each replication, the receivers are allowed to be placed anywhere within the subregion (50m x 50m x 20m). To simulate an external building, the audio source is placed along the left side of the region, (1m x 60m x 50m).

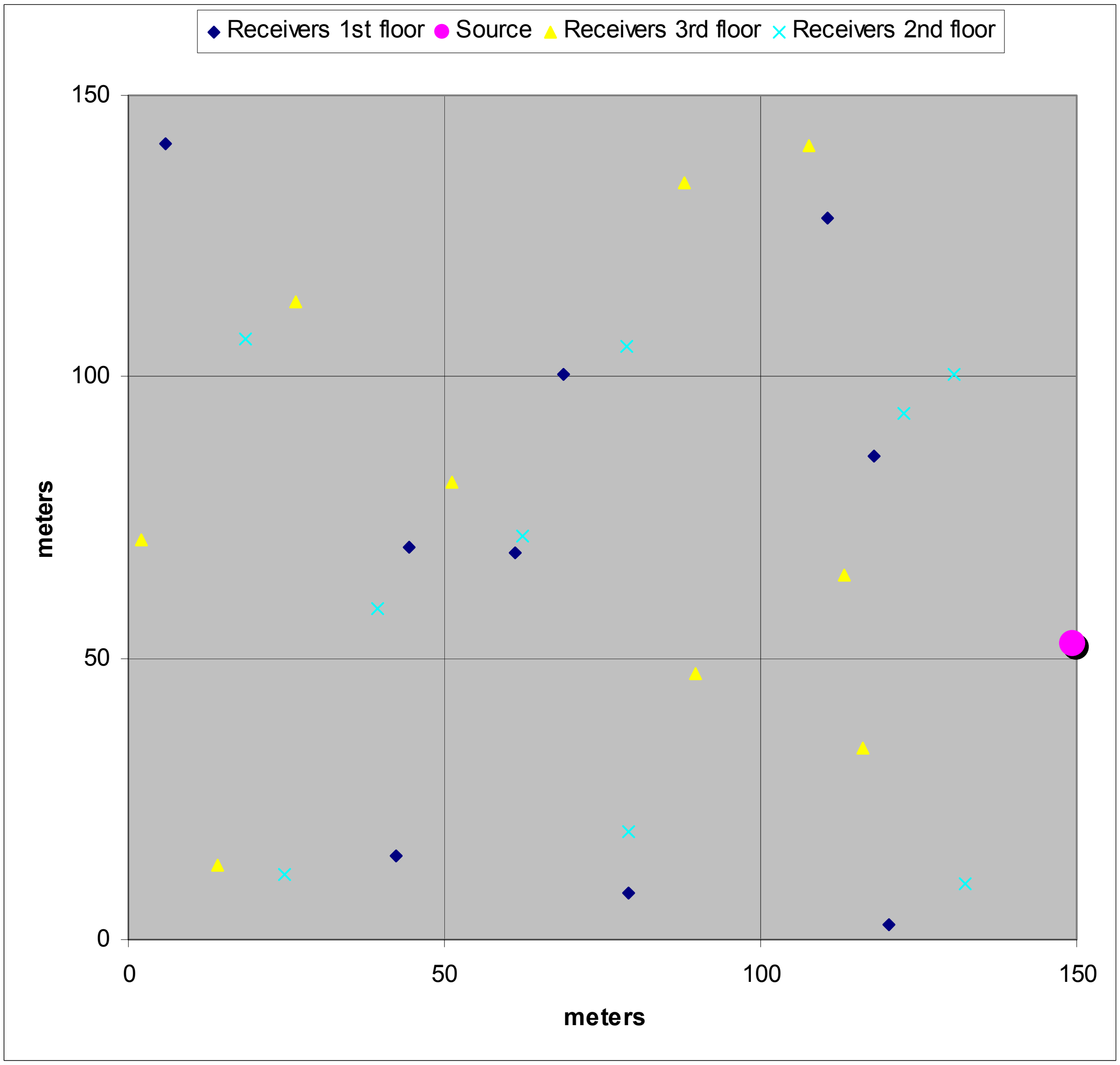

Figure 3.6 X/Y Plane representation of Topology #5: 150m x 150m x 50m

The final topology, topology #5, is a variation of scenario #4, with the audio source internal to the monitored building versus external. The building is again 150 meters square in the horizontal and 20 meters high. The detection area is divided into 9 subregions (Figure 3.6). For each replication, the receivers are allowed to be placed anywhere within the subregion (50m x 50m x 20m). The audio source is placed anywhere within the building, (150m x 150m x 50m).

Evaluation Technique

The evaluation technique used during this experiment is simulation. This technique was chosen due to the nature of the research. The goal is to create a geolocating algorithm and to measure its performance. The results of the experiment are compared to the GPS TOA model.

Workload

The workload submitted to the system is a series of audio events which simulate the output of the system's receivers. The relative arrival times and receivers location is used by the geolocation algorithm to generate an event location and event time.

Experimental Design

The experimental design is a full factorial experiment. The two factors to be explored are topologies and percentage of receivers experiencing echo. The topologies are broken up into five scenarios. The six levels of echo are 0%, 20%, 40%, 60%, 80%, and 100% of the receivers experiencing echo. The amount of echo each receiver experiences is randomly generated between 0% and 100%.

Within each replication, receivers are randomly placed. For each receiver, a random number is generated between zero and one. If this number is below the echo rate, a second random number is generated, again between one and two. This is the amount of echo that receiver is experiencing. Therefore, receivers experiencing will measure travel times that are no more than twice the direct path travel time.

Analyze and Interpret results

Analysis of Variation (ANOVA) and Confidence Intervals (CI) are used to quantify the impact of each of the factors on the location error metric. These techniques use the various sums of squares from the data to calculate the relative variation between the factors and to quantify the impact each factor plays on the measured metrics.

Summary

In this chapter, five distinct topologies were chosen to simulate different sniper detection scenarios. Each topology was simulated at six levels of echo, from 0% to 100% of the receivers experiencing multipath. And each topology/echo rate combination was replicated 35 times.

IV. Analysis and Results

Chapter Overview

In this chapter, the results of the experiments are discussed in detail. Analysis for each of the different topologies is explored as well as a composite analysis of the overall system.

Sample of experiment output

The raw output for each the 1050 individual experiment replications consists of collection of X/Y/Z coordinates for the source and an event time. For every possible 4-tuple chosen from the set of receivers, the algorithm attempts to geolocate the source. The topology of those four receivers or the amount of echo present in the signal may cause the algorithm to fail. If the algorithm produces a valid location, it is added to a candidate location list. An average location is generated from this population. A second list is generated which consists of every candidate location within 100 meters of the population average. This list is also averaged. A third candidate list is generated from the mode of the resulting population rounded to the nearest meter. The location error is the Euclidean distance from the population average, the 100 meter cluster average and the population mode. A fourth location error is calculated for the population mode in the X/Y planes only.

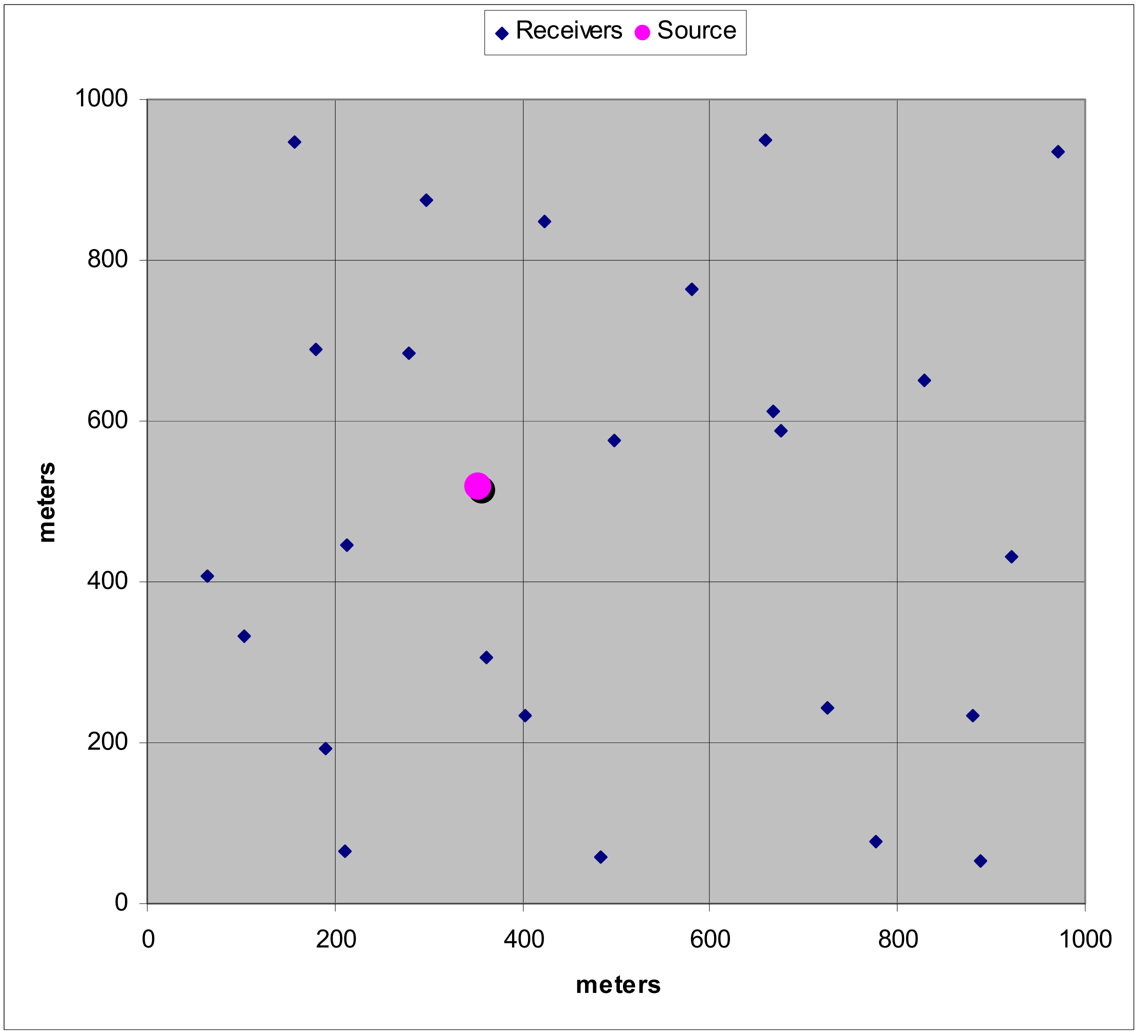

Figure 4.1 Sample input: 25 receivers and 1 source shown in X/Y plane

Figure 4.1 shows a sample topology and the relative locations of all receivers to the source (in two dimensions). Each of the grid squares represents a subregion. Each subregion contains a randomly placed receiver.

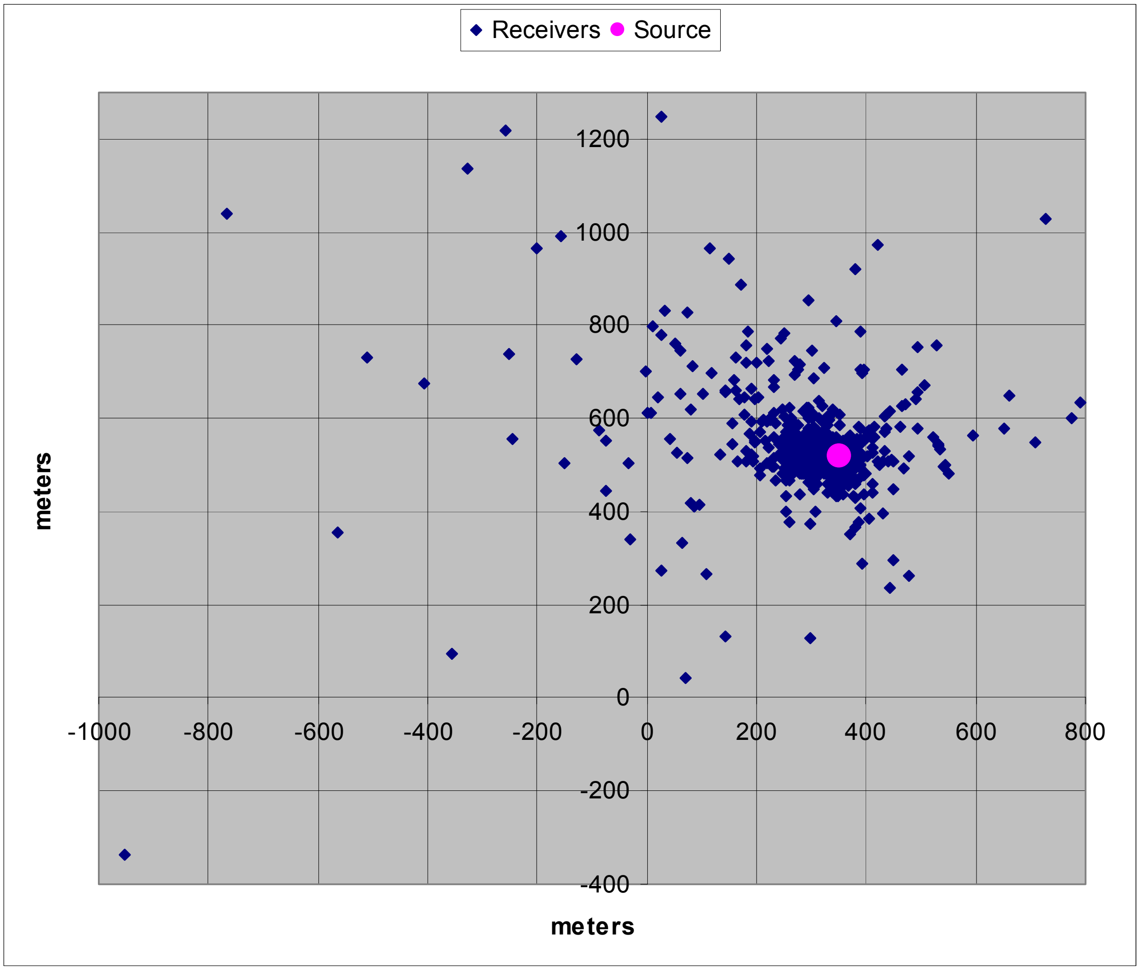

Figure 4.2 Sample output: all valid locations generated by 4-tuples

The output generated by the geolocation algorithm is a series of locations. This series is all the valid locations produced by every 4-tuple combination of the receivers. Some 4-tuples do not generate a valid location answer due to too much echo in the input signals or a bad receiver distribution (i.e., too close together). A few of the locations contain large errors but most are grouped around the actual source location.

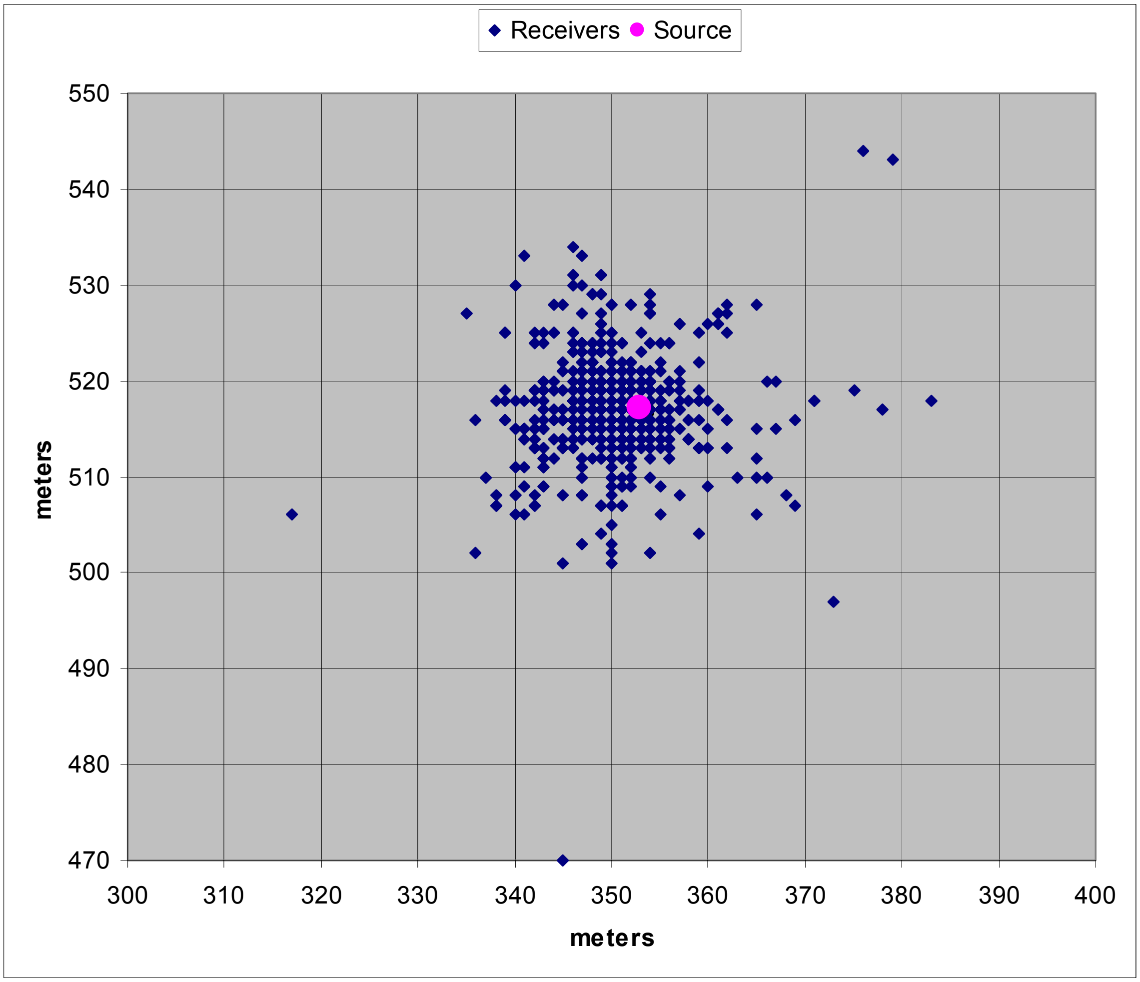

Figure 4.3 Sample output: Valid locations within 100m of population average

Figure 4.3 shows all of the valid locations produced by the geolocating algorithm which lie within 100 meters of the population average. The 100 meter cluster result provides a better location answer than the population average after removing the outliers. Although not performed in this research, an iterative calculation of averaging and removing outliers may produce a better location solution.

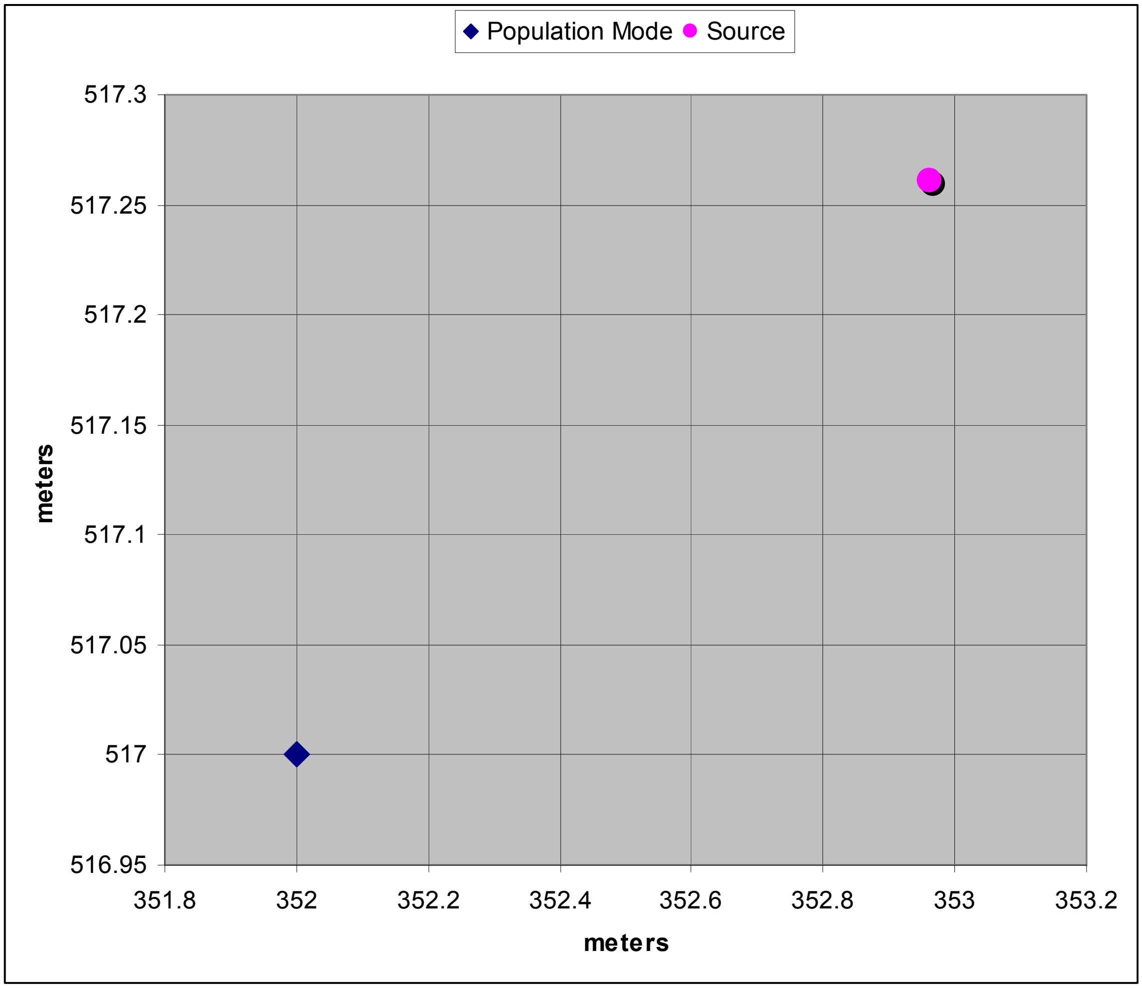

Figure 4.4 Sample output: Mode of valid locations population

Figure 4.4 shows the mode of all valid locations returned from all 4-tuple combinations, rounded to the nearest meter. This answer is typically very near the actual source, at least in the X/Y plane.

Individual topology output

Each of the five topologies was examined at six different echo rates: 0%, 20%, 40%, 60%, 80%, and 100%. The output was examined for the population of all valid locations produced from all possible 4-tuples, all valid locations that fall within 100 meters of the population average, the mode of the population locations rounded to the nearest meter, and the X/Y distance error of the population mode. Each of the following figures shows the average of the 35 replications for each echo level.

Topology #1: 1000m x 1000m x 50m, 25 receivers

The first topology models an outdoor scenario with a monitoring area of 1000 meters square by 50 meters vertical. This area is divided into 25 subregions of 200m by 200m by 50m. The source or shooter can be located anywhere within the monitoring area. Figures 4.4 – 4.6 illustrate the average location error between the output location and the actual source location. Figure 4.7 shows the horizontal location error only.

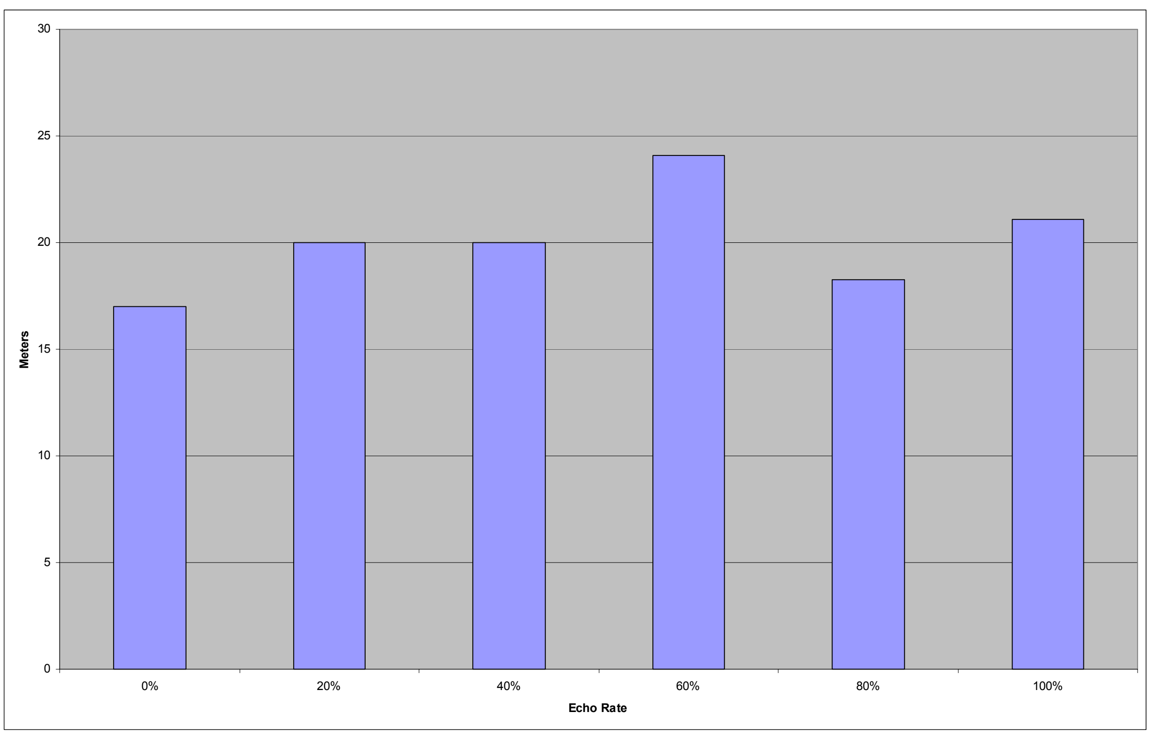

Figure 4.4 Population Average Errors for Topology 1

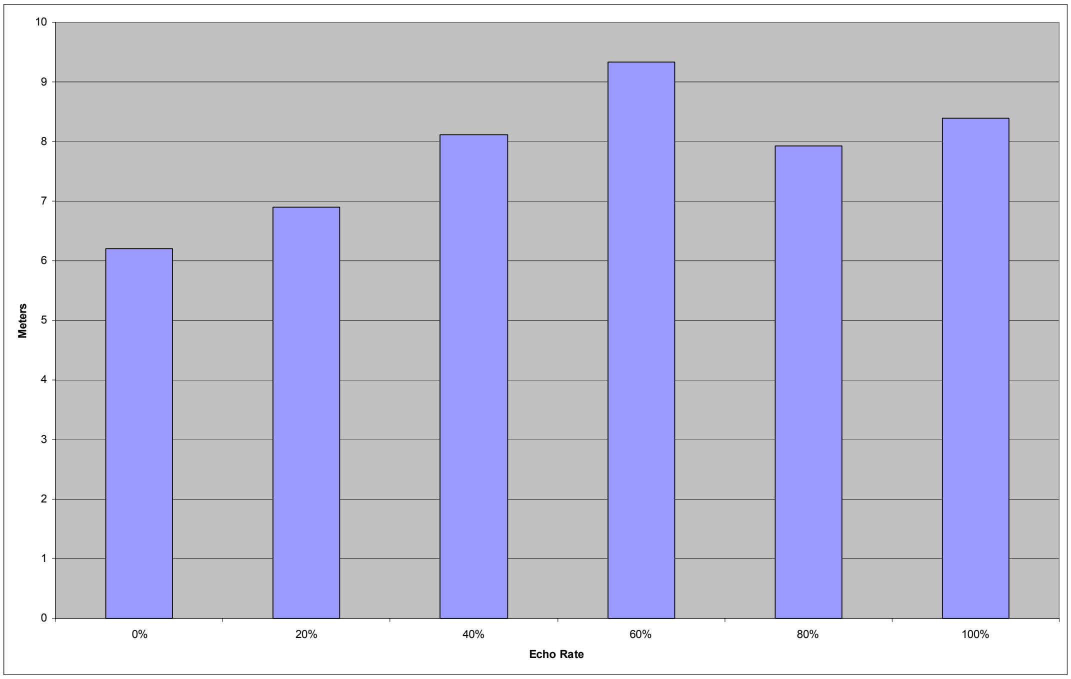

Figure 4.5 100m Cluster Average Errors for Topology 1

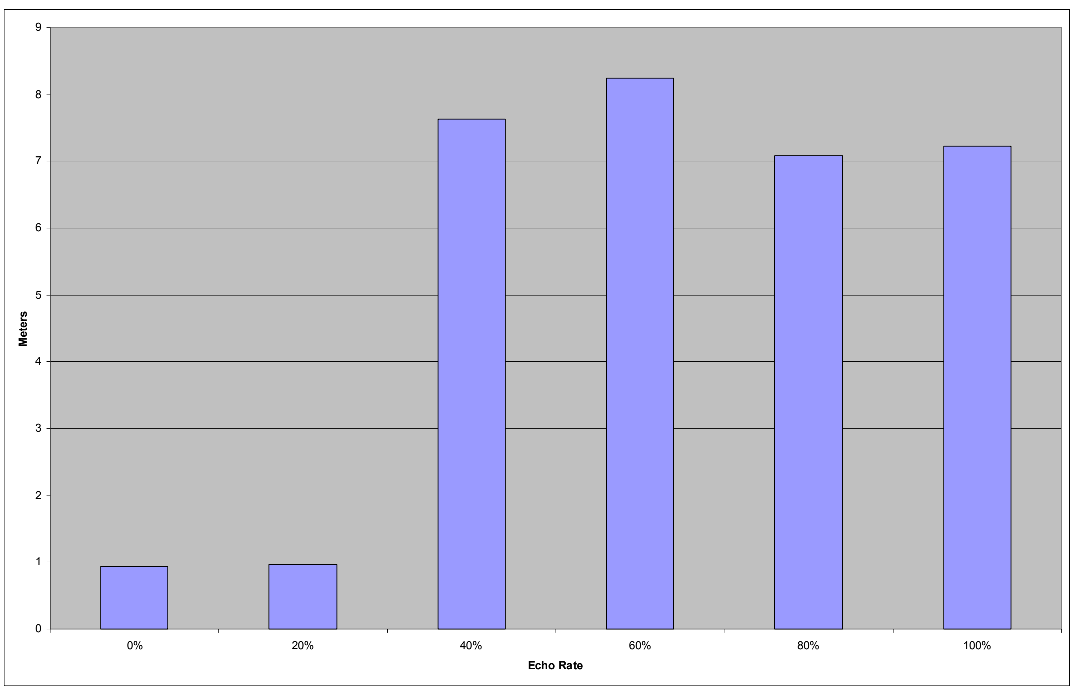

Figure 4.6 Population Mode Errors for Topology 1

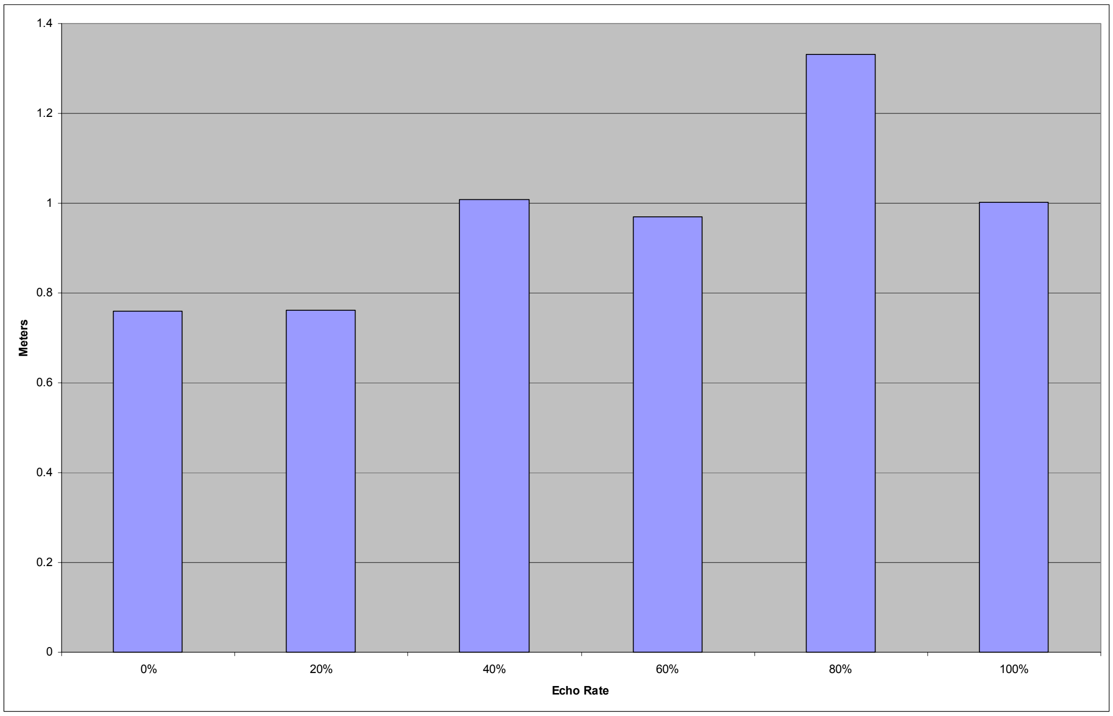

Figure 4.7 Population Mode X/Y Errors for Topology 1

Topology #2: 5000m x 5000m x 50m, 25 receivers

The second topology also represents an outdoor scenario although on a larger scale; the monitoring area is 5000 meters square by 50 meters vertical. This area is also divided into 25 subregions, each of size 1000m by 1000m by 50m. The shooter can be located anywhere within the monitoring area. Figures 4.8 – 4.10 illustrate the average error between the output location and the actual source location. Figure 4.11 shows the horizontal location error only.

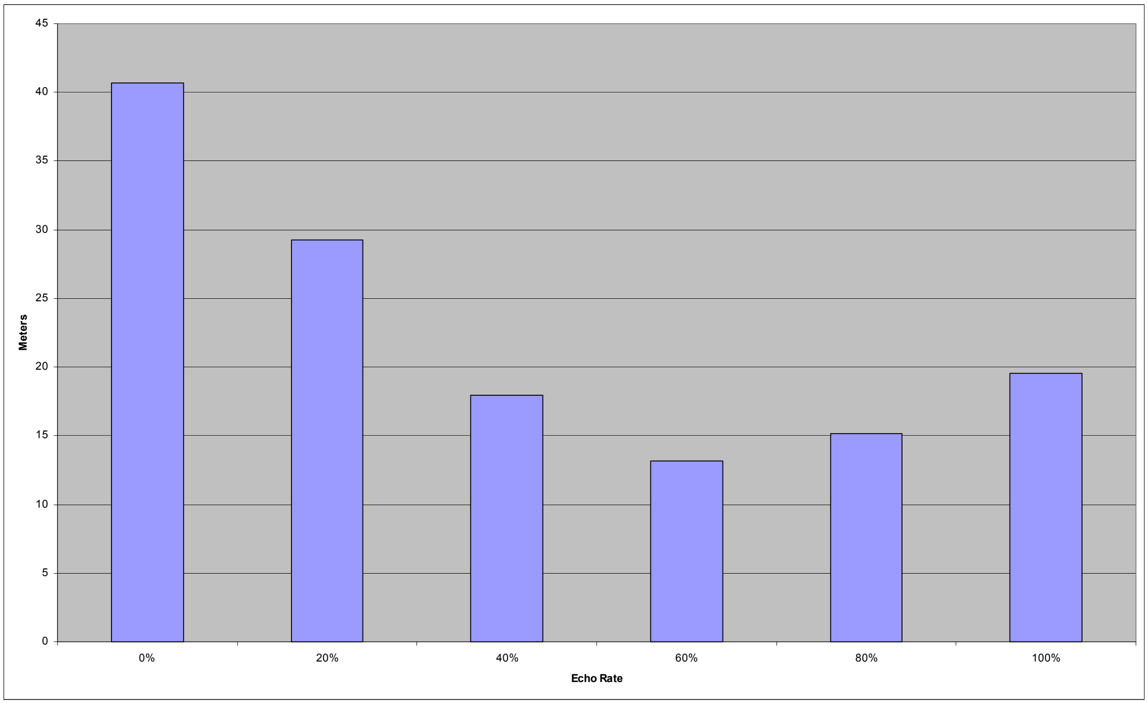

Figure 4.8 Population Average Errors for Topology 2

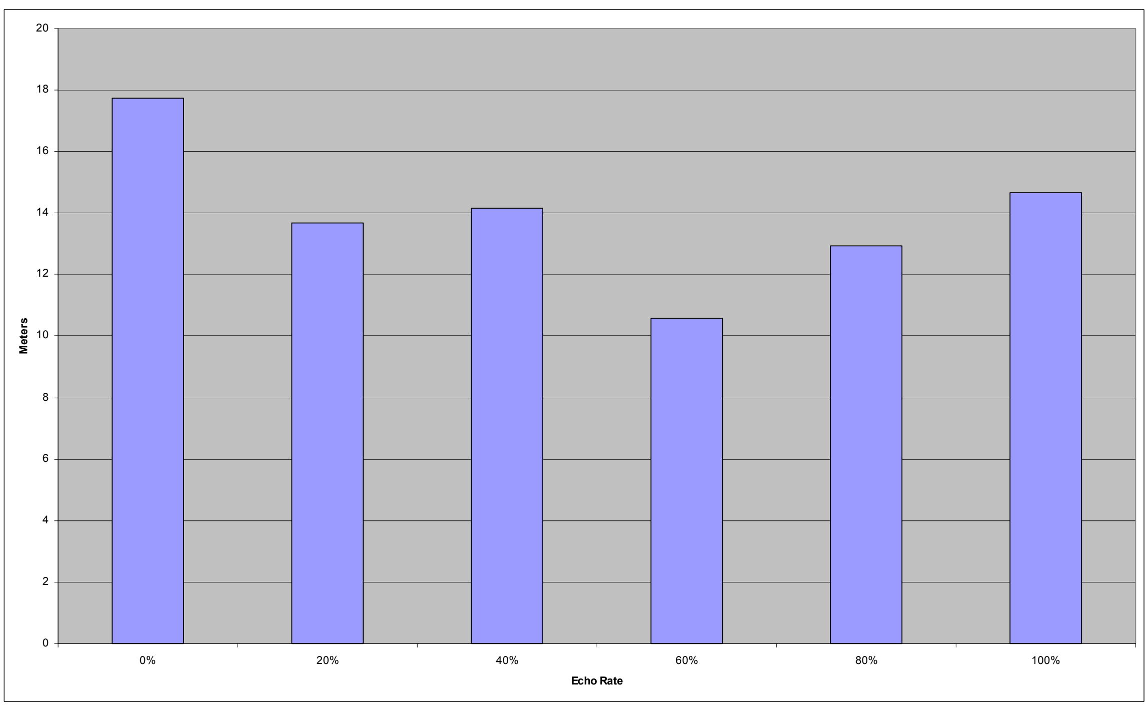

Figure 4.9 100M Cluster Average Errors for Topology 2

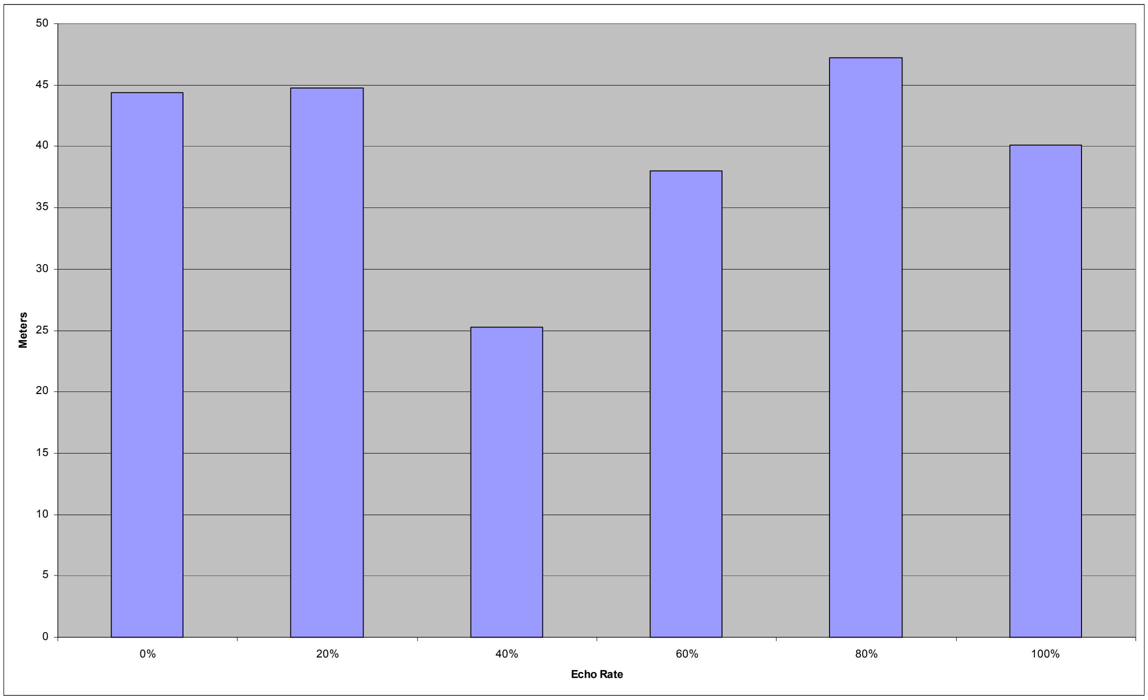

Figure 4.10 Population Mode Errors for Topology 2

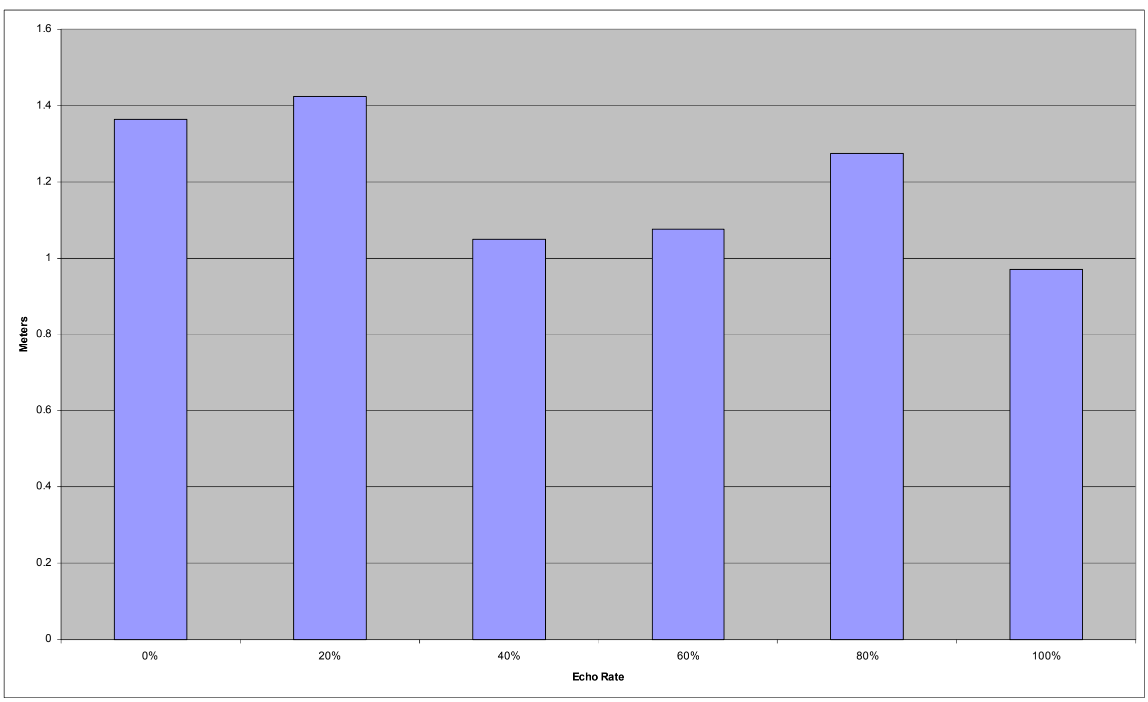

Figure 4.11 Population Mode X/Y Errors for Topology 2

Topology #3: 150m x 150m x 50m, 9 receivers

The third topology is an outdoor urban scenario with the monitoring area being 150 meters square by 50 meters vertical. This area is divided into 9 subregions, each of size 50m by 50m by 50m. The shooter can be located to one side of the monitoring area, simulating a sniper firing from a high-story building window. Figures 4.12 – 4.14 illustrate the average location error between the output location and the actual source location. Figure 4.15 shows the horizontal location error only.

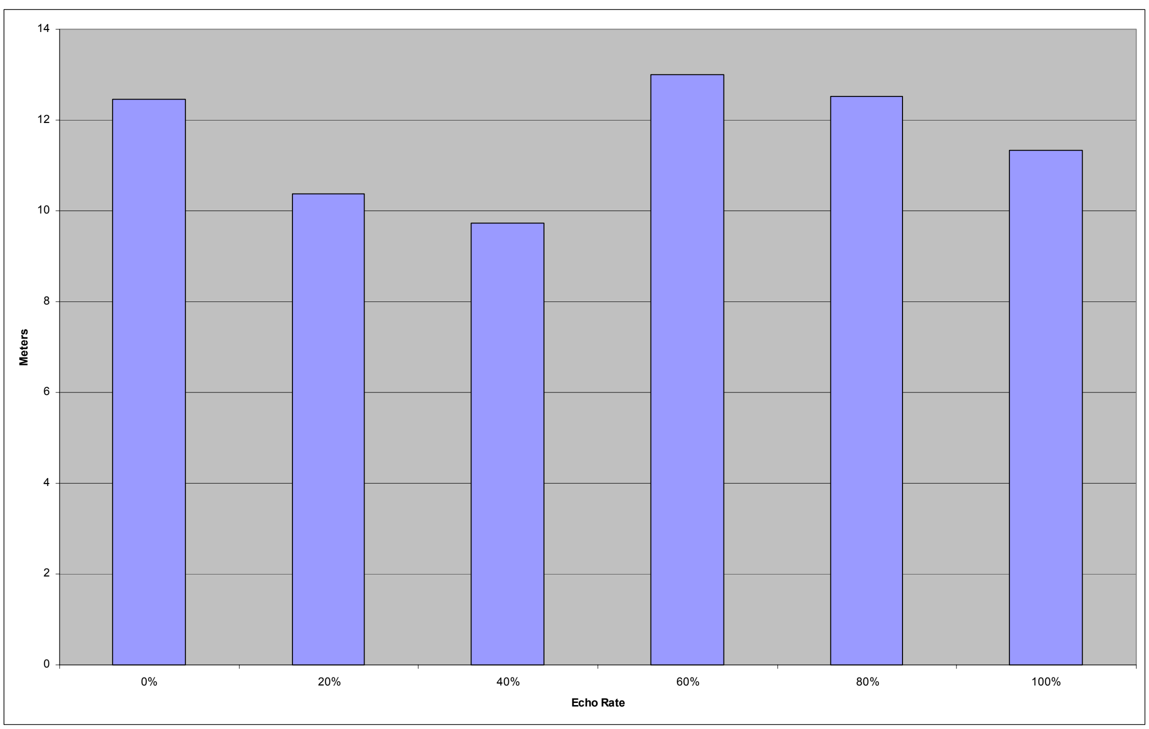

Figure 4.12 Population Average Errors for Topology 3

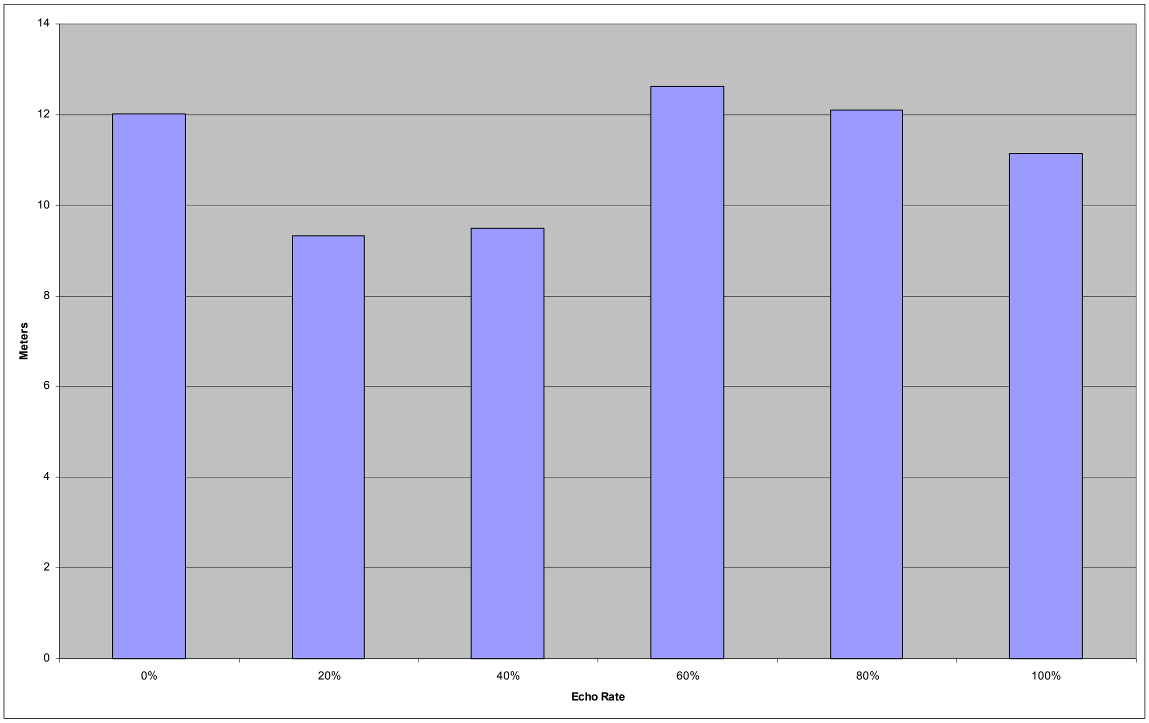

Figure 4.13 100M Cluster Average Errors for Topology 3

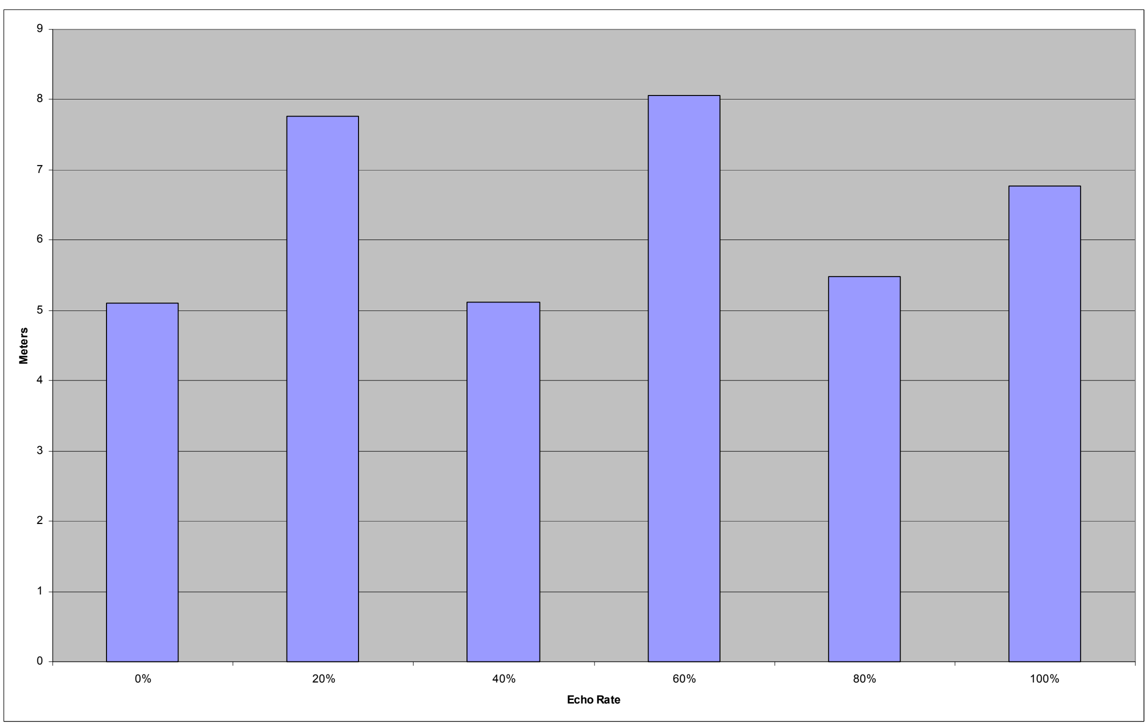

Figure 4.14 Population Mode Errors for Topology 3

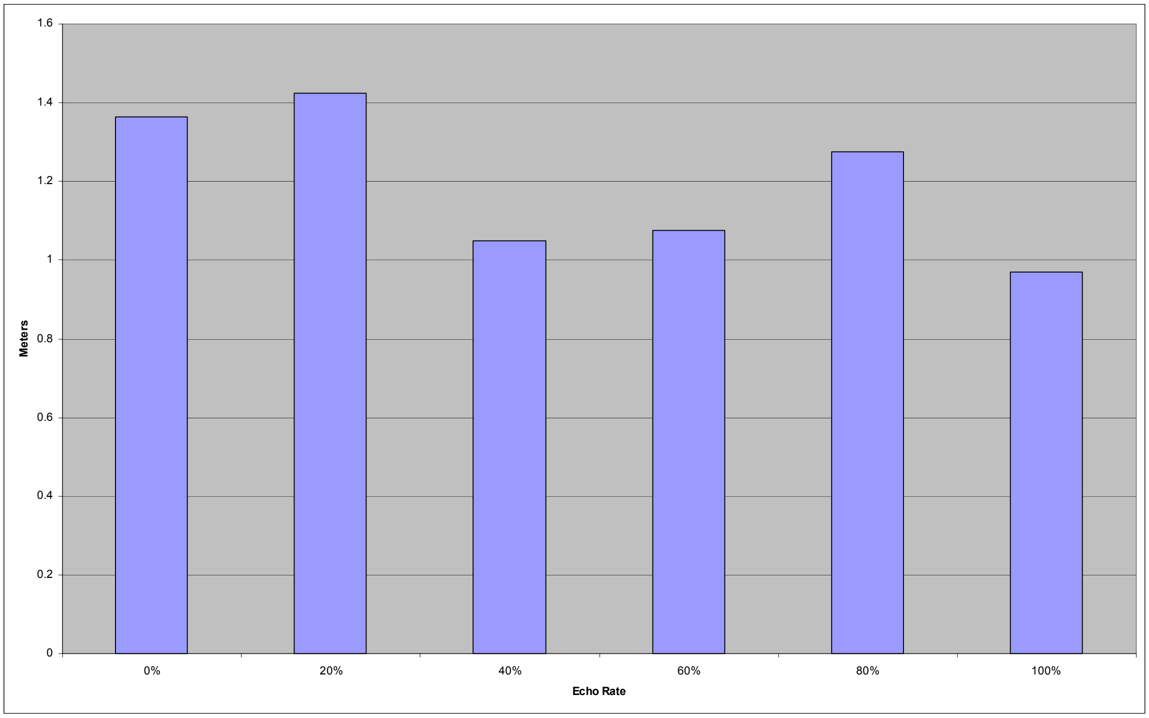

Figure 4.15 Population Mode X/Y Errors for Topology 3

Topology #4: 150m x 150m x 60m, 27 receivers

The fourth topology is an indoor urban scenario with dimensions 150m by 150m by 60m to simulate a building. This area is divided into 27 subregions stacked three deep in each dimension: each of size 50m by 50m by 20m. This shooter can be located to one side of the monitoring area, simulating a sniper firing from second high-story building window. Figures 4.16 – 4.18 illustrate the average error between the output location and the actual source location. Figure 4.19 shows the horizontal location error only.

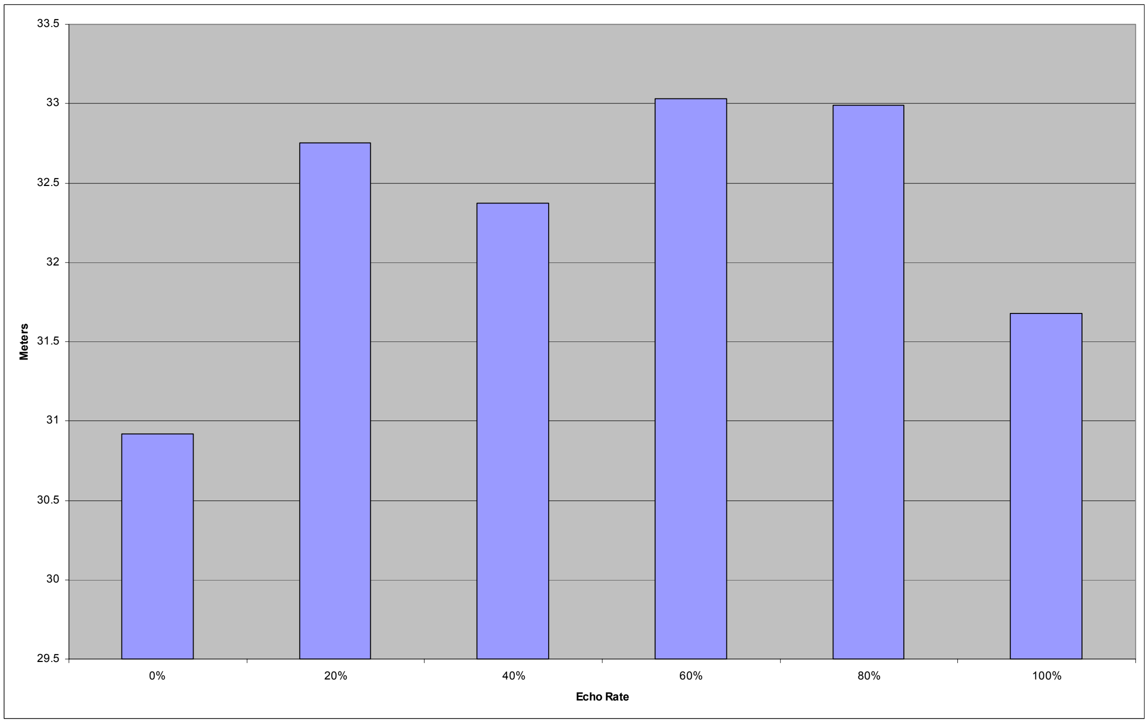

Figure 4.16 Population Average Errors for Topology 4

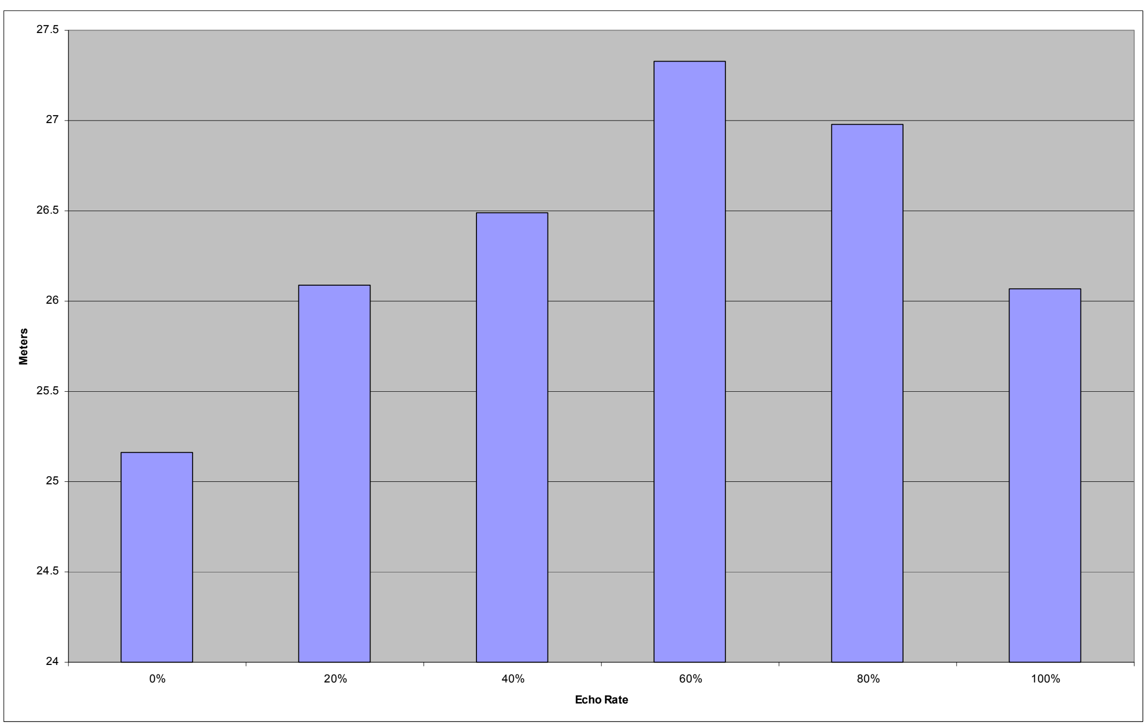

Figure 4.17 Population Average Errors for Topology 4

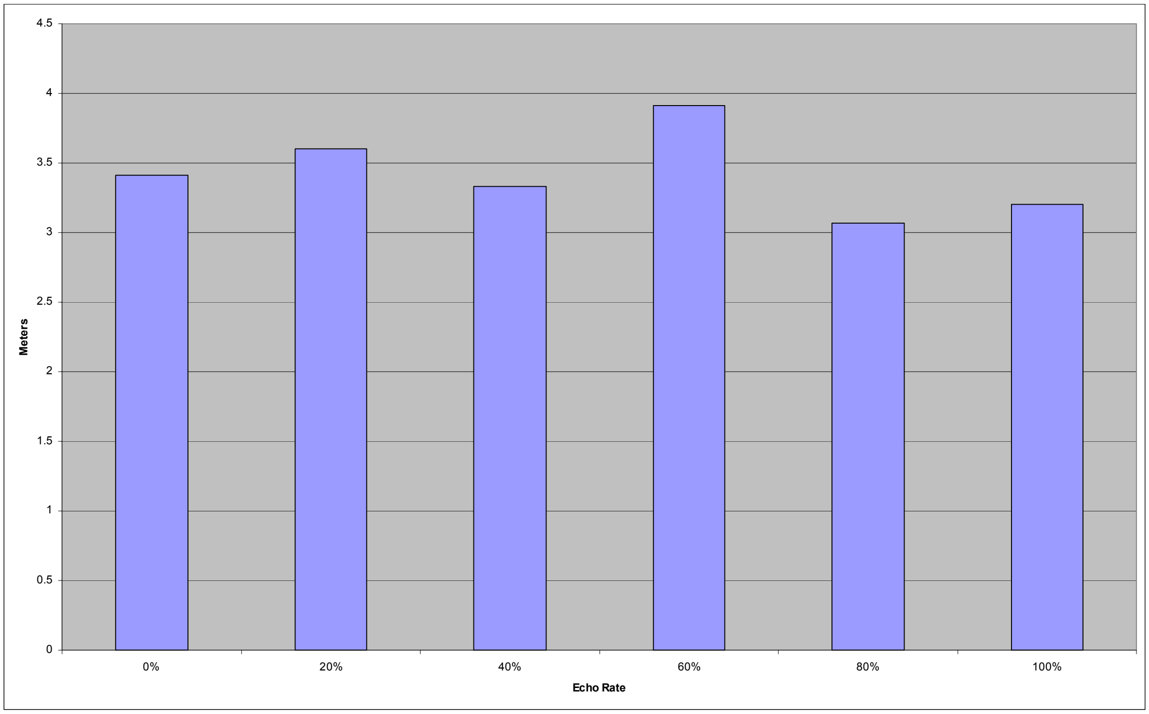

Figure 4.18 Population Mode Errors for Topology 4

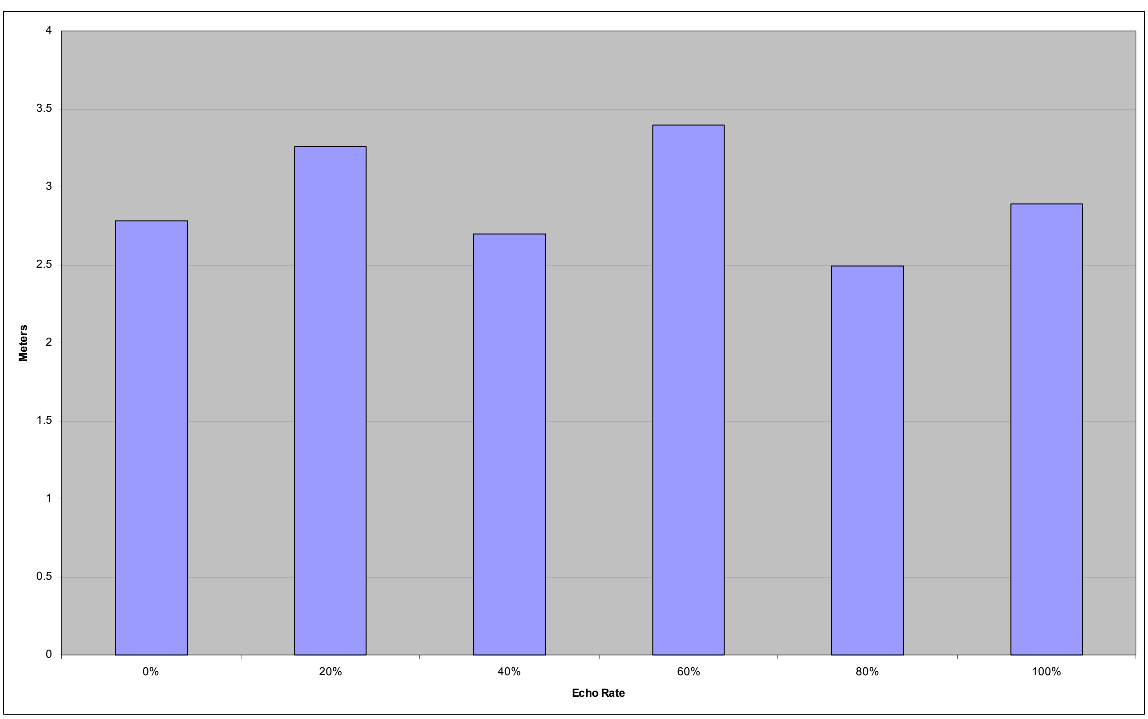

Figure 4.19 Population Mode X/Y Errors for Topology 4

Topology #5: 150m x 150m x 60m, 27 receivers

The fifth and final topology is very similar to the fourth topology. The area is divided into 27 subregions stacked three deep in each dimension: each of size 50m by 50m by 20m. The difference is that the shooter is inside of the monitoring area. Figures 4.20 – 4.24 illustrate the average error between the output location and the actual source location. Figure 4.23 shows the horizontal location error only.

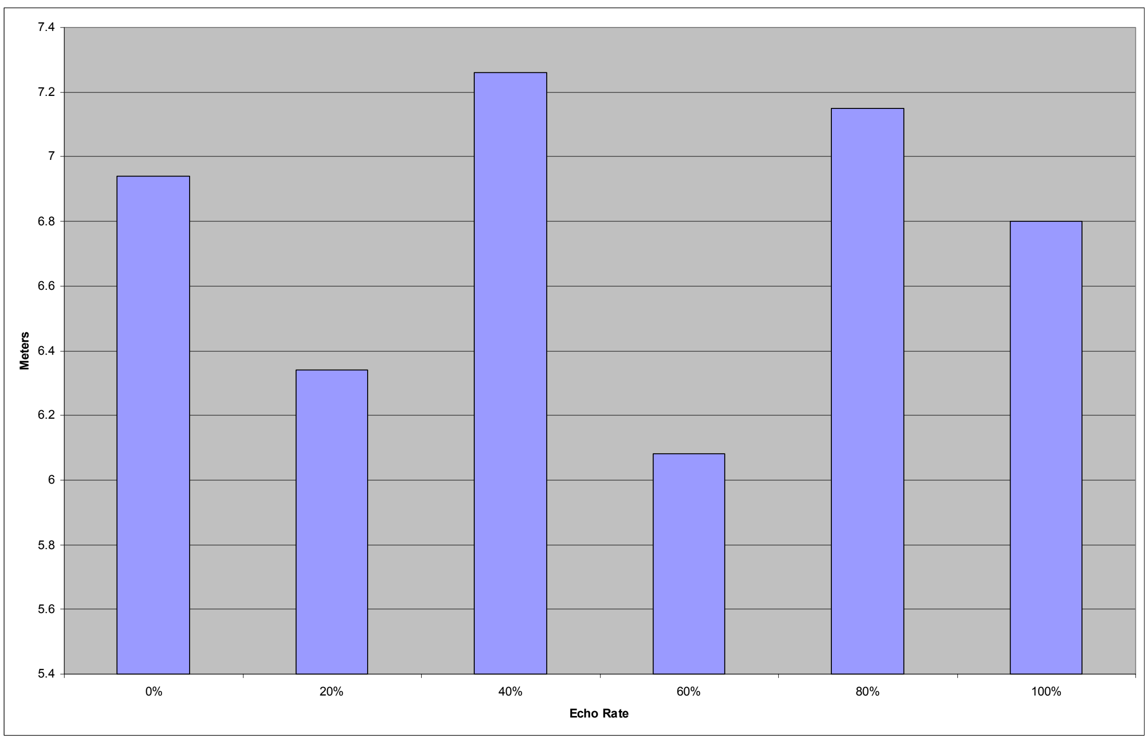

Figure 4.20 Population Average Errors for Topology 5

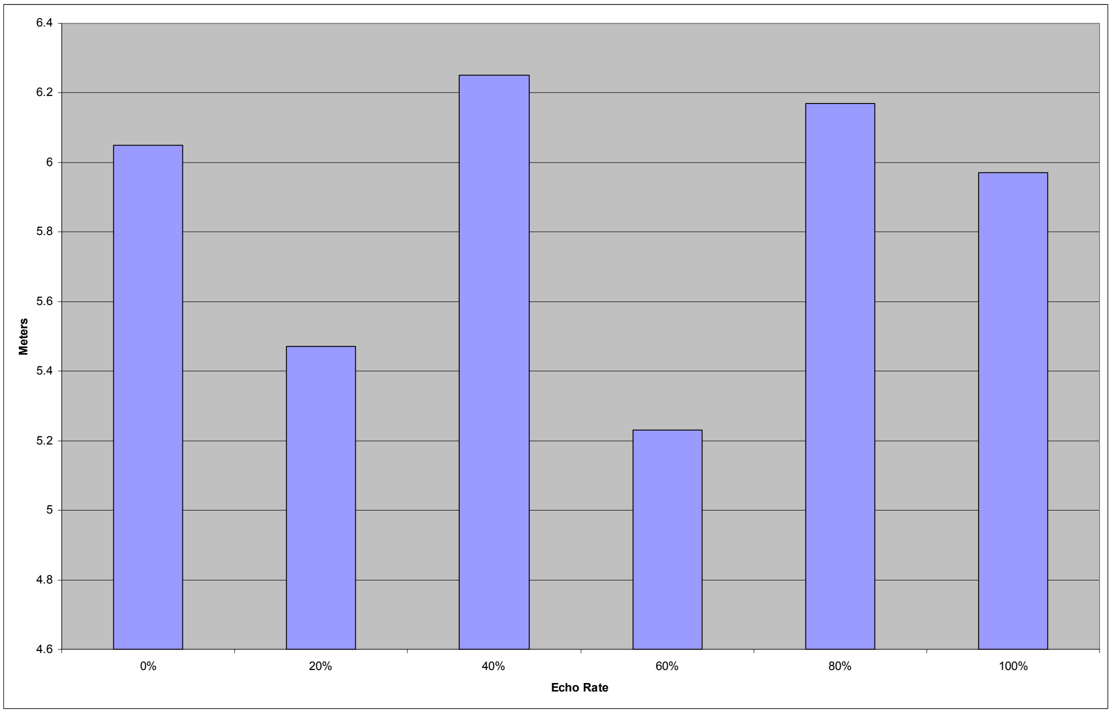

Figure 4.21 100M Cluster Average Errors for Topology 5

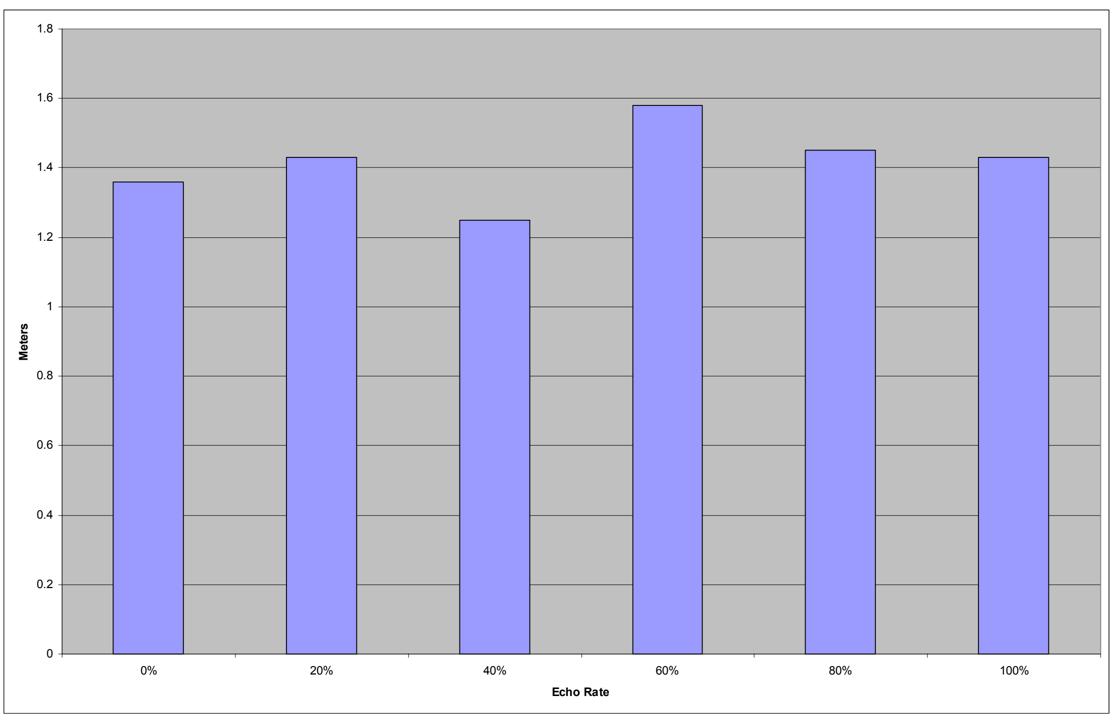

Figure 4.22 Population Mode Errors for Topology 5

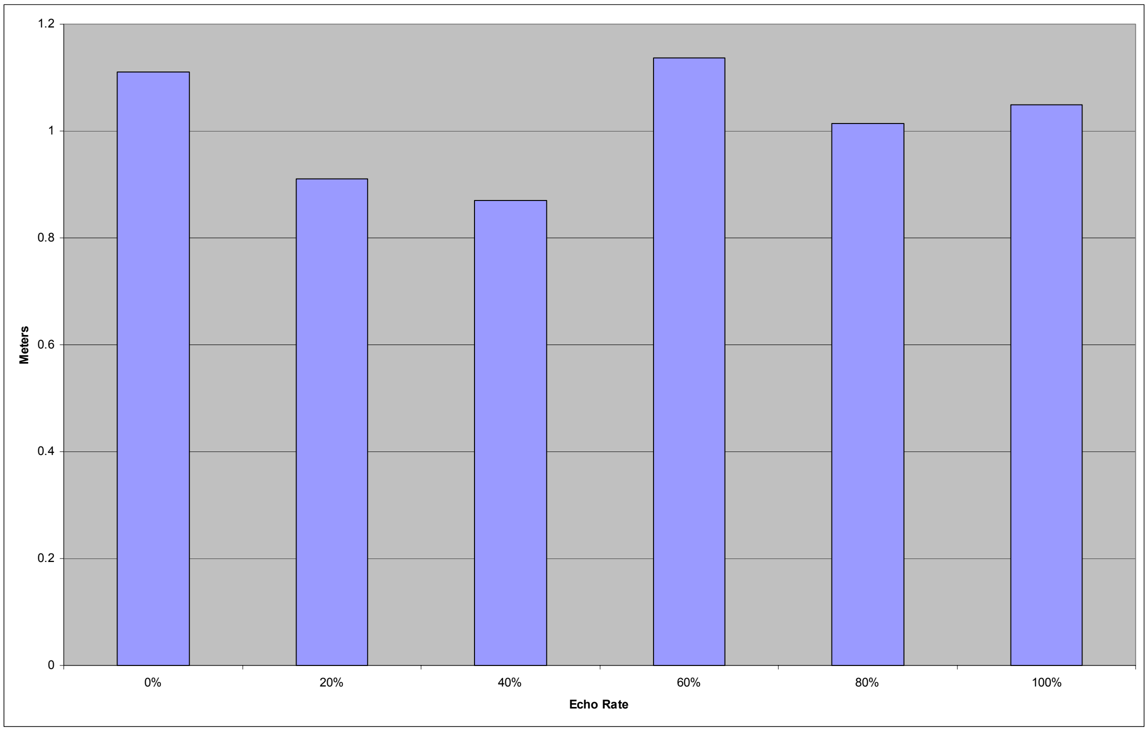

Figure 4.23 Population Mode X/Y Errors for Topology 5

Consolidated output

The following graphs illustrate the consolidated location errors for all five topologies. Figure 4.24 shows that the raw population of valid locations produced by the algorithm do not yield the desired accuracy. Indeed only the fifth topology approaches the 6 meter accuracy target. This is mainly due to the receiver distribution with respect to the source. The other topologies have less separation in the vertical plane with respect to the receiver and therefore are more susceptible to error in the vertical component. This fact figures into Figure 4.27 showing a much higher degree of accuracy because it's measuring only the X/Y error.

Figure 4.25 illustrates the average location error of the 100 meter clusters; all the locations in the population which lie within 100 meters of the population average. This location answer approaches a better answer but still falls short of the desired accuracy.

Figure 4.26 shows the average location error of the mode of the population, rounded to the nearest meter. Except for the second topology, these results are much closer to the goal of 6 meters. The only explanation found for this discrepancy is the distances involved are five times greater than that of the next largest monitored area. The effects introduced by general topology are exacerbated by this large factor producing a much higher location error. But as can be seen in Figure 4.27, almost all of this excessive error is contained in the vertical component. In an outdoor scenario, such as topology #2, the vertical component isn't nearly as important as it would be in an indoor scenario such as topologies #4 and #5.

The relative location of the source to all receivers has a major impact on the accuracy of a TOA geolocation system. It is therefore unclear at this point why the average error distribution between topologies 1 and 2 is different over the range of echo rates. Topology 2 is simply five times larger than topology 1. Across each of the other topologies, the relationship between possible source location and possible receiver locations is different enough to account for the different distributions. Further research is required to answer the question and characterize these differences.

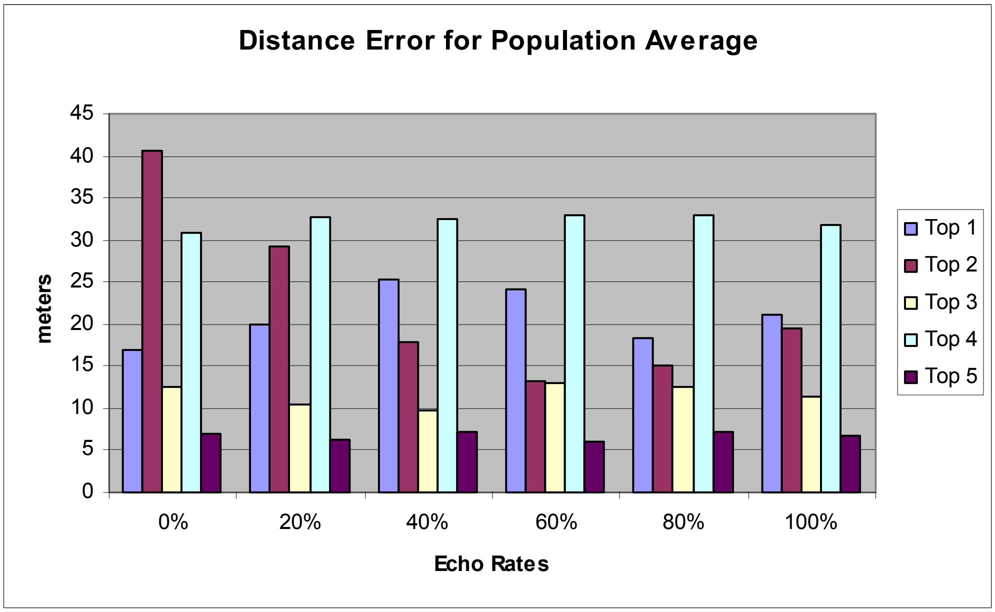

Figure 4.24 Population Average Errors for All Topologies

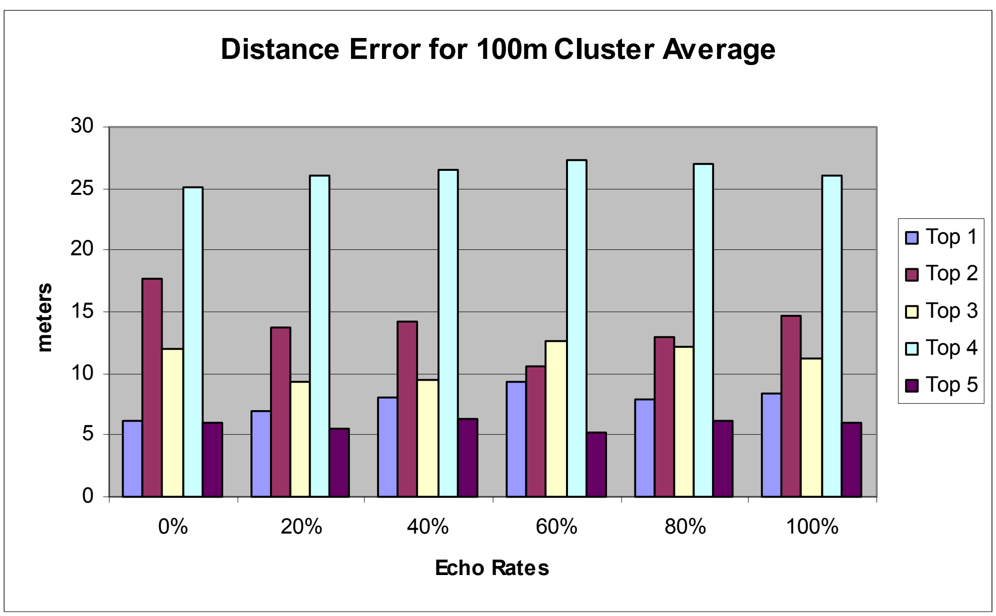

Figure 4.25 Population Average Errors for All Topologies

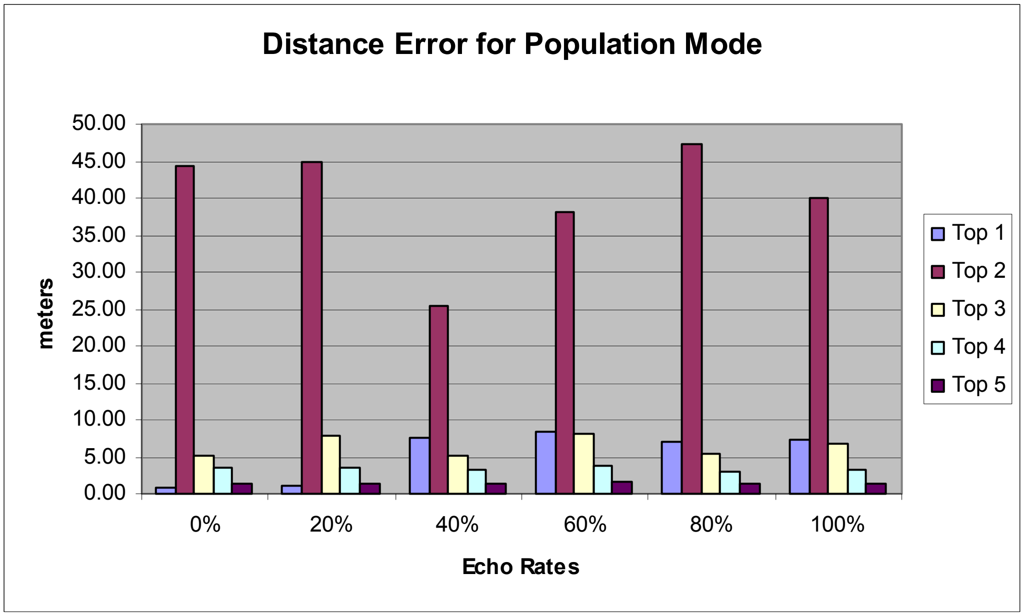

Figure 4.26 Population Mode Errors for All Topologies

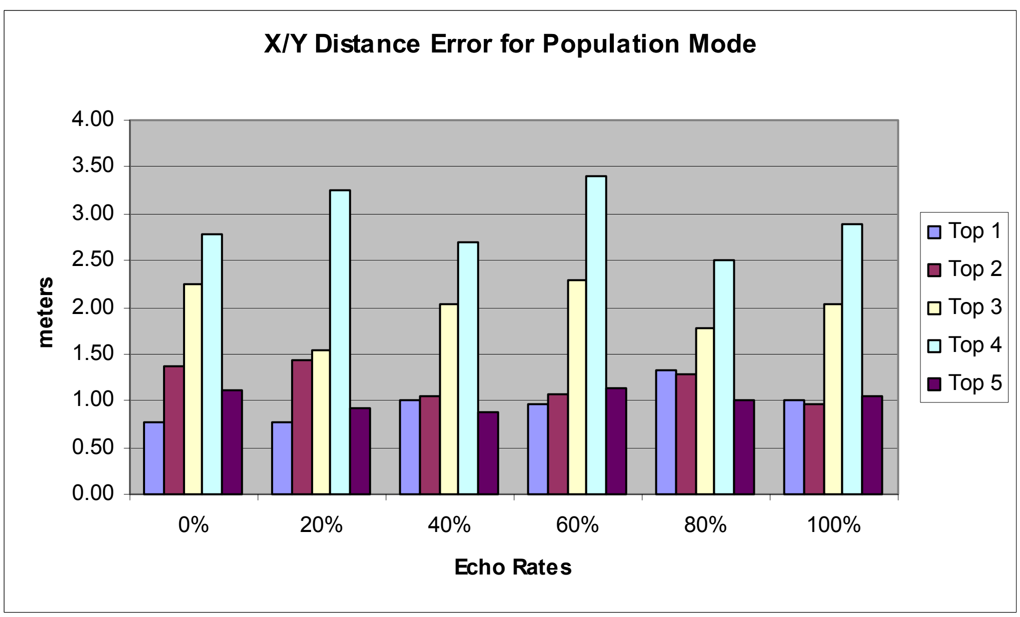

Figure 4.27 Population Mode X/Y Errors for All Topologies

Output Distributions

Graphs 4.28 – 4.31 illustrate the histrogram distribution of the output and the 95% confidence interval for the four location answers. The histrograms show that the majority of the output data lie near the bottom of the graph (near the desired location accuracy).

Population Loc Error Across All Echo Rates and Topologies

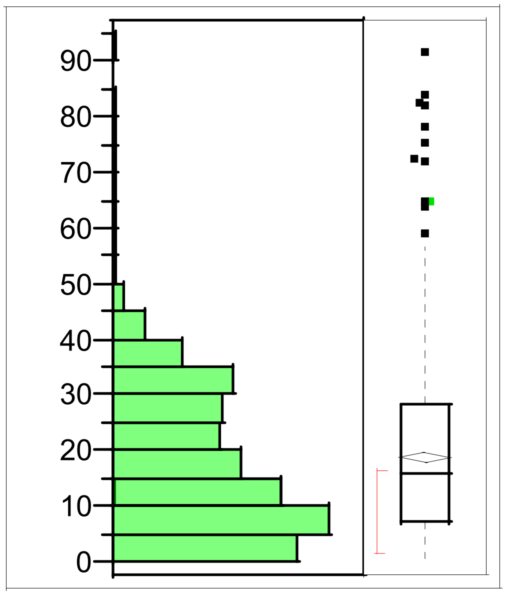

Moments

Mean	18.662943
Std Dev	13.717821
Std Err Mean	0.4233411
upper 95% Mean	19.493635
lower 95% Mean	17.832251
N	1050

Confidence Intervals

Parameter	Estimate	Lower CI	Upper CI	1-Alpha
Mean	18.66294	17.83225	19.49363	0.950
Std Dev	13.71782	13.15516	14.33114	

Figure 4.28 Population Location Error Histrogram Distribution

A 95% confidence interval on the population average shows that 95% of the time, the location error in the population is between 17.8 and 19.5. While this figure isn't within the desired accuracy, it is approaching the 6 meter limit.

100M Cluster Loc Error Across All Echo Rates and Topologies

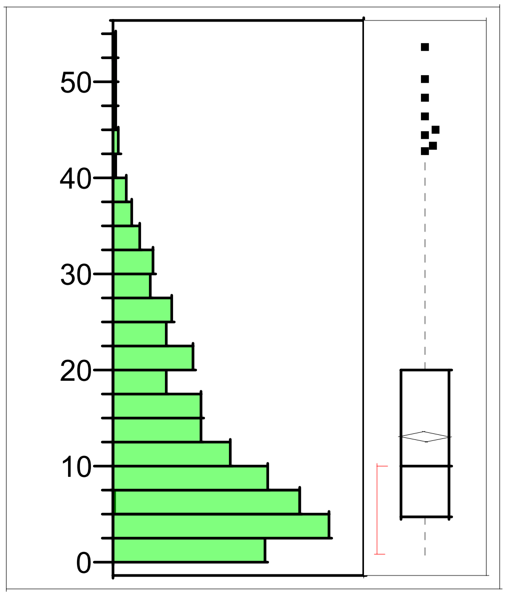

Moments

Mean	13.019924
Std Dev	10.19876
Std Err Mean	0.3147406
upper 95% Mean	13.637517
lower 95% Mean	12.402331
N	1050

Confidence Intervals

Parameter	Estimate	Lower CI	Upper CI	1-Alpha
Mean	13.01992	12.40233	13.63752	0.950
Std Dev	10.19876	9.780438	10.65474	

Figure 4.29 100M Cluster Location Error Histrogram Distribution

The distribution of the 100 meter cluster data is skewed toward zero as well. The 95% CI shows that expected values of this metric are between 12.4 and 13.6. Again, not within the target accuracy of 6 meters but much closer than the population average metric.

Pop Mode Loc Error Across All Echo Rates and Topologies

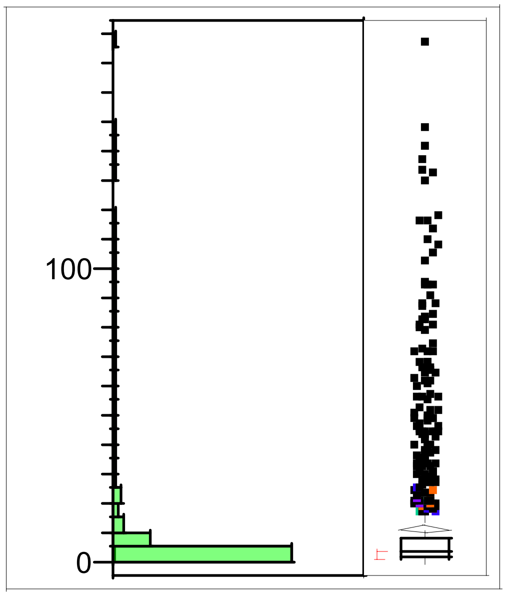

Moments

Mean	11.317771
Std Dev	21.832041
Std Err Mean	0.6737514
upper 95% Mean	12.639825
lower 95% Mean	9.9957175
N	1050

Confidence Intervals

Parameter	Estimate	Lower CI	Upper CI	1-Alpha
Mean	11.31777	9.995718	12.63983	0.950
Std Dev	21.83204	20.93656	22.80814	

Figure 4.30 Population Mode Location Error Histogram Distribution

The distribution of the population mode is highly skewed toward the desired accuracy of 6 meters. The 95% CI shows an expected value between 10.0 and 12.6. As is shown in the following distribution, most of this error is in the vertical component due to the distribution of receivers in relation to the source.

Pop Mode X/Y Loc Error Across All Echo Rates and Topologies

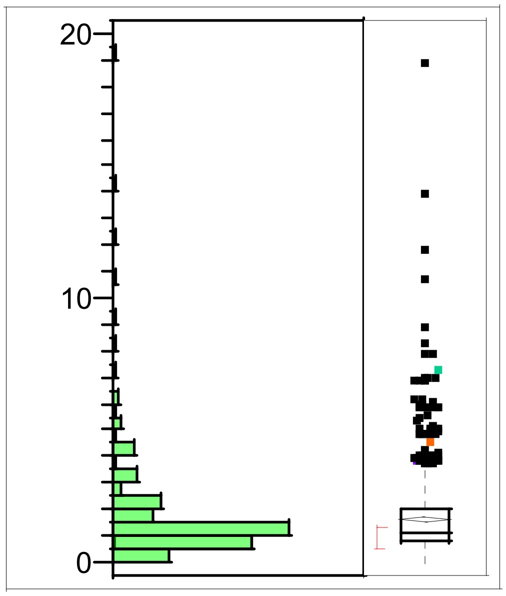

Moments

Mean	1.6171143
Std Dev	1.5514445
Std Err Mean	0.0478786
upper 95% Mean	1.7110631
lower 95% Mean	1.5231655
N	1050

Confidence Intervals

Parameter	Estimate	Lower CI	Upper CI	1-Alpha
Mean	1.617114	1.523166	1.711063	0.950
Std Dev	1.551445	1.487809	1.620809	

Figure 4.31 Population Mode X/Y Location Error Histrogram Distribution

The distribution of the X/Y location error for the population mode indicates that the desired accuracy can be achieved when ignoring the vertical component. That is to say the majority of the error in the population mode is in the vertical component. Therefore the 95% CI on the X/Y location error of the population average of 1.5 to 1.7 meets the desired 6 meter accuracy.

ANOVA

The following table shows the ANOVA of the four output locations with respect to both factors: echo rate and topology.

Table 4.1 Least Squares Fit

Response Population Loc Error

Source	Nparm	DF	Sum of Squares	F Ratio	Prob > F
Echo Rate	5	5	1047.246	2.2801	0.0448
Topology	4	4	27009.275	73.5084	<.0001
Echo Rate*Topology	20	20	18183.872	9.8978	<.0001

Response 100M Cluster Loc Error

Source	Nparm	DF	Sum of Squares	F Ratio	Prob > F
Echo Rate	5	5	216.6282	0.8384	0.5225
Topology	4	4	9270.0387	44.8448	<.0001
Echo Rate*Topology	20	20	1505.5379	1.4566	0.0882

Response Pop Mode Loc Error

Source	Nparm	DF	Sum of Squares	F Ratio	Prob > F
Echo Rate	5	5	2059.683	1.5670	0.1667
Topology	4	4	49047.339	46.6428	<.0001
Echo Rate*Topology	20	20	11534.470	2.1938	0.0018

Response Pop Mode X/Y Loc Error

Source	Nparm	DF	Sum of Squares	F Ratio	Prob > F
Echo Rate	5	5	7.726700	0.8350	0.5248
Topology	4	4	97.975157	13.2353	<.0001
Echo Rate*Topology	20	20	44.361031	1.1985	0.2467

Summary

In this chapter, the output as analyzed to determine if the desired location accuracy of 6 meters could be attained and to determine the affect that the topology and the echo rate had on the location accuracy. In each experiment, a raw population of all valid location answers was averaged, as well as all locations within 100 meters of the population average and the mode of the population average. Every combination of topology and echo rate was replicated 35 times. The average of these replications was plotted for each topology separately and then plotted together for the population average, the 100 meter cluster and the population mode.

The desired accuracy of 6 meters can be met consistently in the X/Y (horizontal) component of the population mode measurement. In other words, the horizontal error in the mode of the population of locations produced from the algorithm typically falls well under the 6 meter ceiling. In most cases, the three-dimensional location error in the population mode will fall within this desired accuracy as well. Additional sensors could be added to any of the topologies to increase the output accuracy.

There remains some question relating to why the output across the different echo rates does not follow a similar shape for each of the topologies. More disturbing is the comparison between topologies 1 and 2, which only differ in the size of the monitored area. It is expected that the general shape of the outputs over the different echo rates would be similar. Yet they are different. This research does not answer the question of why they are different.

V. Conclusions and Recommendations

Chapter Overview

This is the chapter conclusions are drawn from the results presented in chapter 4. The questions asked in chapter 1 are also answered. Recommendations are made concerning the future of this research, both in future research and construction of the sniper detection system.

Conclusions of Research

The experiments run over the five topologies investigated show the feasibility of the geolocation algorithm in a multipath environment. The key to overcoming the echo is a large number of receivers distributed equally over the area to be monitored. By sampling every possible 4-tuple combination, a more accurate location answer is produced versus a simple 4-receiver system or an overdetermined system of equal receivers. Pilot studies that were not included in this thesis strengthen this assertion. Further statistical analysis of the population of valid locations produced from considering all 4-tuple combinations of receiver may yield a better location result than the population mode measurement.

Significance of Research

This research proves the feasibility of a sniper detection system (or a system used to determine any discernable audio event) using only time-of-arrival input data in a multipath environment. Given the current world situation, an accurate, real time sniper detection system which operates in a true multipath environment would prove invaluable, both in saving lives and acting as a deterrent.

Additionally, this concept of using audio signals and a TOA algorithm can be used in reverse: multiple audio sources whose locations are known and a single receiver whose location is to be calculated. This situation is much more representative of the GPS model.

Recommendations for Future Research

The next step in building a viable sniper detection system using the TOA algorithm is to investigate the signal analyzer. The incoming audio signals must be analyzed in real time for the suspect audio signature and an accurate time stamp must then be applied to the signal. These time stamps must then be sent to the central processing system (with the TOA algorithm), along with the exact location of each receiver (using GPS). In addition, research needs to be performed on synchronizing the clocks on the receivers and the central processing system. An accurate time-stamp is imperative to the successful operation of the geolocation algorithm. The clock error assumed within this experiment was 3ms.

Another follow-up research topic would be to identify why the shape of the location error graph across the different echo rates is different across the different topologies. An exploration of different topologies would also be worthwhile.

Summary

This focus of this research was to prove the viability of an algorithm to geolocate an audio signal in a multipath environment. The results indicate that the method used to calculate a location, sampling of every 4-tuple combination in a receiver-rich system, provides an accurate location, even when all receivers are experiencing echo. Further research and study are needed to bring such a system out of the laboratory and into the battle field.

Appendix A, Raw Data

Topology #1, 0% echo

Replication	Number of valid locs	Number valid locs w/in 100 m	Pop avg dis from source	100m avg dis from source	Pop mode dis from source	Percent of Echo	Pop mode X/Y dis
1	8064	6425	14.40	1.25	1.24	0.00	1.00
2	5723	2841	22.62	8.46	1.16	0.00	1.01
3	4325	1840	12.90	6.97	0.85	0.00	0.74
4	4823	1412	30.63	0.92	1.20	0.00	0.79
5	4522	1871	11.68	3.67	0.86	0.00	0.59
6	6635	4937	21.02	9.73	1.17	0.00	1.14
7	8185	6715	6.53	2.64	1.01	0.00	0.88
8	4253	2811	9.35	5.97	0.59	0.00	0.59
9	3346	1063	19.39	14.65	1.23	0.00	1.18
10	4032	1147	14.51	2.55	0.85	0.00	0.80
11	4798	3196	15.19	3.19	0.50	0.00	0.50
12	4776	2872	21.92	3.12	0.69	0.00	0.32
13	8232	6880	6.65	1.51	0.59	0.00	0.31
14	5019	3154	14.67	8.48	1.08	0.00	0.59
15	4196	1728	32.01	7.30	0.63	0.00	0.08
16	4350	2739	17.14	6.34	0.64	0.00	0.63
17	4477	2373	17.09	8.28	0.94	0.00	0.92
18	5772	4142	11.79	6.20	0.89	0.00	0.79
19	3604	1268	6.39	7.06	1.39	0.00	1.04
20	4638	3079	9.55	0.84	0.53	0.00	0.24
21	4514	1506	5.26	1.19	1.31	0.00	1.19
22	4697	2401	27.22	7.07	1.06	0.00	0.91
23	4275	2215	42.96	20.10	1.24	0.00	0.74
24	4820	2477	17.32	4.34	0.71	0.00	0.60
25	6920	5037	15.01	5.19	0.87	0.00	0.54
26	3999	1208	12.40	9.51	0.58	0.00	0.56
27	4754	1859	17.74	1.44	0.84	0.00	0.61
28	5573	3268	16.85	1.72	1.08	0.00	0.93
29	4468	2965	27.02	12.25	1.29	0.00	1.29
30	8237	6943	9.57	9.08	0.73	0.00	0.47
31	5677	2762	14.96	0.60	0.96	0.00	0.96
32	3864	1747	18.44	7.05	1.26	0.00	1.08
33	8525	6968	11.40	9.92	0.76	0.00	0.69
34	5970	4132	31.11	13.94	0.96	0.00	0.92
35	5582	3747	11.70	4.58	1.38	0.00	0.95
AVG	5304.14	3192.23	16.98	6.20	0.94	0.00	0.76
STDEV	1446.81	1789.48	8.38	4.49	0.27	0.00	0.29

Table A1 Topology #1, 0% echo

Topology #1, 20% echo

Replication	Number of valid locs	Number valid locs w/in 100 m	Pop avg dis from source	100m avg dis from source	Pop mode dis from source	Percent of Echo	Pop mode X/Y dis
1	7909	6368	6.47	3.90	1.16	0.24	0.67
2	4933	3304	21.44	11.93	1.17	0.28	0.93
3	7013	5636	21.87	12.94	1.23	0.08	0.76
4	5188	2883	26.86	5.85	0.95	0.36	0.58
5	4535	1623	9.50	1.53	0.97	0.24	0.97
6	4310	2233	17.15	12.00	0.70	0.12	0.62
7	3908	2465	29.27	10.82	0.64	0.16	0.64
8	3670	1304	6.41	9.45	1.02	0.16	0.82
9	7771	6402	3.01	5.10	0.87	0.24	0.46
10	4557	2995	12.80	7.29	0.90	0.28	0.81
11	5020	2259	36.49	7.28	0.55	0.16	0.21
12	4936	2656	65.65	2.20	0.66	0.08	0.66
13	4540	1762	20.06	13.28	0.89	0.28	0.19
14	4528	2994	27.57	14.20	0.99	0.24	0.97
15	4443	2754	19.29	2.89	0.81	0.28	0.81
16	4021	1304	15.74	6.24	1.15	0.36	1.11
17	6656	5307	12.14	7.25	0.95	0.16	0.75
18	6116	4449	11.39	2.19	1.39	0.12	1.03
19	6307	4707	19.73	7.47	1.09	0.12	0.83
20	7600	6304	10.83	4.92	0.82	0.08	0.77
21	4235	1676	23.82	4.02	1.13	0.28	1.06
22	3451	1502	10.25	1.25	1.27	0.16	0.93
23	4635	2433	21.22	7.45	1.04	0.08	1.01
24	4704	2128	31.52	12.44	0.63	0.16	0.57
25	4247	1653	41.07	7.55	0.99	0.24	0.43
26	7264	5760	5.33	1.63	0.37	0.20	0.35
27	4999	2527	20.03	7.90	0.85	0.12	0.84
28	2729	1214	20.97	8.68	1.53	0.24	1.21
29	8284	6598	22.60	7.32	1.11	0.20	1.00
30	6913	5392	12.00	5.24	1.37	0.36	1.24
31	4400	1736	14.73	2.87	1.28	0.12	1.07
32	4738	3298	16.82	8.19	0.48	0.40	0.44
33	8395	6907	8.34	2.79	1.09	0.24	0.65
34	3516	1612	17.35	6.11	0.50	0.24	0.50
35	4957	2269	39.63	9.29	0.93	0.40	0.77
AVG	5297.94	3326.11	19.98	6.90	0.96	0.21	0.76
STDEV	1512.67	1833.43	12.32	3.67	0.27	0.09	0.27

Table A2 Topology #1, 20% echo

Topology #1, 40% echo

Replication	Number of valid locs	Number valid locs w/in 100 m	Pop avg dis from source	100m avg dis from source	Pop mode dis from source	Percent of Echo	Pop mode X/Y dis
1	3652	2064	13.40	7.07	7.17	0.32	1.45
2	5223	2368	10.37	9.94	4.14	0.32	0.45
3	3077	1447	10.11	4.12	5.42	0.44	0.68
4	3662	2075	13.33	5.63	21.52	0.40	1.10
5	4479	3399	20.99	12.79	7.99	0.44	0.61
6	5466	4354	20.56	5.43	8.63	0.48	0.70
7	5951	4273	30.27	11.06	5.60	0.28	0.78
8	3031	1275	13.30	4.43	7.01	0.24	0.70
9	4297	4297	10.20	10.20	1.04	0.36	1.00
10	3442	1338	21.19	7.52	8.98	0.36	2.17
11	2804	1169	23.00	1.95	9.69	0.40	0.41
12	4363	2463	22.66	1.91	1.28	0.48	0.33
13	3980	1855	19.70	7.42	5.34	0.32	1.43
14	4740	3127	16.49	10.02	8.58	0.44	0.29
15	3296	1365	12.99	12.91	13.84	0.28	1.64
16	5048	3410	18.24	2.02	9.83	0.32	1.29
17	3905	2788	39.00	17.73	7.37	0.24	0.72
18	2991	1108	7.61	12.40	16.41	0.44	2.15
19	6112	5080	11.37	10.34	6.76	0.48	0.42
20	3364	1483	23.13	9.76	3.29	0.24	1.03
21	3896	2786	30.59	2.65	7.91	0.72	1.44
22	8222	7192	20.71	14.05	1.03	0.36	0.80
23	3679	1607	24.13	6.67	3.97	0.36	0.42
24	3602	1550	12.19	15.52	2.26	0.20	2.09
25	4070	2454	15.76	8.83	8.75	0.40	1.34
26	3404	1644	20.09	1.58	26.42	0.24	0.51
27	5351	3975	20.23	1.11	5.29	0.36	0.65
28	4833	3328	29.58	11.13	3.86	0.36	0.89
29	7039	5879	17.68	4.14	3.22	0.28	1.15
30	4427	2061	14.33	1.90	1.93	0.48	0.99
31	4147	2500	38.65	10.40	18.30	0.44	1.27
32	2273	1061	23.45	23.16	1.80	0.40	1.17
33	4342	2657	40.98	10.51	1.29	0.32	0.82
34	3256	1478	16.11	0.20	19.76	0.16	1.27
35	8221	7006	17.02	7.35	1.39	0.24	1.12
AVG	4389.86	2797.6	19.98	8.11	7.63	0.36	1.01
STDEV	1396.10	1615.39	8.35	5.20	6.27	0.11	0.50

Table A3 Topology #1, 40% echo

Topology #1, 60% echo

Replication	Number of valid locs	Number valid locs w/in 100 m	Pop avg dis from source	100m avg dis from source	Pop mode dis from source	Percent of Echo	Pop mode X/Y dis
1	4331	1634	27.63	13.41	25.56	0.56	1.69
2	3674	2105	25.27	10.10	0.68	0.40	0.68
3	3647	1817	28.37	3.78	21.63	0.56	1.40
4	6938	5743	18.07	8.53	3.98	0.56	0.60
5	5974	5193	0.84	1.32	12.14	0.64	0.14
6	3162	1940	13.53	4.98	15.93	0.56	0.60
7	2954	1639	38.58	20.01	6.92	0.68	0.64
8	2550	1294	8.90	4.56	1.19	0.68	1.18
9	4161	2485	24.75	4.38	8.03	0.64	0.94
10	3426	1714	55.87	15.88	1.11	0.60	1.10
11	3206	1027	25.64	1.18	12.00	0.60	2.41
12	4932	2898	39.07	17.27	4.19	0.68	0.94
13	4860	3113	18.76	15.88	5.89	0.64	0.90
14	5104	3438	15.19	8.64	11.66	0.52	0.87
15	3849	2166	27.78	23.92	3.47	0.56	0.60
16	4175	2442	15.27	2.30	20.99	0.68	0.23
17	5497	4113	8.18	2.24	3.53	0.52	0.35
18	4420	2571	24.77	3.75	2.48	0.56	0.39
19	3228	1732	16.46	11.46	5.99	0.44	1.56
20	4867	3496	12.59	8.64	7.57	0.52	1.36
21	7822	6466	13.27	2.41	6.28	0.44	0.54
22	3846	2610	38.42	17.98	3.65	0.44	0.97
23	3946	2477	21.99	8.62	4.79	0.48	0.33
24	3395	2066	28.27	3.37	19.18	0.64	0.62
25	3692	2247	28.83	8.26	3.32	0.56	0.90
26	3318	2140	9.76	3.47	7.88	0.60	1.72
27	3748	1042	29.46	14.07	20.09	0.56	4.66
28	3785	2218	27.59	2.62	1.54	0.72	0.45
29	3469	1546	31.07	16.59	3.77	0.64	0.20
30	3370	1342	22.52	4.78	24.73	0.44	1.01
31	4762	3580	16.16	1.43	0.55	0.64	0.55
32	3977	2476	32.52	21.90	6.24	0.44	0.70
33	6903	5160	33.45	13.83	2.07	0.52	1.25
34	3805	2423	30.64	15.85	5.45	0.68	0.85
35	4098	1867	33.43	9.46	4.22	0.52	0.61
AVG	4254.03	2634.86	24.08	9.34	8.25	0.57	0.97
STDEV	1182.54	1314.50	10.92	6.59	7.29	0.09	0.81

Table A4 Topology #1, 60% echo

Topology #1, 80% echo

Replication	Number of valid locs	Number valid locs w/in 100 m	Pop avg dis from source	100m avg dis from source	Pop mode dis from source	Percent of Echo	Pop mode X/Y dis
1	3709	2527	18.88	20.91	4.75	0.64	1.04
2	4496	3283	40.29	22.53	1.54	0.64	1.26
3	4373	2230	26.16	8.14	11.30	0.68	2.04
4	3912	1745	6.36	13.92	3.97	0.84	1.65
5	3799	2037	10.87	1.08	6.42	0.80	1.22
6	3755	2248	24.31	5.14	13.18	0.76	0.81
7	6415	5294	9.58	1.41	4.02	0.64	1.14
8	4221	2701	13.03	7.24	4.14	0.76	1.09
9	3746	2503	34.33	13.29	9.13	0.72	2.07
10	2699	1645	32.56	1.54	12.95	0.80	1.03
11	4756	3573	22.97	1.85	1.95	0.72	0.60
12	3589	1845	10.72	2.75	4.40	0.88	1.23
13	6172	4863	9.08	6.36	9.31	0.84	1.46
14	5610	4242	11.50	10.19	6.43	0.68	1.32
15	3842	1881	41.80	9.66	21.12	0.88	1.13
16	3511	1725	29.09	14.30	8.57	0.64	1.07
17	3195	1105	8.58	4.86	1.98	0.84	1.98
18	3599	1399	25.59	27.27	3.19	0.64	2.41
19	7179	6222	10.02	9.28	0.98	0.72	0.73
20	3457	1744	18.22	0.86	6.31	0.80	1.58
21	6899	5888	4.48	1.29	3.40	0.68	0.78
22	5485	4183	6.48	11.21	2.46	0.84	1.28
23	5099	3483	20.19	12.41	18.47	0.72	0.86
24	5171	3723	8.37	7.13	4.38	0.84	1.54
25	4842	3126	29.51	7.59	4.54	0.88	0.67
26	4576	3330	23.97	5.49	2.27	0.76	0.50
27	3621	2367	13.25	1.01	9.54	0.64	0.78
28	4254	1695	14.19	4.68	22.06	0.64	1.68
29	6257	4587	8.91	3.87	3.69	0.88	0.68
30	3622	2000	33.39	12.42	10.40	0.84	1.00
31	3331	1743	8.82	1.45	4.00	0.72	0.80
32	5515	4009	15.54	1.09	11.93	0.76	0.40
33	6216	4913	18.70	10.39	0.69	0.80	0.49
34	4839	2891	16.34	2.89	5.52	0.68	0.90
35	3689	979	13.67	12.02	8.83	0.80	7.38
AVG	4555.74	2963.69	18.28	7.93	7.08	0.75	1.33
STDEV	1151.20	1389.21	10.16	6.53	5.45	0.08	1.16

Table A5 Topology #1, 80% echo

Topology #1, 100% echo

Replication	Number of valid locs	Number valid locs w/in 100 m	Pop avg dis from source	100m avg dis from source	Pop mode dis from source	Percent of Echo	Pop mode X/Y dis
1	3549	2098	26.28	11.03	2.54	0.96	1.19
2	3423	1650	44.10	8.22	12.59	0.96	1.08
3	4177	1713	14.19	4.15	10.06	1.00	4.04
4	4248	2478	9.61	1.24	12.05	0.96	1.46
5	5196	3381	23.22	8.42	8.54	1.00	0.93
6	4345	2979	20.66	1.90	1.67	1.00	0.35
7	3800	1738	43.74	21.81	7.43	1.00	1.42
8	4458	3546	9.83	6.92	7.09	1.00	0.28
9	3966	2164	17.11	3.33	14.00	0.92	0.81
10	7069	5965	18.84	11.20	1.47	0.96	1.31
11	4287	3077	11.68	4.66	2.86	0.92	1.89
12	5920	4582	30.33	14.35	3.12	0.96	0.97
13	4159	1860	21.10	10.04	5.41	0.92	1.99
14	4895	3186	24.43	14.19	3.74	0.96	0.97
15	4210	2544	23.77	14.10	3.08	0.96	0.80
16	4006	2506	22.55	8.59	5.46	1.00	1.05
17	4385	2520	11.06	10.27	21.22	1.00	2.16
18	4004	2354	22.55	7.79	19.56	0.96	0.32
19	3525	2000	21.36	12.24	1.10	0.92	0.77
20	3556	1835	24.92	3.58	9.37	1.00	0.60
21	5021	3179	15.71	9.67	1.29	0.96	1.13
22	3954	1264	33.54	7.05	10.43	0.96	0.05
23	7290	5827	43.54	20.43	0.56	1.00	0.30
24	6239	5070	10.57	3.88	2.16	0.96	0.25
25	5312	4147	4.90	5.41	3.18	1.00	1.22
26	4250	2966	13.63	4.69	6.50	0.88	0.36
27	4646	3305	21.35	1.55	4.59	1.00	0.76
28	4786	3464	12.20	2.53	3.44	0.92	0.72
29	4477	2302	17.60	17.65	21.79	0.96	1.22
30	3326	2107	17.90	9.44	17.19	0.92	0.23
31	5579	3968	11.30	3.31	2.06	0.92	1.08
32	3701	2337	28.70	15.92	0.76	0.88	0.55
33	4389	2584	21.42	2.04	23.24	1.00	0.98
34	5182	3922	13.64	9.02	1.63	0.92	1.27
35	3666	2461	31.18	2.98	1.95	0.96	0.54
AVG	4542.74	2945.11	21.10	8.39	7.23	0.96	1.00
STDEV	960.60	1140.28	9.77	5.44	6.65	0.04	0.73

Table A6 Topology #1, 100% echo

Topology #2, 0% echo

Replication	Number of valid locs	Number valid locs w/in 100 m	Pop avg dis from source	100m avg dis from source	Pop mode dis from source	Percent of Echo	Pop mode X/Y dis
1	519	307	17.07	4.68	23.44	0.00	0.32
2	827	405	28.62	17.68	104.11	0.00	1.19
3	931	402	22.45	13.10	39.46	0.00	1.09
4	859	335	18.36	21.35	97.09	0.00	2.40
5	737	194	73.40	15.16	27.07	0.00	1.08
6	1891	1337	12.80	3.96	1.58	0.00	0.45
7	1107	473	30.28	20.55	22.27	0.00	1.35
8	1008	545	79.05	13.15	8.41	0.00	1.08
9	1189	519	37.21	15.75	46.92	0.00	1.22
10	940	528	76.20	25.00	35.69	0.00	0.98
11	1253	659	30.32	10.45	7.04	0.00	0.84
12	3099	2157	18.94	9.10	21.94	0.00	1.21
13	1064	274	55.62	24.16	114.64	0.00	3.93
14	652	204	33.29	8.04	130.94	0.00	2.15
15	848	330	48.05	50.82	178.71	0.00	0.86
16	973	461	46.96	13.47	2.93	0.00	1.30
17	798	199	23.81	2.32	46.13	0.00	3.85
18	2041	1455	46.44	30.67	20.18	0.00	0.33
19	943	475	35.89	12.35	6.27	0.00	1.09
20	1176	657	33.14	5.56	28.70	0.00	0.95
21	1177	522	8.64	18.03	45.35	0.00	0.73
22	2307	1608	25.60	0.88	10.88	0.00	0.81
23	688	296	34.61	29.04	11.84	0.00	1.44
24	705	274	65.70	8.70	9.28	0.00	0.96
25	529	200	26.46	5.46	15.43	0.00	1.09
26	845	286	54.26	44.91	50.04	0.00	1.36
27	1043	509	64.73	40.80	0.83	0.00	0.75
28	742	366	37.71	7.64	53.01	0.00	1.22
29	611	247	11.11	17.97	25.21	0.00	1.77
30	1007	482	82.66	40.37	36.14	0.00	1.14
31	807	290	92.52	17.78	74.18	0.00	1.13
32	830	228	25.87	18.82	83.97	0.00	3.94
33	686	226	72.65	2.35	54.50	0.00	0.53
34	574	204	21.51	15.52	68.13	0.00	2.12
35	940	413	32.71	34.91	51.28	0.00	1.08
AVG	1038.46	516.2	40.70	17.73	44.39	0.00	1.36
STDEV	533.17	442.83	22.67	12.73	40.96	0.00	0.91

Table A7 Topology #2, 0% echo

Topology #2, 20% echo

Replication	Number of valid locs	Number valid locs w/in 100 m	Pop avg dis from source	100m avg dis from source	Pop mode dis from source	Percent of Echo	Pop mode X/Y dis
1	878	412	14.96	14.63	37.44	0.20	0.88
2	879	305	41.60	12.64	7.82	0.20	3.32
3	1263	644	27.99	33.91	82.44	0.08	0.32
4	1955	1179	19.94	8.08	32.12	0.08	0.69
5	570	169	37.97	27.28	34.70	0.08	5.53
6	1471	1016	23.76	6.05	28.57	0.08	1.03
7	829	433	34.22	15.74	19.90	0.20	1.04
8	2269	1590	25.08	21.40	50.59	0.24	0.81
9	1096	487	83.21	37.89	119.38	0.32	1.56
10	880	248	32.65	7.84	35.11	0.28	2.01
11	868	208	10.78	3.27	58.76	0.04	3.30
12	831	201	53.59	31.40	72.90	0.20	1.69
13	1413	907	49.18	15.19	7.00	0.08	0.77
14	1195	697	22.94	9.08	26.34	0.04	1.23
15	596	255	53.12	14.20	142.83	0.16	1.55
16	757	273	84.46	8.18	27.56	0.16	1.76
17	1119	622	18.27	3.63	56.80	0.28	0.96
18	1709	1066	17.41	2.48	3.35	0.24	1.19
19	970	416	30.61	5.35	138.29	0.24	0.45
20	849	236	8.73	19.16	75.79	0.04	1.78
21	1313	798	18.41	2.21	13.00	0.20	1.00
22	2338	1477	28.03	17.89	31.05	0.12	1.13
23	1758	1090	14.62	26.79	30.05	0.28	0.22
24	1338	803	27.84	2.71	26.28	0.08	1.04
25	956	378	29.20	9.57	95.90	0.12	1.71
26	833	199	18.00	11.60	89.65	0.08	0.73
27	1183	773	36.93	17.47	63.07	0.12	0.68
28	2930	1840	6.74	13.81	2.78	0.20	1.12
29	1880	1316	39.21	13.83	5.19	0.20	1.45
30	2421	1664	9.60	14.96	11.16	0.40	1.03
31	1517	962	31.74	21.41	2.78	0.08	0.72
32	2490	1704	9.82	1.25	50.26	0.08	1.06
33	648	156	8.93	11.46	12.30	0.24	2.45
34	878	376	24.05	5.84	67.74	0.24	2.47
35	1202	630	30.67	10.62	7.77	0.24	1.15
AVG	1316.63	729.43	29.26	13.68	44.76	0.17	1.42
STDEV	604.28	500.39	18.41	9.30	38.28	0.09	1.02

Table A8 Topology #2, 20% echo

Topology #2, 40% echo

Replication	Number of valid locs	Number valid locs w/in 100 m	Pop avg dis from source	100m avg dis from source	Pop mode dis from source	Percent of Echo	Pop mode X/Y dis
1	1531	1105	17.75	10.54	9.03	0.44	0.25
2	292	237	21.29	22.64	32.53	0.28	1.20
3	905	663	2.93	15.34	25.36	0.48	0.31
4	623	409	43.89	15.45	25.36	0.24	0.52
5	2096	1523	18.35	10.75	4.12	0.32	0.63
6	1152	793	1.85	7.15	4.85	0.36	0.58
7	242	196	18.11	25.63	91.95	0.44	1.45
8	1370	1075	1.91	4.28	5.76	0.24	0.74
9	2546	1837	15.39	6.17	3.60	0.56	1.07
10	538	370	2.51	14.31	4.23	0.28	1.28
11	2067	1415	29.30	20.37	1.10	0.40	0.47
12	676	492	38.59	38.09	36.41	0.28	1.58
13	449	335	5.94	2.27	24.37	0.24	2.35
14	994	676	3.23	5.67	8.16	0.36	1.18
15	1145	828	30.93	24.07	7.36	0.52	1.50
16	638	450	21.03	20.07	73.42	0.36	0.68
17	364	275	30.15	19.96	50.33	0.28	2.24
18	2638	2008	16.48	6.97	15.07	0.40	0.53
19	990	803	16.41	21.19	20.28	0.44	1.23
20	1104	868	4.13	11.11	28.30	0.20	1.11
21	2561	1916	2.10	2.07	3.82	0.28	0.95
22	2588	1865	22.95	15.44	3.54	0.48	1.32
23	1085	822	2.05	1.08	31.36	0.40	1.15
24	1007	742	27.66	11.89	21.72	0.36	0.50
25	680	490	21.84	15.55	62.92	0.36	0.98
26	1952	1457	17.21	1.03	3.16	0.40	0.99
27	324	252	30.73	30.02	3.48	0.40	1.14
28	495	371	23.35	15.60	58.01	0.20	1.98
29	944	679	3.31	6.84	41.07	0.44	1.38
30	636	526	18.50	3.35	37.06	0.32	1.08
31	1466	966	34.18	25.28	35.09	0.28	1.15
32	455	338	33.47	29.95	38.92	0.48	0.53
33	1032	790	42.60	22.16	2.05	0.28	1.01
34	984	666	3.19	10.97	50.49	0.24	0.83
35	212	162	5.63	2.01	20.66	0.40	0.84
AVG	1108.03	811.43	17.97	14.15	25.28	0.36	1.05
STDEV	723.99	529.14	12.88	9.49	22.77	0.09	0.50

Table A9 Topology #2, 40% echo

Topology #2, 60% echo

Replication	Number of valid locs	Number valid locs w/in 100 m	Pop avg dis from source	100m avg dis from source	Pop mode dis from source	Percent of Echo	Pop mode X/Y dis
1	3049	2161	38.79	7.83	4.43	0.48	0.58
2	366	231	17.98	6.35	65.98	0.56	1.07
3	392	245	4.03	1.71	62.46	0.48	1.29
4	439	328	1.79	5.72	95.88	0.60	0.31
5	447	355	32.22	34.62	29.72	0.60	1.82
6	297	198	6.50	2.67	106.98	0.44	1.70
7	442	317	6.11	8.80	45.73	0.56	2.20
8	2020	1405	10.21	3.55	13.93	0.48	0.74
9	1058	709	20.09	0.78	6.20	0.40	0.88
10	332	223	11.84	4.23	49.16	0.48	0.55
11	369	258	16.07	13.02	72.89	0.60	1.32
12	425	318	11.14	5.69	66.80	0.60	2.03
13	294	239	16.78	6.18	80.02	0.56	1.63
14	360	253	14.14	24.95	14.75	0.52	0.66
15	788	527	3.01	8.52	47.47	0.68	0.40
16	925	654	13.77	1.53	2.11	0.48	0.60
17	733	549	3.44	9.33	3.66	0.72	0.72
18	1937	1434	1.63	9.63	52.90	0.60	0.21
19	387	277	4.20	4.24	35.14	0.56	1.22
20	1706	1282	8.27	15.71	2.26	0.56	0.43
21	1499	1147	9.54	17.57	28.50	0.52	0.78
22	590	467	32.00	31.15	1.81	0.60	0.30
23	485	336	13.49	7.75	13.33	0.44	2.38
24	1033	741	2.88	4.40	65.94	0.56	0.82
25	365	257	17.51	10.53	85.92	0.60	0.62
26	2418	1883	8.61	22.20	2.77	0.52	0.76
27	1776	1257	27.95	23.36	10.81	0.48	1.10
28	482	354	10.44	10.71	18.28	0.48	1.49
29	1289	879	6.22	4.29	69.59	0.52	0.80
30	223	165	15.66	14.71	11.74	0.56	2.56
31	404	297	27.52	10.33	8.47	0.64	1.22
32	2326	1701	16.00	6.07	14.66	0.56	0.85
33	353	263	6.99	11.36	48.73	0.52	0.51
34	293	234	14.61	7.57	22.57	0.64	2.30
35	689	499	9.21	13.74	68.15	0.56	0.83
AVG	885.46	641.23	13.16	10.59	37.99	0.55	1.08
STDEV	742.05	543.18	9.29	8.19	31.01	0.07	0.64

Table A10 Topology #2, 60% echo

Topology #2, 80% echo

Replication	Number of valid locs	Number valid locs w/in 100 m	Pop avg dis from source	100m avg dis from source	Pop mode dis from source	Percent of Echo	Pop mode X/Y dis
1	577	433	12.00	19.96	45.52	0.80	0.54
2	563	433	27.74	8.97	43.60	0.72	0.34
3	342	223	6.00	11.36	134.72	0.76	2.27
4	475	322	3.57	0.46	24.36	0.72	1.22
5	479	349	8.61	15.31	20.99	0.84	2.03
6	432	313	9.70	2.32	81.17	0.72	0.91
7	594	468	10.07	2.41	4.35	0.72	0.49
8	492	309	17.27	16.27	118.08	0.80	1.09
9	845	621	36.53	45.42	61.32	0.80	1.81
10	508	372	5.92	17.24	35.38	0.76	0.97
11	436	301	3.22	8.60	45.03	0.72	0.60
12	412	295	16.85	9.37	9.93	0.88	0.44
13	1275	982	16.12	12.18	9.32	0.84	0.92
14	364	277	8.51	13.25	84.40	0.72	1.25
15	289	193	17.71	1.43	8.01	0.80	1.62
16	654	418	38.50	22.13	29.11	0.80	0.99
17	508	392	13.79	8.49	18.52	0.76	1.88
18	774	593	33.40	12.91	45.46	0.76	1.05
19	2679	2020	12.66	16.62	16.59	0.64	0.76
20	1467	1156	9.66	12.68	10.33	0.60	0.30
21	2756	1963	23.40	5.29	19.30	0.68	0.77
22	341	282	1.46	6.69	44.15	0.80	2.50
23	343	226	25.12	18.09	149.69	0.68	0.85
24	757	541	29.74	35.16	7.70	0.72	1.66
25	152	91	14.73	16.80	133.71	0.84	2.17
26	298	223	15.07	8.15	24.63	0.68	2.23
27	406	328	7.53	3.67	34.23	0.92	1.28
28	321	248	12.22	9.78	40.25	0.92	1.17
29	213	150	10.47	11.06	22.30	0.72	2.57
30	902	664	14.97	3.47	40.45	0.76	1.09
31	313	236	16.48	25.56	85.40	0.88	2.23
32	2639	1987	16.10	5.00	37.71	0.84	0.42
33	526	351	19.84	4.79	89.68	0.68	1.14
34	266	201	12.97	25.80	57.71	0.76	2.73
35	610	408	2.32	15.90	21.17	0.80	0.32
AVG	714.51	524.83	15.15	12.93	47.26	0.77	1.27
STDEV	671.82	502.93	9.39	9.59	39.22	0.08	0.72

Table A11 Topology #2, 80% echo

Topology #2, 100% echo

Replication	Number of valid locs	Number valid locs w/in 100 m	Pop avg dis from source	100m avg dis from source	Pop mode dis from source	Percent of Echo	Pop mode X/Y dis
1	2272	1822	59.82	33.67	4.14	0.92	1.20
2	377	301	31.43	40.26	95.71	0.92	1.15
3	375	298	16.61	10.99	22.69	1.00	1.57
4	2977	2119	7.68	1.10	5.12	0.92	1.07
5	1130	731	24.49	11.08	3.93	0.92	1.05
6	462	345	30.04	9.01	14.07	0.84	0.90
7	413	296	29.81	32.82	69.81	0.88	0.37
8	203	156	37.11	25.61	9.70	0.92	1.85
9	643	454	4.98	13.42	14.24	0.96	1.86
10	257	160	5.82	9.95	109.79	0.96	0.55
11	1148	855	37.79	15.02	2.21	0.96	0.76
12	2983	2100	18.99	6.37	18.65	0.96	1.20
13	638	390	29.68	24.22	2.71	1.00	1.23
14	456	320	6.89	20.24	64.40	0.96	0.61
15	1425	1131	21.41	13.93	39.67	0.96	0.99
16	437	326	18.29	6.67	111.81	0.96	1.19
17	620	428	11.00	11.74	22.63	0.96	0.75
18	481	378	4.09	6.93	41.18	0.80	0.30
19	1369	927	26.44	19.78	31.22	1.00	0.28
20	1832	1306	13.58	21.72	21.07	0.96	0.59
21	1681	1193	30.23	15.00	6.06	0.92	0.55
22	2324	1628	19.39	5.83	15.47	0.96	0.57
23	2143	1623	30.03	14.40	38.84	1.00	1.05
24	448	270	7.57	2.86	34.42	0.92	0.61
25	316	214	1.20	3.05	57.38	0.96	0.80
26	1427	991	1.53	5.83	34.05	0.96	0.31
27	228	191	23.51	20.32	117.39	1.00	2.14
28	1413	988	29.96	25.53	88.49	0.92	1.21
29	591	395	29.64	25.52	69.76	0.96	1.35
30	357	301	12.32	23.04	34.52	1.00	2.06
31	280	196	22.93	9.87	47.71	1.00	0.84
32	875	620	11.21	2.66	12.25	0.96	0.40
33	471	316	2.36	1.44	13.51	1.00	0.16
34	404	308	5.88	12.50	82.53	0.92	0.72
35	274	201	19.17	10.74	45.51	0.96	1.71
AVG	963.71	693.66	19.51	14.66	40.08	0.95	0.97
STDEV	801.97	582.68	12.98	9.80	34.19	0.05	0.52

Table A12 Topology #2, 100% echo

Topology #3, 0% echo

Replication	Number of valid locs	Number valid locs w/in 100 m	Pop avg dis from source	100m avg dis from source	Pop mode dis from source	Percent of Echo	Pop mode X/Y dis
1	30	30	11.87	11.87	5.51	0.00	2.18
2	44	44	5.45	5.45	6.17	0.00	4.00
3	50	47	9.16	1.85	1.26	0.00	1.05
4	54	53	12.27	14.37	1.26	0.00	1.13
5	60	60	21.46	21.46	3.32	0.00	2.14
6	61	61	6.96	6.96	5.04	0.00	5.03
7	39	39	11.26	11.26	9.45	0.00	7.04
8	53	53	9.26	9.26	2.56	0.00	1.74
9	61	61	4.07	4.07	2.60	0.00	1.37
10	47	47	23.74	23.74	39.52	0.00	2.83
11	16	16	46.87	46.87	0.83	0.00	0.52
12	44	44	12.80	12.80	1.32	0.00	1.21
13	36	36	3.08	3.08	5.21	0.00	1.43
14	39	39	1.32	1.32	1.16	0.00	1.02
15	34	34	1.54	1.54	1.30	0.00	1.02
16	68	68	3.94	3.94	1.41	0.00	1.01
17	42	42	16.07	16.07	0.37	0.00	0.18
18	47	46	6.03	3.09	3.44	0.00	1.65
19	51	51	11.08	11.08	8.11	0.00	1.71
20	29	29	6.01	6.01	8.77	0.00	4.07
21	24	24	1.57	1.57	8.02	0.00	8.01
22	68	68	4.21	4.21	2.86	0.00	1.53
23	66	66	2.60	2.60	1.11	0.00	1.08
24	65	65	32.35	32.35	1.63	0.00	1.63
25	41	39	26.98	21.60	6.18	0.00	6.16
26	20	20	9.34	9.34	2.53	0.00	1.00
27	47	47	5.99	5.99	6.32	0.00	1.01
28	55	55	14.26	14.26	11.47	0.00	2.44
29	38	38	14.36	14.36	1.06	0.00	1.05
30	60	60	15.66	15.66	3.26	0.00	1.32
31	45	45	23.67	23.67	5.58	0.00	5.58
32	52	52	1.36	1.36	6.75	0.00	1.00
33	51	51	20.38	20.38	1.87	0.00	1.39
34	31	31	2.41	2.41	8.03	0.00	1.46
35	59	58	36.39	34.44	3.23	0.00	1.44
AVG	46.49	46.26	12.45	12.01	5.10	0.00	2.24
STDEV	13.63	13.60	10.86	10.76	6.67	0.00	1.93

Table A13 Topology #3, 0% echo

Topology #3, 20% echo

Replication	Number of valid locs	Number valid locs w/in 100 m	Pop avg dis from source	100m avg dis from source	Pop mode dis from source	Percent of Echo	Pop mode X/Y dis
1	43	42	13.09	10.83	2.45	0.11	2.30
2	33	32	11.32	8.81	8.36	0.22	1.62
3	32	32	1.69	1.69	5.41	0.11	1.01
4	52	52	1.35	1.35	3.52	0.22	3.00
5	51	51	21.09	21.09	24.84	0.11	5.75
6	63	63	12.81	12.81	1.39	0.33	0.59
7	59	58	2.46	2.06	4.53	0.00	1.00
8	43	43	3.97	3.97	1.17	0.11	1.12
9	54	54	1.67	1.67	5.13	0.11	1.05
10	39	39	11.02	11.02	1.26	0.11	0.24
11	36	36	5.13	5.13	13.98	0.11	1.24
12	44	44	14.20	14.20	4.95	0.11	3.14
13	52	51	19.64	17.34	2.50	0.22	1.23
14	51	47	19.52	10.37	3.21	0.00	1.09
15	68	68	11.59	11.59	2.49	0.11	2.22
16	25	25	30.70	30.70	52.54	0.22	2.25
17	60	54	17.83	4.68	7.47	0.11	1.00
18	39	38	8.02	5.42	1.14	0.22	1.13
19	65	65	5.62	5.62	1.98	0.11	1.02
20	42	42	10.55	10.55	8.67	0.11	1.00
21	14	14	4.57	4.57	2.28	0.11	1.00
22	19	19	23.24	23.24	3.95	0.33	3.10
23	23	23	8.20	8.20	7.04	0.33	1.52
24	51	50	3.02	5.26	24.84	0.22	1.21
25	26	26	10.46	10.46	2.24	0.22	1.24
26	54	54	1.92	1.92	4.66	0.44	1.32
27	23	23	11.57	11.57	16.79	0.33	1.26
28	41	41	8.16	8.16	19.09	0.22	2.89
29	59	59	10.84	10.84	6.67	0.11	1.63
30	49	49	1.96	1.96	2.97	0.33	0.13
31	53	53	0.98	0.98	5.66	0.11	1.05
32	49	47	12.48	7.93	1.20	0.11	1.02
33	69	68	12.71	10.97	1.50	0.22	1.24
34	40	40	12.72	12.72	13.91	0.44	1.01
35	32	32	16.84	16.84	1.91	0.33	1.09
AVG	44.37	43.83	10.37	9.33	7.76	0.19	1.53
STDEV	14.30	14.02	7.13	6.72	10.09	0.11	1.04

Table A14 Topology #3, 20% echo

Topology #3, 40% echo

Replication	Number of valid locs	Number valid locs w/in 100 m	Pop avg dis from source	100m avg dis from source	Pop mode dis from source	Percent of Echo	Pop mode X/Y dis
1	6	6	17.43	17.43	17.31	0.44	1.86
2	29	29	8.92	8.92	11.64	0.22	1.22
3	62	62	10.70	10.70	2.76	0.33	1.56
4	59	59	12.20	12.20	6.72	0.44	1.37
5	22	22	17.27	17.27	3.74	0.67	2.03
6	50	50	17.34	17.34	2.04	0.33	0.10
7	82	82	11.72	11.72	1.50	0.33	1.46
8	15	15	5.87	5.87	2.23	0.33	2.13
9	51	51	8.53	8.53	3.87	0.33	1.03
10	23	23	5.89	5.89	4.96	0.44	4.02
11	47	47	19.41	19.41	4.75	0.33	3.13
12	57	56	18.39	16.49	2.13	0.56	2.06
13	43	43	8.98	8.98	7.28	0.44	2.57
14	30	30	3.47	3.47	6.69	0.44	1.38
15	69	69	5.52	5.52	4.22	0.67	4.00
16	47	46	2.45	3.08	3.87	0.56	1.13
17	55	55	7.14	7.14	6.97	0.33	1.01
18	44	44	24.70	24.70	32.37	0.44	8.47
19	55	55	2.47	2.47	3.03	0.22	1.00
20	55	54	16.59	14.86	2.80	0.56	2.12
21	66	66	9.14	9.14	5.04	0.33	3.08
22	49	49	2.82	2.82	2.69	0.67	1.03
23	50	50	1.88	1.88	1.41	0.67	1.07
24	31	31	9.71	9.71	1.82	0.78	1.39
25	24	24	15.86	15.86	2.52	0.33	1.92
26	30	30	15.20	15.20	4.91	0.56	4.02
27	44	44	3.92	3.92	7.76	0.11	1.00
28	27	27	10.12	10.12	8.46	0.33	6.00
29	35	35	8.87	8.87	4.01	0.33	1.24
30	20	20	5.51	5.51	5.93	0.44	2.04
31	63	61	10.93	6.34	1.77	0.33	1.00
32	34	34	3.81	3.81	1.06	0.56	0.19
33	41	41	6.78	6.78	1.70	0.22	1.20
34	37	37	5.14	5.14	7.91	0.22	1.02
35	47	47	5.48	5.48	3.60	0.44	1.54
AVG	42.83	42.69	9.72	9.50	5.12	0.42	2.04
STDEV	16.82	16.70	5.79	5.66	5.72	0.16	1.64

Table A15 Topology #3, 40% echo

Topology #3, 60% echo

Replication	Number of valid locs	Number valid locs w/in 100 m	Pop avg dis from source	100m avg dis from source	Pop mode dis from source	Percent of Echo	Pop mode X/Y dis
1	46	46	2.22	2.22	12.04	0.78	0.74
2	25	25	33.05	33.05	4.13	0.78	1.05
3	30	30	25.26	25.26	26.26	0.33	7.08
4	62	62	13.55	13.55	5.43	0.78	1.37
5	44	44	27.09	27.09	14.83	0.67	14.08
6	62	62	7.16	7.16	2.20	0.56	1.14
7	51	51	5.45	5.45	2.26	0.67	1.33
8	54	52	17.57	14.34	5.06	0.22	1.19
9	25	25	12.48	12.48	1.39	0.67	1.06
10	42	41	18.89	16.75	1.08	0.67	1.01
11	32	32	7.90	7.90	2.74	0.44	1.00
12	49	48	8.31	6.53	2.28	0.44	1.04
13	20	20	17.65	17.65	1.91	0.67	1.91
14	70	70	1.88	1.88	4.42	0.78	1.96
15	38	38	10.28	10.28	3.73	0.44	3.35
16	51	51	21.66	21.66	2.04	0.89	1.25
17	69	69	19.91	19.91	4.83	0.56	1.00
18	53	53	11.79	11.79	1.29	0.44	0.47
19	62	62	21.09	21.09	9.11	0.67	4.03
20	48	48	33.16	33.16	30.16	0.44	10.90
21	49	49	1.96	1.96	2.93	0.67	1.69
22	37	37	6.52	6.52	2.02	0.78	2.02
23	61	61	4.60	4.60	2.55	0.67	1.12
24	41	41	9.35	9.35	12.27	0.44	0.28
25	31	31	6.23	6.23	2.78	0.56	1.04
26	58	57	6.63	5.13	5.75	1.00	1.27
27	34	34	2.77	2.77	2.28	0.78	2.04
28	37	37	18.72	18.72	4.09	0.44	1.17
29	79	78	9.45	8.22	5.39	0.78	2.35
30	38	38	11.22	11.22	25.26	0.67	0.16
31	26	26	11.96	11.96	21.14	0.56	1.70
32	51	50	11.28	9.38	1.98	0.22	1.23
33	68	67	18.71	17.17	41.30	0.56	1.57
34	52	52	13.41	13.41	4.85	0.44	1.12
35	44	44	6.24	6.24	10.19	0.44	4.08
AVG	46.83	46.6	13.01	12.63	8.06	0.60	2.28
STDEV	14.51	14.35	8.37	8.37	9.58	0.18	2.88

Table A16 Topology #3, 60% echo

Topology #3, 80% echo

Replication	Number of valid locs	Number valid locs w/in 100 m	Pop avg dis from source	100m avg dis from source	Pop mode dis from source	Percent of Echo	Pop mode X/Y dis
1	61	61	3.38	3.38	1.30	0.67	1.28
2	46	45	5.97	3.85	2.37	0.67	2.22
3	51	50	2.78	1.15	4.11	0.78	1.22
4	59	57	27.52	23.70	1.74	0.89	1.35
5	76	76	3.45	3.45	8.14	0.89	1.61
6	47	47	11.61	11.61	1.16	0.89	1.13
7	62	62	5.28	5.28	0.49	0.78	0.38
8	43	43	19.01	19.01	1.51	0.78	1.08
9	33	33	8.93	8.93	5.66	0.67	1.28
10	48	48	27.48	27.48	3.98	0.78	2.45
11	43	43	4.82	4.82	1.52	0.89	1.10
12	53	52	22.55	20.06	6.69	0.44	3.72
13	22	22	9.38	9.38	17.20	0.67	1.68
14	36	36	5.72	5.72	11.30	0.78	1.40
15	67	67	2.06	2.06	2.23	0.67	2.23
16	21	21	13.37	13.37	20.40	0.67	4.11
17	14	14	9.89	9.89	3.98	0.67	1.55
18	33	33	19.96	19.96	7.57	0.89	3.00
19	83	82	12.18	11.00	5.37	1.00	1.17
20	44	44	8.76	8.76	10.28	1.00	7.03
21	67	67	16.99	16.99	5.53	0.44	1.34
22	65	64	31.86	30.29	4.17	0.67	3.03
23	52	52	11.36	11.36	2.75	0.67	0.04
24	62	62	26.98	26.98	2.91	0.78	1.02
25	50	49	22.42	20.21	1.35	0.67	0.20
26	28	28	16.49	16.49	13.81	1.00	0.65
27	41	40	6.66	6.85	2.05	0.78	1.85
28	42	42	15.37	15.37	2.46	0.78	2.07
29	51	51	14.98	14.98	6.84	0.67	1.32
30	53	53	7.81	7.81	4.77	0.78	3.45
31	58	58	1.99	1.99	1.23	0.78	1.22
32	55	55	1.93	1.93	6.17	1.00	1.00
33	20	20	19.01	19.01	1.86	0.78	1.03
34	54	54	9.05	9.05	13.56	0.22	1.08
35	62	62	11.45	11.45	5.46	0.44	2.05
AVG	48.63	48.37	12.53	12.10	5.48	0.74	1.78
STDEV	15.95	15.83	8.28	7.95	4.81	0.17	1.31

Table A17 Topology #3, 80% echo

Topology #3, 100% echo

Replication	Number of valid locs	Number valid locs w/in 100 m	Pop avg dis from source	100m avg dis from source	Pop mode dis from source	Percent of Echo	Pop mode X/Y dis
1	45	45	8.30	8.30	11.71	1.00	2.22
2	31	31	17.91	17.91	2.61	1.00	1.25
3	57	57	4.06	4.06	4.25	0.89	1.11
4	36	36	2.50	2.50	4.60	0.78	2.76
5	47	47	6.97	6.97	2.04	1.00	2.00
6	57	57	13.67	13.67	1.21	0.89	0.89
7	32	32	21.94	21.94	9.37	0.78	6.27
8	50	50	6.73	6.73	1.95	0.89	1.27
9	18	18	4.04	4.04	17.82	0.78	1.04
10	63	62	30.62	29.07	45.65	1.00	19.09
11	52	52	2.25	2.25	1.48	1.00	1.26
12	52	51	12.67	10.82	10.73	0.89	1.44
13	31	31	9.60	9.60	1.11	1.00	1.07
14	18	18	2.78	2.78	4.05	1.00	4.00
15	41	41	18.40	18.40	1.15	1.00	1.05
16	20	20	9.33	9.33	2.83	1.00	1.32
17	34	34	15.09	15.09	5.28	1.00	0.02
18	17	17	18.94	18.94	3.29	1.00	2.47
19	56	56	2.58	2.58	3.23	0.89	1.67
20	54	54	13.80	13.80	3.57	1.00	1.74
21	47	47	10.54	10.54	5.80	1.00	1.25
22	30	30	16.08	16.08	7.43	1.00	2.48
23	48	48	13.58	13.58	1.77	0.89	1.04
24	36	36	13.74	13.74	1.46	1.00	1.43
25	67	64	7.43	5.62	1.37	1.00	1.19
26	28	28	2.41	2.41	3.09	1.00	1.00
27	47	47	31.29	31.29	13.72	1.00	1.00
28	19	19	5.14	5.14	7.85	1.00	0.34
29	29	29	7.87	7.87	5.65	1.00	0.38
30	56	56	1.64	1.64	1.20	0.89	0.40
31	42	41	16.89	16.68	20.34	1.00	2.30
32	30	30	3.41	3.41	4.08	1.00	1.10
33	67	67	13.86	13.86	21.49	0.78	1.19
34	83	82	26.53	25.46	2.13	0.89	1.00
35	34	34	3.88	3.88	1.63	1.00	1.04
AVG	42.11	41.91	11.33	11.14	6.77	0.95	2.03
STDEV	16.02	15.76	8.03	7.89	8.70	0.08	3.17

Table A18 Topology #3, 100% echo

Topology #4, 0% echo

Replication	Number of valid locs	Number valid locs w/in 100 m	Pop avg dis from source	100m avg dis from source	Pop mode dis from source	Percent of Echo	Pop mode X/Y dis
1	5922	5681	38.89	34.86	1.67	0.00	1.11
2	6540	6294	28.43	25.04	2.03	0.00	1.54
3	4792	4634	33.94	29.89	3.16	0.00	3.06
4	4406	4080	29.19	20.65	2.09	0.00	2.09
5	5443	5231	30.61	27.28	2.24	0.00	2.02
6	5191	4830	28.15	20.17	3.67	0.00	2.18
7	6556	6329	30.11	26.92	6.05	0.00	6.04
8	4628	4387	30.07	24.49	3.10	0.00	3.00
9	5954	5636	30.01	24.24	4.07	0.00	4.06
10	4950	4673	22.67	16.26	2.76	0.00	0.52
11	5649	5348	31.53	25.97	1.30	0.00	1.22
12	4572	4362	30.71	25.71	2.17	0.00	2.17
13	6122	5788	28.16	22.22	5.90	0.00	4.02
14	5646	5397	20.08	15.38	1.94	0.00	1.09
15	3302	3116	35.51	28.82	3.30	0.00	3.14
16	3838	3617	37.95	31.60	4.15	0.00	3.14
17	5224	4813	35.37	26.23	4.07	0.00	4.00
18	4287	3999	40.22	32.26	5.82	0.00	5.30
19	5257	4927	32.21	25.36	2.72	0.00	2.13
20	4034	3762	35.39	28.33	4.40	0.00	4.00
21	5086	4816	32.27	26.18	2.09	0.00	1.12
22	3874	3644	31.55	24.67	5.38	0.00	5.18
23	5476	5203	30.84	24.99	6.42	0.00	3.87
24	4788	4489	31.15	24.34	3.13	0.00	3.05
25	6007	5698	22.19	16.60	3.18	0.00	3.01
26	5692	5408	34.63	29.47	2.44	0.00	1.00
27	5702	5513	23.84	20.35	6.37	0.00	6.05
28	4354	4224	18.97	15.60	3.23	0.00	3.12
29	5971	5785	33.75	31.30	2.97	0.00	1.25
30	4597	4423	34.81	30.84	1.09	0.00	0.48
31	4198	3987	27.69	22.15	2.68	0.00	0.94
32	5927	5597	27.89	21.58	4.27	0.00	4.19
33	6269	5825	24.28	15.51	3.03	0.00	3.01
34	4443	4215	48.47	43.26	4.18	0.00	4.11
35	4511	4193	30.63	22.21	2.14	0.00	1.19
AVG	5120.23	4854.97	30.92	25.16	3.41	0.00	2.78
STDEV	833.24	812.32	5.85	5.94	1.46	0.00	1.55

Table A19 Topology #4, 0% echo

Topology #4, 20% echo

Replication	Number of valid locs	Number valid locs w/in 100 m	Pop avg dis from source	100m avg dis from source	Pop mode dis from source	Percent of Echo	Pop mode X/Y dis
1	4510	4186	25.49	17.47	0.76	0.15	0.36
2	5334	4996	26.45	19.38	5.11	0.26	5.06
3	5321	4925	34.28	25.43	2.56	0.19	2.02
4	4226	3977	38.55	32.17	4.10	0.19	4.00
5	5390	5189	39.42	35.34	4.00	0.33	4.00
6	4247	4032	28.54	23.13	1.06	0.11	1.06
7	5536	5260	25.40	20.19	2.64	0.19	2.58
8	3912	3527	28.35	15.67	0.66	0.22	0.54
9	6058	5746	23.78	18.39	2.82	0.19	2.31
10	5302	5184	45.65	43.68	7.71	0.41	7.03
11	4483	4303	29.83	25.61	6.46	0.19	6.04
12	4584	4392	35.69	31.60	5.19	0.15	5.08
13	4086	3926	44.02	39.58	12.02	0.22	12.00
14	5291	4895	36.03	28.23	3.12	0.19	1.08
15	4046	3787	34.35	26.57	4.11	0.11	4.00
16	3172	2846	42.38	29.92	3.15	0.19	3.13
17	5440	5154	23.20	17.44	4.29	0.19	4.07
18	5946	5686	24.56	20.36	2.64	0.15	2.00
19	4209	3985	34.64	29.67	3.63	0.30	3.11
20	4938	4672	35.47	29.69	2.74	0.26	2.29
21	5081	4425	35.64	19.97	3.14	0.15	3.03
22	2970	2836	41.75	37.02	3.40	0.11	3.35
23	5273	4956	30.45	24.26	3.48	0.22	3.03
24	3263	3150	42.21	38.74	2.61	0.22	2.00
25	4533	4247	33.85	26.65	3.51	0.22	2.02
26	4445	4067	36.56	26.39	5.32	0.15	5.06
27	5936	5650	28.61	23.92	2.11	0.19	2.06
28	5009	4685	40.58	33.73	3.06	0.30	3.02
29	3742	3552	31.58	25.71	1.80	0.22	1.08
30	5523	5210	34.72	28.23	4.31	0.22	4.01
31	5523	5210	34.72	28.23	4.31	0.22	4.01
32	6176	5700	33.82	24.50	3.33	0.22	3.12
33	4753	4483	18.84	12.65	4.22	0.26	4.20
34	4387	4130	27.04	20.72	1.91	0.19	1.70
35	6458	6086	19.84	12.77	0.68	0.00	0.61
AVG	4831.51	4544.43	32.75	26.09	3.60	0.20	3.26
STDEV	865.82	827.65	6.88	7.50	2.12	0.07	2.18

Table A20 Topology #4, 20% echo

Topology #4, 40% echo

Replication	Number of valid locs	Number valid locs w/in 100 m	Pop avg dis from source	100m avg dis from source	Pop mode dis from source	Percent of Echo	Pop mode X/Y dis
1	5068	4832	34.47	29.82	1.24	0.30	1.24
2	4861	4601	33.35	26.85	2.34	0.30	2.04
3	3572	3436	52.64	48.84	2.89	0.63	2.69
4	4990	4649	29.12	21.60	1.35	0.26	1.17
5	4609	4387	28.73	23.45	5.72	0.33	5.23
6	4414	4197	17.60	11.76	3.22	0.33	0.12
7	6126	5769	26.96	20.30	2.02	0.41	2.02
8	6000	5605	33.11	26.38	0.30	0.56	0.21
9	4523	4367	35.24	31.43	5.27	0.41	5.17
10	4220	4006	36.60	31.34	2.45	0.41	1.14
11	4072	3901	34.67	30.81	4.25	0.44	4.25
12	6490	6220	26.37	22.00	7.98	0.22	6.02
13	5521	5170	27.95	20.39	3.43	0.44	3.01
14	3139	2993	40.39	35.04	4.11	0.37	4.05
15	6240	5955	24.05	19.69	2.26	0.22	1.45
16	5182	4755	33.72	24.76	1.41	0.41	1.18
17	4555	4232	46.87	38.68	5.44	0.33	5.17
18	5684	5461	20.98	17.67	3.59	0.37	2.18
19	4519	4244	23.08	15.54	4.38	0.52	4.07
20	5228	4978	30.39	25.53	1.79	0.37	0.32
21	5430	5176	32.66	28.43	2.99	0.33	1.54
22	4064	3919	26.64	22.21	2.70	0.30	2.05
23	5797	5347	38.45	29.99	4.06	0.41	4.04
24	5346	4987	21.63	14.04	2.21	0.33	1.46
25	4541	4352	35.43	30.68	3.72	0.41	3.35
26	3719	3537	32.15	26.39	3.56	0.44	2.08
27	4870	4633	41.78	37.01	2.93	0.52	2.28
28	3888	3618	35.30	27.62	1.07	0.41	1.01
29	5736	5372	32.06	25.16	5.05	0.41	5.00
30	5707	5493	32.19	28.69	3.46	0.48	3.01
31	6959	6534	23.32	16.72	2.89	0.41	2.00
32	4453	4082	31.42	21.82	2.56	0.37	2.17
33	3752	3569	41.09	35.75	7.26	0.44	7.17
34	5363	5030	28.04	21.00	4.28	0.26	3.43
35	4274	4062	44.44	39.77	2.50	0.30	1.06
AVG	4940.34	4670.54	32.37	26.49	3.33	0.38	2.70
STDEV	894.27	837.62	7.58	7.91	1.67	0.09	1.75

Table A21 Topology #4, 40% echo

Topology #4, 60% echo

Replication	Number of valid locs	Number valid locs w/in 100 m	Pop avg dis from source	100m avg dis from source	Pop mode dis from source	Percent of Echo	Pop mode X/Y dis
1	4906	4652	37.85	33.13	2.25	0.56	1.44
2	5545	5281	39.16	34.41	1.18	0.52	1.06
3	4635	4515	36.60	33.87	4.49	0.74	4.07
4	5144	4942	24.83	20.71	2.04	0.59	1.02
5	3705	3483	38.75	32.00	3.93	0.56	3.00
6	4657	4550	36.66	34.10	4.65	0.63	3.00
7	4347	4175	39.49	35.19	6.85	0.59	6.14
8	5907	5521	31.79	24.44	3.62	0.41	3.10
9	5879	5672	19.01	15.43	5.15	0.74	5.07
10	4153	3945	36.42	30.72	6.44	0.70	6.02
11	4362	4006	36.44	26.80	3.27	0.52	3.01
12	5840	5531	21.20	15.62	2.55	0.63	1.31
13	4907	4648	22.20	16.22	5.62	0.41	5.00
14	2879	2750	33.86	29.22	2.62	0.74	2.46
15	3545	3300	30.71	22.22	3.41	0.70	2.57
16	5636	5339	29.18	23.78	7.18	0.67	7.15
17	4817	4575	29.36	23.57	4.09	0.52	4.07
18	5660	5385	28.47	22.98	5.35	0.52	5.00
19	4531	4338	39.43	34.89	1.72	0.78	1.31
20	4257	3958	30.51	22.46	2.03	0.59	2.03
21	5313	5015	25.90	19.28	8.07	0.59	8.00
22	5921	5506	37.70	29.27	6.31	0.70	6.21
23	5973	5558	29.81	22.32	1.51	0.52	1.05
24	3002	2858	33.99	28.31	5.11	0.67	5.11
25	5951	5643	20.87	15.39	3.46	0.70	3.02
26	5283	4894	44.65	36.61	3.62	0.59	1.54
27	4236	4140	56.16	54.10	2.03	0.74	2.02
28	4160	4012	32.35	28.35	2.26	0.74	2.19
29	3380	3188	46.25	39.84	5.49	0.63	5.25
30	5900	5690	26.68	23.15	3.39	0.44	3.05
31	3748	3612	36.46	32.62	5.17	0.63	3.12
32	7015	6766	25.83	22.19	3.10	0.59	3.00
33	4716	4412	25.02	17.56	1.89	0.52	1.58
34	5941	5702	34.26	30.12	5.20	0.67	5.02
35	4602	4143	38.24	25.82	1.85	0.63	1.03
AVG	4870.09	4620.14	33.03	27.33	3.91	0.61	3.40
STDEV	972.12	929.85	7.83	8.14	1.81	0.10	1.92

Table A22 Topology #4, 60% echo

Topology #4, 80% echo

Replication	Number of valid locs	Number valid locs w/in 100 m	Pop avg dis from source	100m avg dis from source	Pop mode dis from source	Percent of Echo	Pop mode X/Y dis
1	5366	5164	33.56	29.52	7.01	0.74	7.01
2	4119	3945	33.34	28.49	3.86	0.59	3.29
3	6163	5739	28.03	20.05	3.46	0.81	3.08
4	4754	4476	42.04	35.79	5.40	0.63	5.04
5	5624	5423	33.93	30.23	2.53	0.78	2.26
6	5182	4930	32.20	27.09	2.34	0.59	2.04
7	4742	4397	44.26	36.01	4.11	0.78	4.11
8	5901	5637	21.85	17.09	2.50	0.67	1.70
9	4362	4130	27.88	21.93	4.03	0.74	4.00
10	4803	4453	31.33	23.51	2.50	0.70	1.38
11	5939	5607	29.45	23.23	1.46	0.74	1.39
12	4499	4301	36.89	32.26	1.05	0.78	1.01
13	4620	4193	37.56	26.57	5.00	0.81	5.00
14	4124	3974	41.20	37.52	4.05	0.78	4.04
15	5189	5044	34.31	31.50	1.96	0.85	1.96
16	3953	3825	34.59	31.33	1.74	0.74	1.39
17	4932	4628	31.01	24.83	3.31	0.78	1.47
18	6291	6045	26.46	22.50	2.07	0.81	0.41
19	5140	4852	24.97	19.14	3.64	0.78	1.01
20	5817	5530	30.32	25.00	2.89	0.89	2.00
21	4247	3849	30.66	19.21	3.37	0.85	2.14
22	2812	2730	45.72	42.61	4.36	0.85	4.36
23	4646	4524	42.23	39.75	1.33	0.70	1.16
24	5386	5137	32.98	28.23	3.39	0.78	3.11
25	5512	5128	28.12	20.26	3.24	0.81	1.32
26	4621	4247	33.11	24.06	6.07	0.78	6.06
27	5590	5258	42.11	35.66	3.26	0.74	0.86
28	4554	4403	36.63	33.40	1.06	0.78	1.01
29	5580	5230	28.28	21.42	2.02	0.67	2.02
30	5512	5211	22.95	16.70	2.03	0.74	2.02
31	4890	4527	36.19	28.27	1.88	0.93	0.33
32	4798	4514	34.82	29.35	1.78	0.74	1.35
33	4901	4449	30.96	18.57	3.40	0.67	3.32
34	5993	5602	27.32	20.31	1.22	0.85	0.65
35	4800	4610	27.46	22.83	4.14	0.67	4.02
AVG	5010.34	4734.63	32.99	26.98	3.07	0.76	2.49
STDEV	724.97	687.85	5.95	6.77	1.42	0.08	1.66

Table A23 Topology #4, 80% echo

Topology #4, 100% echo

Replication	Number of valid locs	Number valid locs w/in 100 m	Pop avg dis from source	100m avg dis from source	Pop mode dis from source	Percent of Echo	Pop mode X/Y dis
1	5007	4798	36.47	32.05	1.28	1.00	1.21
2	4028	3777	41.18	34.73	4.01	1.00	3.04
3	5803	5557	27.76	23.80	3.17	0.93	3.05
4	4333	4108	45.00	39.65	9.02	0.96	9.00
5	4913	4769	27.94	25.02	0.88	0.93	0.54
6	5450	5150	21.69	15.22	1.68	1.00	1.02
7	4663	4474	29.64	25.10	3.17	0.93	3.01
8	5381	5134	40.21	35.80	6.77	1.00	6.27
9	6549	6089	27.39	19.30	4.50	0.96	4.17
10	4954	4725	35.22	31.02	4.17	1.00	4.12
11	4547	4171	32.13	22.23	2.69	0.85	2.62
12	4091	3859	37.00	31.12	3.35	0.96	2.26
13	4681	4530	26.54	23.51	2.46	0.93	2.33
14	5059	4806	37.82	32.86	4.01	0.93	4.01
15	5208	4916	25.72	19.61	4.28	0.93	4.23
16	4265	3958	34.10	25.94	2.20	1.00	1.20
17	4667	4539	37.77	35.18	3.34	0.96	3.18
18	3986	3808	25.67	20.74	2.54	0.96	2.19
19	5396	5171	18.95	14.91	3.87	0.96	3.12
20	5156	4872	41.26	35.52	2.22	0.96	2.22
21	5102	4772	22.44	15.30	2.58	1.00	2.02
22	5765	5481	36.08	31.24	3.52	0.89	3.42
23	5242	4991	38.09	33.07	2.63	0.93	2.32
24	5286	4955	27.56	20.44	2.65	0.93	2.26
25	5993	5467	27.83	17.81	1.04	0.96	1.00
26	6287	5914	29.80	23.08	2.41	0.96	2.04
27	3711	3501	36.77	30.61	2.74	0.85	2.21
28	6475	6199	28.83	24.43	4.23	0.85	4.14
29	5628	5253	27.17	19.61	2.10	0.96	2.06
30	4454	4289	24.78	20.49	1.90	0.93	1.07
31	6021	5740	38.92	34.38	4.29	0.89	4.02
32	5325	5065	30.89	25.79	5.23	1.00	5.02
33	4609	4441	29.10	25.32	1.48	1.00	1.17
34	6218	5835	24.46	17.70	1.52	1.00	1.51
35	4468	4194	36.52	29.99	4.17	0.96	4.15
AVG	5106.31	4837.37	31.68	26.07	3.20	0.95	2.89
STDEV	738.15	689.68	6.43	6.85	1.62	0.04	1.68

Table A24 Topology #4, 100% echo

Topology #5, 0% echo

Replication	Number of valid locs	Number valid locs w/in 100 m	Pop avg dis from source	100m avg dis from source	Pop mode dis from source	Percent of Echo	Pop mode X/Y dis
1	10579	10398	10.62	9.14	1.99	0.00	1.52
2	11030	10916	9.28	8.41	1.35	0.00	0.57
3	10891	10798	5.52	4.78	0.99	0.00	0.90
4	9155	9067	4.98	4.16	0.81	0.00	0.62
5	11318	11222	7.59	7.16	0.90	0.00	0.83
6	7637	7532	14.21	13.18	1.49	0.00	1.12
7	13543	13433	6.27	5.50	1.94	0.00	0.81
8	14547	14533	1.72	1.70	1.33	0.00	1.09
9	9685	9543	6.91	5.70	1.49	0.00	0.57
10	12618	12565	3.77	3.48	0.74	0.00	0.43
11	6439	6313	17.05	15.26	3.62	0.00	3.61
12	15388	15383	1.24	1.22	0.66	0.00	0.66
13	14120	14068	2.84	2.54	1.60	0.00	1.17
14	9659	9521	6.63	5.51	1.81	0.00	1.34
15	11782	11612	7.43	5.98	0.77	0.00	0.76
16	7436	7244	12.03	9.48	2.86	0.00	2.81
17	7299	7159	12.66	11.12	2.02	0.00	2.01
18	13986	13946	2.07	1.86	0.75	0.00	0.73
19	14097	13998	4.65	4.01	1.55	0.00	1.25
20	8462	8346	6.78	5.62	1.05	0.00	0.90
21	11120	10984	8.08	7.12	1.00	0.00	0.82
22	12316	12165	5.76	4.61	0.49	0.00	0.45
23	8409	8226	12.06	10.18	0.66	0.00	0.23
24	7849	7729	14.06	12.93	2.31	0.00	1.98
25	10967	10898	6.47	5.89	1.32	0.00	1.29
26	11417	11300	2.91	2.42	1.25	0.00	0.48
27	8420	8308	8.88	7.97	1.31	0.00	0.99
28	13207	13131	5.25	4.85	1.61	0.00	1.60
29	13886	13832	4.18	3.88	0.39	0.00	0.34
30	12627	12486	6.26	5.43	0.96	0.00	0.96
31	10284	10124	6.12	4.78	1.45	0.00	1.38
32	14365	14296	3.77	3.39	0.89	0.00	0.87
33	9820	9637	3.72	2.27	1.53	0.00	1.53
34	13642	13609	2.63	2.49	1.36	0.00	1.07
35	8720	8624	8.57	7.76	1.22	0.00	1.15
AVG	11049.14	10941.31	6.94	6.05	1.36	0.00	1.11
STDEV	2475.40	2506.53	3.87	3.46	0.66	0.00	0.68

Table A25 Topology #5, 0% echo

Topology #5, 20% echo

Replication	Number of valid locs	Number valid locs w/in 100 m	Pop avg dis from source	100m avg dis from source	Pop mode dis from source	Percent of Echo	Pop mode X/Y dis
1	9634	9500	8.12	7.08	1.07	0.04	0.57
2	12761	12733	1.77	1.70	1.61	0.22	0.04
3	11425	11333	3.29	2.75	1.26	0.26	0.75
4	9426	9293	8.94	7.61	2.43	0.15	0.90
5	12538	12437	2.97	2.43	1.42	0.26	0.57
6	14992	14962	1.37	1.30	1.00	0.11	0.86
7	9219	9022	9.75	7.63	1.36	0.19	1.20
8	10058	9909	9.89	8.81	0.95	0.11	0.94
9	11096	11034	3.32	3.06	0.89	0.11	0.81
10	7369	7222	14.97	13.16	4.05	0.33	3.54
11	7680	7508	13.96	11.83	0.99	0.11	0.77
12	13577	13498	2.86	2.58	0.83	0.11	0.80
13	13577	13498	2.86	2.58	0.83	0.11	0.80
14	10438	10166	7.47	4.88	1.38	0.22	1.37
15	11662	11531	10.34	9.50	1.03	0.30	0.08
16	6986	6846	11.15	9.01	2.96	0.33	2.43
17	14089	14055	2.96	2.76	2.11	0.19	1.13
18	11811	11702	3.02	2.50	1.07	0.22	0.19
19	13304	13243	6.50	6.08	1.77	0.22	1.41
20	13465	13412	3.47	3.13	1.30	0.19	1.28
21	10287	10173	5.24	4.57	0.32	0.19	0.31
22	11223	11126	5.08	4.56	1.26	0.15	0.91
23	10706	10544	7.92	6.50	2.72	0.33	0.68
24	9147	8942	6.75	4.79	0.66	0.11	0.15
25	10748	10675	4.89	4.52	1.30	0.15	0.86
26	13682	13634	3.43	3.19	0.87	0.19	0.50
27	10279	10058	12.02	10.29	1.46	0.22	0.58
28	12467	12395	3.93	3.49	0.49	0.07	0.49
29	9992	9868	10.55	9.51	1.93	0.15	1.11
30	11606	11557	2.41	2.23	1.57	0.30	1.10
31	14419	14381	4.17	3.91	0.71	0.19	0.52
32	9606	9480	13.86	12.75	2.00	0.33	0.92
33	11773	11670	6.47	5.70	1.67	0.41	0.97
34	11864	11742	3.08	2.42	1.66	0.30	1.32
35	12144	12037	3.25	2.70	1.17	0.22	1.02
AVG	11287.1	11176.7	6.34	5.47	1.43	0.20	0.91
STDEV	1990.60	2031.62	3.86	3.34	0.75	0.09	0.64

Table A26 Topology #5, 20% echo

Topology #5, 40% echo

Replication	Number of valid locs	Number valid locs w/in 100 m	Pop avg dis from source	100m avg dis from source	Pop mode dis from source	Percent of Echo	Pop mode X/Y dis
1	10485	10363	8.03	6.87	1.07	0.37	0.77
2	8915	8746	9.34	7.93	1.30	0.48	0.64
3	8884	8659	10.64	8.26	1.76	0.30	1.21
4	10682	10595	6.26	5.70	1.84	0.30	0.37
5	7388	7250	12.86	11.00	0.73	0.41	0.54
6	9752	9642	7.29	6.36	1.73	0.26	1.68
7	7181	7044	14.70	13.10	1.55	0.33	0.67
8	8510	8320	7.13	4.99	0.74	0.33	0.67
9	14185	14136	1.18	1.00	1.26	0.30	0.64
10	14691	14658	2.00	1.87	1.43	0.56	1.22
11	8377	8302	7.89	7.08	0.57	0.41	0.26
12	12578	12428	4.84	3.72	1.58	0.44	0.79
13	9570	9453	8.07	6.96	0.98	0.30	0.90
14	13041	12896	5.76	4.93	0.80	0.56	0.71
15	11543	11490	6.11	5.77	2.26	0.26	1.83
16	12534	12457	2.86	2.38	0.17	0.37	0.16
17	8075	7862	11.06	8.52	1.41	0.33	0.90
18	13511	13409	4.10	3.41	0.78	0.44	0.72
19	9385	9272	6.79	5.85	2.18	0.33	0.64
20	12065	11979	2.99	2.67	0.81	0.37	0.79
21	11324	11253	5.56	5.16	1.81	0.52	1.62
22	10584	10478	6.60	5.81	1.69	0.33	0.88
23	8886	8714	8.11	6.30	1.45	0.52	1.44
24	12812	12745	1.66	1.23	0.47	0.33	0.41
25	13654	13628	3.99	3.90	1.21	0.41	0.10
26	8142	8047	12.44	11.48	1.99	0.30	1.88
27	12597	12526	3.88	3.52	0.57	0.33	0.52
28	10766	10634	5.47	4.43	1.62	0.48	1.05
29	7388	7215	12.21	10.20	2.25	0.37	1.69
30	6442	6262	24.31	21.61	1.44	0.30	1.26
31	12318	12251	3.32	2.95	0.45	0.26	0.42
32	10441	10355	9.99	9.39	0.33	0.48	0.29
33	12992	12897	4.97	4.48	1.57	0.26	0.96
34	8614	8499	6.26	5.20	1.03	0.48	0.95
35	12743	12650	5.36	4.79	1.00	0.41	0.85
AVG	10601.6	10489	7.26	6.25	1.25	0.38	0.87
STDEV	2262.49	2296.02	4.46	3.93	0.57	0.09	0.47

Table A27 Topology #5, 40% echo

Topology #5, 60% echo

Replication	Number of valid locs	Number valid locs w/in 100 m	Pop avg dis from source	100m avg dis from source	Pop mode dis from source	Percent of Echo	Pop mode X/Y dis
1	11200	11091	4.52	3.69	1.00	0.52	0.96
2	8289	8109	15.16	13.29	2.79	0.63	1.58
3	10743	10629	4.87	4.25	1.33	0.59	1.31
4	12858	12827	1.91	1.75	1.25	0.59	1.23
5	9122	8994	7.37	6.02	4.22	0.52	1.03
6	12687	12606	3.72	3.35	1.10	0.59	0.79
7	9353	9296	4.98	4.63	2.35	0.67	2.08
8	11524	11335	10.90	9.37	1.39	0.74	1.01
9	12945	12905	3.00	2.77	1.45	0.67	1.26
10	10661	10531	8.39	7.53	1.43	0.41	1.34
11	13028	12924	4.97	4.14	2.21	0.67	0.50
12	13070	12975	3.39	3.06	0.75	0.52	0.60
13	11919	11814	4.37	3.71	1.81	0.56	1.43
14	11791	11710	4.98	4.36	1.65	0.56	1.06
15	5667	5491	14.54	11.61	4.03	0.56	4.03
16	9108	8924	11.61	9.77	1.25	0.63	0.15
17	14264	14194	5.24	4.75	1.35	0.41	1.32
18	12116	12003	5.06	4.43	2.03	0.56	1.24
19	14071	14018	4.97	4.61	1.15	0.74	0.58
20	9181	9093	6.71	6.16	1.14	0.63	0.95
21	14725	14706	2.41	2.36	1.24	0.67	1.10
22	10007	9812	7.51	5.73	1.35	0.63	0.95
23	11462	11319	2.90	1.96	1.63	0.56	1.16
24	12159	12076	4.88	4.53	0.75	0.44	0.70
25	11391	11243	6.63	5.65	1.56	0.48	1.51
26	6542	6430	14.24	12.63	1.98	0.67	1.97
27	12411	12284	4.01	3.71	1.00	0.70	0.99
28	12585	12511	3.35	3.04	1.29	0.63	1.23
29	10247	10023	7.69	5.75	1.85	0.59	1.01
30	13311	13215	2.90	2.53	1.39	0.41	0.51
31	6783	6595	15.11	12.30	1.74	0.41	1.37
32	10727	10669	1.21	1.08	1.66	0.74	0.73
33	13969	13921	1.03	0.85	1.09	0.63	1.04
34	14044	13982	3.33	2.90	0.70	0.63	0.63
35	13718	13663	5.02	4.67	0.43	0.59	0.43
AVG	11362.2	11254.8	6.08	5.23	1.58	0.59	1.14
STDEV	2277.01	2311.03	3.93	3.29	0.80	0.10	0.65

Table A28 Topology #5, 60% echo

Topology #5, 80% echo

Replication	Number of valid locs	Number valid locs w/in 100 m	Pop avg dis from source	100m avg dis from source	Pop mode dis from source	Percent of Echo	Pop mode X/Y dis
1	8008	7796	9.79	7.12	1.35	0.70	1.29
2	11269	11200	2.57	2.09	1.06	0.63	1.04
3	7787	7660	9.41	8.06	1.48	0.74	1.25
4	12514	12450	3.03	2.80	0.87	0.74	0.81
5	10055	9903	7.22	5.88	1.70	0.70	0.82
6	10645	10536	10.16	9.21	1.69	0.81	0.98
7	10050	9918	8.09	6.99	1.35	0.78	0.61
8	13756	13683	2.08	1.81	1.23	0.81	0.87
9	9731	9581	9.33	8.23	1.09	0.70	0.50
10	12733	12635	6.43	5.78	2.00	0.70	1.11
11	6990	6801	21.68	18.94	2.37	0.74	1.33
12	9880	9756	10.60	9.44	2.47	0.81	2.47
13	13068	13015	3.76	3.53	0.93	0.63	0.92
14	10790	10617	4.86	3.22	1.68	0.81	0.29
15	11569	11468	3.24	2.78	1.31	0.78	1.02
16	12863	12707	7.35	6.29	1.77	0.74	1.77
17	11314	11130	7.69	6.39	2.06	0.85	1.39
18	15483	15426	2.36	2.02	1.29	0.74	1.12
19	13265	13217	2.49	2.29	1.57	0.56	0.66
20	11975	11850	7.48	6.42	0.57	0.74	0.51
21	8402	8261	5.38	4.14	0.90	0.70	0.86
22	14221	14178	1.95	1.78	1.59	0.70	1.03
23	10235	9999	7.48	5.47	1.27	0.81	0.20
24	10299	10186	7.33	6.78	1.43	0.85	1.19
25	13294	13224	4.46	3.96	1.43	0.56	1.22
26	11258	11180	3.60	3.08	1.39	0.78	0.60
27	8663	8559	10.77	9.76	0.78	0.59	0.78
28	11254	11147	5.97	5.38	1.51	0.74	1.15
29	7877	7782	9.51	8.66	1.37	0.74	1.10
30	8347	8197	10.09	8.29	1.34	0.74	1.11
31	9132	9020	21.98	20.89	2.85	0.67	2.71
32	9419	9253	10.21	8.71	2.40	0.70	0.53
33	14193	14125	3.01	2.58	0.97	0.78	0.88
34	11127	10955	7.53	6.10	0.98	0.56	0.98
35	13632	13587	1.22	1.14	0.81	0.81	0.42
AVG	11002.8	10885.8	7.15	6.17	1.45	0.73	1.01
STDEV	2145.26	2177.52	4.70	4.28	0.52	0.08	0.52

Table A29 Topology #5, 80% echo

Topology #5, 100% echo

Replication	Number of valid locs	Number valid locs w/in 100 m	Pop avg dis from source	100m avg dis from source	Pop mode dis from source	Percent of Echo	Pop mode X/Y dis
1	11464	11326	5.15	4.42	1.58	0.96	1.56
2	10574	10472	7.86	7.22	1.36	0.93	0.44
3	11787	11714	5.74	5.29	1.75	0.93	0.47
4	9834	9717	9.73	8.97	2.66	0.96	2.59
5	12599	12502	4.08	3.42	1.73	0.96	0.94
6	14247	14212	1.46	1.36	1.53	0.96	1.16
7	12332	12252	5.74	5.10	1.13	1.00	0.70
8	12051	11993	4.93	4.56	1.41	0.93	1.01
9	7568	7339	15.22	12.47	0.83	0.96	0.77
10	12203	12164	2.20	2.03	0.77	0.96	0.54
11	7673	7556	6.14	4.92	1.56	0.93	1.52
12	9242	9072	12.36	10.80	3.00	1.00	2.91
13	13247	13126	3.89	3.37	0.62	0.81	0.44
14	13420	13338	5.32	4.83	1.12	0.93	0.84
15	13426	13369	3.57	3.27	2.00	1.00	0.58
16	13958	13906	1.50	1.33	1.27	1.00	0.88
17	12727	12643	3.56	3.03	1.70	0.96	1.02
18	10739	10585	7.56	6.30	1.76	0.93	1.25
19	8760	8629	12.42	11.06	2.31	0.85	2.28
20	9062	8940	7.97	6.80	1.23	1.00	0.79
21	12101	12009	8.31	7.63	1.66	0.96	1.64
22	7405	7267	8.83	7.76	1.52	0.96	0.70
23	12725	12679	4.07	3.73	1.49	0.96	1.11
24	10085	9927	7.33	6.65	1.39	1.00	1.39
25	9493	9416	11.13	10.59	1.98	0.89	1.97
26	7132	6908	18.51	15.43	1.09	0.93	0.50
27	13418	13341	3.52	3.03	0.91	0.96	0.72
28	9019	8885	10.73	9.61	1.38	0.96	1.28
29	13552	13492	5.66	5.25	1.33	0.93	0.45
30	11235	11093	5.80	4.77	0.86	0.93	0.58
31	13106	13013	4.23	3.55	0.38	1.00	0.29
32	11311	11232	6.87	6.24	0.96	1.00	0.91
33	13944	13923	2.54	2.44	0.86	0.96	0.40
34	8888	8757	6.00	5.03	1.24	0.96	1.09
35	8860	8719	8.18	6.65	1.75	1.00	1.02
AVG	11119.6	11014.7	6.80	5.97	1.43	0.95	1.05
STDEV	2144.51	2182.88	3.82	3.27	0.54	0.04	0.63

Table A25 Topology #5, 100% echo

Bibliography

1. [AcL94] Ackroyd N., R. Lorimer, *Global Navigation: A GPS User's Guide*, Lloyd's of London Press LTD, 1994.

2. [Cal03] Calvert, J.B., "Sound Waves", http://www.du.edu/~jcalvert/waves/soundwav.htm, September, 2003

3. [DGB, 96] Duckworth, G.L., D.C.Gilbert, J.E.Barger, "Acoustic Counter-Sniper System", SPIE Proceedings 2938, Command Control, communications, and Intelligence Systems for Law Enforcement, presented at the SPIE International Symposium on Enabling Technologies for Law Enforcement and Security, Boston, MA, 19-21 November, 1996.

4. [FiS99] Figler, B.D., T.J.Spera, "Improved sniper location system", Proceedings of the SPIE - The International Society for Optical engineering, Vol. 3577, 1999.

5. [KFC82] Kinsler, Lawrence E. ,Austin R. Frey, Alan B. Coppens, James V.Sanders, "Fundamentals of Acoustics", John Wiley & Sons, 1982.

6. [MiE01] Misra, Pratap, Per Enge, *Global Positioning System; Signals, Measurements, and Performance*, Ganga-Jamuna Press, 2001.

7. [LSC02] Lewis, G., S. Shaw, M. Crowe, C. Cranford, K. Torvik, P. Scharf, Dr. Peter Scharf, Bob Stellingworth, "Urban Gunshot and sniper location: technologies and demonstration results", Proceedings of the SPIE – The International Society for Optical engineering, Vol. 4708, 2002.

8. [SmA87] Smith, J.O., J.S.Abel, "The spherical interpolation method of source localization", IEEE Journal of Oceanic Engineering, Vol. OE-12, No. 1, Jan 1987.

9. [Una93] Unattributed, "ICD-GPS-200, Revision C, Initial Release", Oct 93.

10. [Una00] Unattributed, “Echo”, http://www.infoplease.com/ce6/sci/A0816696.html, The Columbia Electronic Encyclopedia, 2000.

11. [Wei03] Weimer, Melissa Ray , “Waveform Analysis Using The Fourier Transform”, http://www.dataq.com/applicat/articles/an11.htm, Aug 2003.

12. [Wel87] D. Wells, *Guide to GPS Positioning*, Canadian GPS Associates, 1987.

13. [WoE85] Wong, G.S.K., T.F.W.Embleton, “Variations of the speed of sound in air with humidity and temperature”, Journal of the Acoustical Society of America, Vol. 77, No. 5, May 1985.

Vita

1st Lieutenant Jeffrey A. Boggs graduated from Havana High School in Havana, Illinois. He entered undergraduate studies at the Community College of Aurora and the University of Colorado at Denver in August 1992. He later graduated from Rollins College, Florida in May 2000. He was commissioned through Officer Training School in August of 2000.

His first assignment on active duty, following basic training and technical school, was at Patrick AFB, FL in February 1986. In May 1988, he was assigned to Detachment 45, Buckley ANGB, CO, where he served as a Mission "B" Controller. In May 1996, he was stationed at Patrick AFB, FL, at the Air Force Technical Applications Center, as a Satellite Analyst. Following his commissioning in 2000, he was assigned to the 333rd Training Squadron, Keesler AFB, MS for technical training. In Jan 2001, he was assigned to the 78th Communications Squadron at Robins AFB, GA as an ACE Lieutenant. In August 2002, he entered the Graduate School of Engineering and Management, Air Force Institute of Technology. Upon graduation, he will be assigned to the Air Force Weather Agency, Offutt AFB, NE.

REPORT DOCUMENTATION PAGE			Form Approved OMB No. 074-0188

The public reporting burden for this collection of information is estimated to average 1 hour per response, including the time for reviewing instructions, searching existing data sources, gathering and maintaining the data needed, and completing and reviewing the collection of information. Send comments regarding this burden estimate or any other aspect of the collection of information, including suggestions for reducing this burden to Department of Defense, Washington Headquarters Services, Directorate for Information Operations and Reports (0704-0188), 1215 Jefferson Davis Highway, Suite 1204, Arlington, VA 22202-4302. Respondents should be aware that notwithstanding any other provision of law, no person shall be subject to an penalty for failing to comply with a collection of information if it does not display a currently valid OMB control number.
PLEASE DO NOT RETURN YOUR FORM TO THE ABOVE ADDRESS.

1. REPORT DATE *(DD-MM-YYYY)*	2. REPORT TYPE	3. DATES COVERED *(From – To)*
23-03-2004	Master's Thesis	March 2003 – March 2004

4. TITLE AND SUBTITLE	**5a. CONTRACT NUMBER**
GEOLOCATION OF AN AUDIO SOURCE IN A MULTIPATH ENVIRONMENT USING TIME-OF-ARRIVAL	**5b. GRANT NUMBER**
	5c. PROGRAM ELEMENT NUMBER
6. AUTHOR(S)	**5d. PROJECT NUMBER**
Boggs, Jeffrey A., 1st Lieutenant, USAF	**5e. TASK NUMBER**
	5f. WORK UNIT NUMBER

7. PERFORMING ORGANIZATION NAMES(S) AND ADDRESS(S) Air Force Institute of Technology Graduate School of Engineering and Management (AFIT/EN) 2950 Hobson Way, Building 640 WPAFB OH 45433-8865	**8. PERFORMING ORGANIZATION REPORT NUMBER** AFIT/GCS/ENG/04-03
9. SPONSORING/MONITORING AGENCY NAME(S) AND ADDRESS(ES) National Security Agency (NSA) / R5 Attn: Mr. William Kroah DSN: (301) 688-0348 Ft George G. Meade, MD 20755-6000 E-mail: wtk@afterlife.ncsc.mil	**10. SPONSOR/MONITOR'S ACRONYM(S)**
	11. SPONSOR/MONITOR'S REPORT NUMBER(S)

12. DISTRIBUTION/AVAILABILITY STATEMENT

APPROVED FOR PUBLIC RELEASE; DISTRIBUTION UNLIMITED.

13. SUPPLEMENTARY NOTES

14. ABSTRACT

The Air Force and the Department of Defense (DoD) are continually searching for ways to protect U.S. forces, both stateside and abroad. One continuing threat, especially in the current world environment, is gunfire from an unseen sniper. Designated areas, such as a forward deployed base or motorcade route, need to be continuously monitored for sniper fire. Once detected, these gunmen need to be located in real time. One possible method for accomplishing this task is to geolocate the audio signals generated using time-of-arrival (TOA) algorithms. These algorithms rely on direct-path measurements for accuracy. Multipath environments therefore pose a problem when measuring signals from the audio spectrum.

The errors induced by a multipath environment can be reduced by introducing additional audio receivers to the detection system. By sampling all possible combinations of a minimum set of receivers (four), a more accurate location can be calculated. An accuracy of six meters can be achieved roughly 69 percent of the time, though most of the error occurs in the vertical component. An accuracy of six meters in the X/Y plane can be achieved approximately 97 percent of the time.

15. SUBJECT TERMS

Global Positioning System, snipers, acoustic detection

16. SECURITY CLASSIFICATION OF:			17. LIMITATION OF ABSTRACT	18. NUMBER OF PAGES	19a. NAME OF RESPONSIBLE PERSON
					Rusty O. Baldwin, Maj, USAF
a. REPORT	b. ABSTRACT	c. THIS PAGE			19b. TELEPHONE NUMBER *(Include area code)*
U	U	U	UU	107	(937) 255-6565, ext 4445 (rbaldwin@afit.edu)